Heinrich Heine
Universität Düsseldorf

p38 MAPKα is a Key Regulator of Cardiac Metabolism

Inaugural dissertation

presented to the Faculty of Mathematics and Natural Sciences at the

Heinrich Heine University Düsseldorf for the degree of Doctor of Natural Sciences

by

Lisa Kalfhues

Düsseldorf, July 2020

from the Institute of Cardiovascular Physiology

Heinrich Heine University, Düsseldorf

Printed by permission of the

Faculty of Mathematics and Natural Science at

Heinrich Heine University Düsseldorf

Examiners:

1. Prof. Dr. Axel Gödecke

2. Prof. Dr. Reza Ahmadian

Date of the oral examination: 08.09.2020

Content

Abstract

The heart utilizes different substrates to maintain a high rate of ATP production to ensure a sufficient cardiac performance, even when nutrient supply changes. Throughout the progression of heart failure (HF), the ability for the heart to switch substrate preference may be impaired even before overt cardiac dysfunction. This loss of metabolic flexibility and insulin sensitivity may even promote HF. The stress-activated p38 mitogen-activated protein kinase α (MAPKα) is known to be implicated in a variety of cardiac pathologies including HF by promoting metabolic remodeling. To elucidate the underlying mechanisms contributing to the establishment of cardiac failure, the influence of p38 MAPKα on cardiac metabolism during the early phase of HF development was investigated.

In this study a mouse model with a cardiomyocyte specific, tamoxifen inducible p38 MAPKα deletion (iCMp38 MAPKα KO) was used. Substrate utilization measured by NMR spectroscopy with ^{13}C-labeled substrates showed that iCMp38 MAPKα KO hearts failed to upregulate glucose utilization after insulin stimulation. This cardiac insulin resistance in iCMp38 MAPKα KO hearts was associated with a decreased Glut4 protein amount (approx. by 50%) and translocation to the plasma membrane after insulin stimulation (approx. by 50%), without compromising phosphorylation levels of other proteins mediating intracellular insulin signal transduction (incl. Akt isoforms, AS160, Pras40, and Gsk3-β).

To induce pressure overload, these mice were exposed to angiotensin II (AngII) by implanting osmotic mini pumps (1.5 mg/kg/d). Heart failure was rapidly induced 48 hours after the onset of AngII treatment. This was confirmed by echocardiography, which revealed a strong left ventricular dilation and a severely impaired cardiac function in iCMp38 MAPKα KO AngII hearts (ejection fraction [%]: KO 18 ±8.9, Ctrl 45.7 ±11.4). The importance of p38 MAPKα signaling was shown by increased p38 MAPKα$^{T180/Y182}$ phosphorylation in Ctrl AngII hearts (by 1.5 ±0.2-fold). Additionally, fatty acid (FA) metabolism alterations were shown by cardiac lipid accumulation and significantly reduced expression levels of the key regulator of FA metabolism, Pgc1-α (0.19 ±0.03-fold) and its cofactor PPARγ (0.45 ±0.26-fold) in iCMp38 MAPKα KO AngII hearts. Surprisingly, AngII treatment also led to increased plasma insulin levels in iCMp38 MAPKα KO mice which enhanced cardiac Akt^{S473} phosphorylation in cardiomyocytes. Activation of Akt in turn reduced activating AMPKα^{T172} and increased inhibitory AMPKα^{S485} phosphorylation, shifting AMPKα to the inactive form. This might contribute to a reduced energy supply in pressure overloaded iCMp38 MAPKα KO hearts. Furthermore, insulin mediated AMPKα inhibition was not found in cardiomyocyte specific Akt KO hearts, underlining the importance of Akt in AMPKα inhibition. Additionally, the alteration in plasma insulin levels suggests a crosstalk between the stressed heart and the pancreas. Although transcriptional insulin expression in isolated pancreatic islets did not differ between control and iCMp38 MAPKα KO mice, a lower insulin protein amount was found in beta-cells from iCMp38 MAPKα KO animals. The reason for this might be a potential increase in insulin secretion leading to the detected hyperinsulinemia.

In conclusion, iCMp38 MAPKα KO mice developed cardiac insulin resistance and an extensive metabolic depression which potentially contributed to the progression of HF. Additionally, iCMp38 MAPKα KO mice were hyperinsulinemic, suggesting a potential interorgan communication between the failing heart and the pancreas. Thus, this study demonstrates for first time that p38 MAPKα signaling is a key regulator in the adaption of cardiac metabolism to elevated workload. Moreover, this mouse model presents a valuable tool to investigate diabetic cardiomyopathy contributing to cardiac failure.

Zusammenfassung

Das Herz verwendet verschiedenste Substrate, um eine ausreichend hohe ATP Produktion zu garantieren. Dadurch kann die kardiale Leistung auch im Falle von sich ändernden Substratverfügbarkeiten zu jedem Zeitpunkt gewährleistet werden. Die Fähigkeit des Herzens seine Substratpräferenzen anzupassen ist bei der Entstehung einer Herzinsuffizienz möglicherweise schon vor Beginn einer kardialen Dysfunktion eingeschränkt. Der Verlust dieser metabolischen Flexibilität sowie eine Insulinresistenz fördern dabei möglicherweise sogar das Voranschreiten der Insuffizienz. Um die molekularen Mechanismen dieser metabolischen Veränderungen zu verstehen, wurde in dieser Arbeit der Einfluss der p38 MAPKα (engl. p38 mitogen-activated protein kinase α) auf den kardialen Stoffwechsel in der frühen Phase der Herzinsuffizienzentwicklung untersucht.

Für diese Untersuchungen wurde ein Mausmodel verwendet, welches eine durch Tamoxifen-induzierbare Deletion der p38 MAPKα (engl. inducible cardiomyocyte (iCM)p38 MAPKα KO), spezifisch in Kardiomyozyten besitzt. Erste NMR-Spektroskopiemessungen mit ^{13}C-markierten Substraten zeigten, dass iCMp38 MAPKα KO-Herzen nicht in der Lage sind, die Glukoseverwertung nach Insulinstimulation zu steigern. Es konnte gezeigt werden, dass diese kardiale Insulinresistenz in iCMp38 MAPKα KO-Herzen aus einer reduzierten Glut4-Menge (um ca. 50%) und zusätzlich aus einer reduzierte Glut4-Tanslokation zur Plasmamembran (um ca. 50%) nach Insulinstimulation resultiert. Die insulininduzierte intrazelluläre Signaltransduktion durch eine Phosphorylierungskaskade (von Akt Isoformen, AS160, Pras40 und Gsk3-β) war dabei nicht beeinträchtigt.

Mittels AngiotesinII (AngII) Applikation über implantierte osmotische Minipumpen (1,5 mg/kg/d) wurde eine Steigerung der Druckbelastung für das Herz induziert. Bereits 48 Stunden nach Implantation konnte eine massiv eingeschränkte kardiale Kontraktilität mittels Echokardiographie festgestellt werden. Dabei zeigte sich neben einer starken linksventrikulären Dilatation auch eine schwerwiegend eingeschränkte Herzfunktion in iCMp38 MAPKα KO AngII-Herzen (Ejektionsfraktion [%]: KO 18 ±8.9, Ktrl 45.7 ±11.4). Die p38 MAPKα selbst zeigte in Kontrollherzen eine signifikant erhöhte p38 MAPKα$^{T180/Y182}$ Phosphorylierung nach AngII Exposition, was auf eine wichtige Funktion dieses Signalwegs schließen lässt. Zusätzlich wurden massive kardiale Fetteinlagerungen und deutlich reduzierte Expressionslevel von wichtigen Faktoren des Fettsäureabbaus (Pgc1-α (auf das 0,19 ±0,03-fache) und dessen Kofaktor PPARγ (auf das 0,45-fache ±0,26-fache) festgestellt. Beides lässt auf Veränderungen im Fettmetabolismus in iCMp38 MAPKα KO AngII-Herzen schließen

Die Behandlung mit AngII führte außerdem zu erhöhten Insulinspiegeln im Plasma von iCMp38 MAPKα KO-Mäusen, was auf eine Interorgankommunikation zwischen dem versagenden Herzen und dem Pankreas schließen lässt. Zwar zeigte die Transkriptexpression von Insulin keine Veränderung, allerdings konnte eine Reduzierung der Insulinmenge in beta-Zellen gezeigt werden. Das deutet auf einen möglichen Einfluss auf die Insulinsekretion hin, allerdings sind hier weitere Untersuchungen notwendig. In iCMp38 MAPKα KO-Herzen führten die erhöhten Insulinspiegel zu einer erhöhten Akt^{S473}-Phosphorylierung, was wiederum in einer reduzierten AMPKα Aktivität resultierte. Dadurch wird möglicherweise die bereits eingeschränkte Energieversorgung im drucküberlasteten Herzen zusätzlich beeinträchtigt. In Kardiomyozyten-spezifischen Akt KO-

Herzen konnte diese insulinvermittelte AMPKα-Hemmung nicht beobachtet werden, was die Wirkung von Akt auf die AMPKα-Inhibierung unterstreicht.

In dieser Arbeit konnte gezeigt werden, dass iCMp38 MAPKα KO-Mäuse eine Hyperinsulinämie, kardiale Insulinresistenz und eine ausgeprägte metabolische Depression entwickeln, was die Entstehung der Herzinsuffizienz begünstigt. Die Arbeit zeigt somit erstmalig, dass die p38 MAPKα einen essentiellen Regulator bei der Anpassung des kardialen Metabolismus an erhöhte Arbeitsbelastung darstellt. Zudem stellen iCMp38 MAPKα KO-Mäuse ein vielversprechendes Modell dar, um die diabetische Kardiomyopathie zu untersuchen, die zum kardialen Versagen beiträgt.

1 Introduction

1.1 The cardiovascular system

The fundamental function of the cardiovascular system is the fast and convective transport of oxygen and nutrients like glucose, amino acids, fatty acids (FA), vitamins and also water to organs and tissues in the periphery. Furthermore, it also removes metabolic products such as carbon dioxide, urea, and creatinine.

The circulatory system includes two distinct loops: the pulmonary circulation and the systemic circulation. The essential component linking the two loops is the heart, which functions as a muscular pump. It consists of four chambers: the left side and the right side each having one atrium and one ventricle. The heart ensures a continuous blood flow by pumping blood from the right ventricle into the pulmonary system to the lung. In the pulmonary alveoli the blood picks up oxygen and delivers carbon dioxide for exhalation. Oxygenated blood is then transported to the left ventricle via its atrium and from there it enters systemic circulation reaching all the tissues and organs of the body. In the systemic capillaries the transfer of oxygen and nutrients to organs and muscles, and the removal of waste products and carbon dioxide occurs. The deoxygenated and carbon dioxide rich blood returns to the right ventricle via the right atrium and enters pulmonary circulation again (Betts *et al.*, 2014).

To maintain the physiological function of the heart and vascular homeostasis, several control mechanisms regulate heart rate, stroke volume, vessel diameter and blood volume. On the one hand, stimulation of the sympathetic/parasympathetic nervous system regulates cardiac function by controlling heart rate and stroke volume. The control of vessel tone or contraction of smooth muscle to affect peripheral resistance, pressure and flow are controlled by the action of released neurotransmitters such as norepinephrine as well as endothelial factors including nitric oxide (NO). In addition, the cardiovascular system is highly regulated by endocrine factors such as hormones and cytokines involving interorgan communication.

In particular, the kidneys affect cardiovascular homeostasis by the regulation of blood volume. Moreover, via the important renin-angiotensin aldosterone system (RAAS), the kidney has a major effect upon the regulation of blood pressure (Peach, 1977). The hormone angiotensin II (AngII), a strong vasoconstrictor and the major effector peptide of the RAAS system, was used during this project to effectively increase blood pressure. To understand its physiological role, this regulatory pathway is explained more in detail, although it is not the only regulatory mechanism controlling the cardiovascular system. Generally, the kidneys respond to decreased blood flow by secreting renin into the blood flow. The released hormone renin then catalyzes the conversion of the plasma protein angiotensinogen into its active form: angiotensin I. Angiotensin I in turn is then converted into angiotensin II, catalyzed by the angiotensin-converting enzyme (ACE) (Fountain *et al.*, 2019). Angiotensin II is a powerful vasoconstrictor, greatly increasing blood pressure by binding to its angiotensin II receptor (AT_1 receptor) (Timmermans *et al.*, 1993) in the kidney and also in extrarenal tissues like heart and blood vessels (Navar *et al.*, 1987).

Blood pressure changes often correlate with alterations in the structure and function of the hearts. Different parameters are commonly used to monitor cardiac structure and function. At the end of filling and just before atrial contraction, the ventricle contains its maximal blood volume, which is known as the **end diastolic volume (EDV)**. The volume of blood remaining in the ventricle at the end of contraction and at the beginning of diastole is known as the **end systolic volume (ESV)**. Changes of EDV and ESV are found in patients with cardiac pathologies such as heart failure, indicate the occurrence of cardiac remodeling (Kerkhof, 2015) and give information about alterations in the volume of the left ventricle (LV). The amount of blood pumped by the ventricle is defined as stroke volume (SV) and is normally calculated by the difference of EDV and ESV measured by echocardiography. SVs are also used to calculate the **ejection fraction (EF)**, which is the portion of the blood that is ejected from the heart with one contraction. To calculate ejection fraction, SV is divided by EDV and is normally expressed as a percentage.

1.2 Metabolism in the healthy heart

The heart continuously contracts to supply the organs and tissues of the body with oxygen and nutrients. Thus, a high rate of adenosine triphosphate (ATP) production and turnover is

a critical requirement to fuel an optimal cardiac performance. Under normal and healthy conditions, the heart produces up to 10-40% of ATP from oxidation of glucose and lactate, and up to 60-90% from beta-oxidation of FAs (Gertz *et al.*, 1988; Opie, 2004; Wisneski *et al.*, 1985). In general, FA oxidation is more energy efficient than glucose or lactate oxidation. While utilization of FAs leads to the generation of 8.2 ATP molecules per carbon, glucose or lactate usage only produces 6.3 ATP molecules per carbon (Chaanine *et al.*, 2011). However, oxidation of glucose and lactate requires less oxygen to produce ATP. These substrates are therefore preferred under condition of limited oxygen supply. To maintain a sufficient rate of ATP production under conditions of increased workload, the heart rapidly switches its substrate preference, a phenomenon known as metabolic flexibility (Balaban, 1990). Thus, the heart is often termed as metabolic omnivore, because it is capable to use all classes of energy substrates such as carbohydrates, lipids, amino acids and ketone bodies to produce ATP (Lopaschuk *et al.*, 2010).

95% of the produced ATP in cardiomyocytes is generated by oxidative phosphorylation and only 5% comes from glycolysis, which explains the high density of mitochondria in cardiomyocytes (approximately 30% of the cell volume) (Schaper *et al.*, 1985; Stanley *et al.*, 2002). Cardiac mitochondria use acetyl-CoA as substrate, which is provided by both FAs and glucose. Since the heart uses a variety of metabolic pathways, metabolic flexibility is regulated at multiple levels. Firstly, FA and glucose metabolism interregulate each other in a process described as Randle cycle (Randle *et al.*, 1963). Randle postulated that increasing FA oxidation in the heart decreases glucose oxidation, and vice versa (Kolwicz *et al.*, 2013). In addition, metabolic pathways can quickly be turned on and off to adapt cardiac metabolism to acute stress by modifications of regulatory enzymes, translocation of transporters to their site of action, and activation or inhibition of metabolic signaling pathways (Hue *et al.*, 2009; Stanley *et al.*, 2005).

1.2.1 Fatty acid metabolism in the heart

Cardiomyocytes metabolize FAs from different sources: free fatty acids (FFA) bound to albumin from plasma or FAs from breakdown of stored triacylglycerol (TAG) within the cell. FAs can enter the cell either by fatty acid translocase (FAT/CD36) or by a non-receptor mediated pathway referred to as passive flip-flop (Kamp *et al.*, 1995). The majority of FAs

undergoes beta-oxidation within the mitochondria, while a minor part of FAs undergoes esterification to TAG. TAGs are stored within the cell in form of lipid droplets (Kienesberger *et al.*, 2013) and serve as a storage depot to fuel ATP production by FA oxidation under conditions of low substrate availability (Saddik *et al.*, 1991). TAG breakdown to fatty acyl-CoA is catalyzed by adipose triglyceride lipase (ATGL), whereas diglyceride acyltransferase (DGAT) regulates the formation of TAGs. To enter beta-oxidation, imported FAs are transformed into fatty acyl-CoA by acyl-CoA synthase, which allows them to enter mitochondria. The translocation process requires CPTI at the outer mitochondrial membrane and CPTII at the inner mitochondrial membrane. CPTI catalyzes the conversion of acyl-CoA to acylcarnitines, which is an essential reaction to shuttle it across the mitochondrial membrane by carnitine-acylcarnitine translocase (CACT). Inside the mitochondria, acylcarnitine is transformed back to acyl-CoA by CPTII. Subsequently, beta-oxidation completely reduces acyl-CoA to acetyl-CoA, which leads to the production of NADH and $FADH_2$ (Lopaschuk *et al.*, 2010). Acetyl-CoA further enters tricarboxylic acid (TCA) cycle and is oxidized to CO_2 and H_2O, which also produces the reduction intermediates NADH and $FADH_2$. These intermediates are used by electron transport chain (ETC) to generate ATP by oxidative phosphorylation (Figure 1.1)

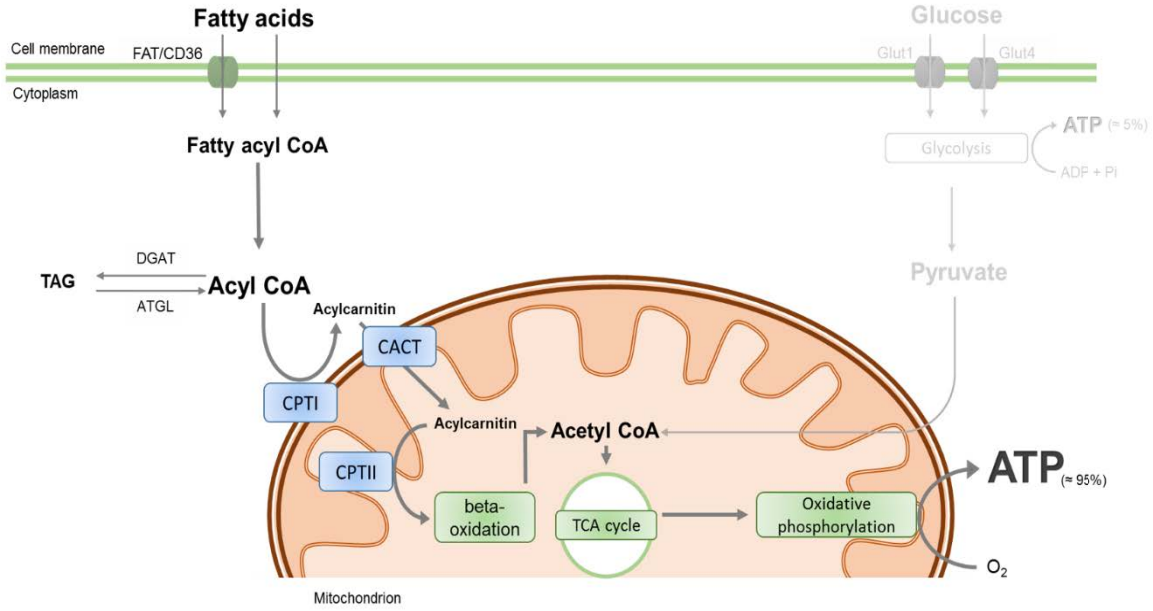

Figure 1.1: Overview of fatty acid metabolism in cardiomyocytes

Fatty acids (FAs) enter the cell via fatty acid translocase (FAT/CD36) and are transformed into acyl-CoA. FAs are then transported into the mitochondria via carnitine-acylcarnitin translocase (CACT)

following the enzymatic transformation into transportable acylcarnitine by carnitine palmitoyltransferase I (CPTI). Once it reaches the mitochondrial lumen, acyl-CoA is reformed by CPTII to fuel beta-oxidation. Acetyl-CoA, the end product of beta-oxidation, subsequently enters the tricarboxylic acid (TCA) cycle and promotes ATP production by electron transport chain (ETC).

1.2.2 Carbohydrate metabolism in the heart

Glucose, and to a lesser extent lactate, are the main carbohydrates utilized by the heart. Circulating glucose can be taken up into cardiomyocytes by specialized glucose transporters: glucose transporter 1 (Glut1) and 4 (Glut4) predominantly (Kraegen *et al.*, 1993). It has been described that the insulin-independent Glut1 is strongly expressed in the fetal heart, whereas the insulin-dependent Glut4 is mainly expressed in the adult heart (Tran *et al.*, 2019). Upon import, glucose is rapidly phosphorylated to glucose-6-phosphate (G6P) by hexokinase. G6P is subsequently processed in multiple metabolic pathways, but the most important route for glucose metabolism in a cell is glycolysis. Glycolysis is highly regulated by enzymes such as 6-phosphofructo-2-kinase (PFK-2), which regulates the activity of the rate-determining enzymes (Kurland *et al.*, 1995). The products of glycolysis are pyruvate, $NADH+H^+$, and ATP. However, ATP from glycolysis only contributes a small portion to the overall amount of ATP produced by the heart. Additionally, pyruvate can also be generated from lactate of different origins: 1) lactate which is transported across the sarcolemma by the monocarboxylate transporter 1 (MCT1), or 2) lactate which was generated from pyruvate catalyzed by lactate dehydrogenase (LDH) due to preferably utilization of FAs. Subsequently, pyruvate is transported into the mitochondria and decarboxylated by pyruvate dehydrogenase (PDH) to produce acetyl-CoA (Patel *et al.*, 2006). The activity of PDH is an important factor regulating the interdependency between FA and carbohydrate metabolism: a reduced PDH activity supports FA oxidation when FA plasma levels are increased and vice versa (Randle, 1986). An increased PHD activity is also mediated by the inhibition of carnitine palmitoyltransferase I (CPTI) which is an important enzyme fueling beta-oxidation (Kerner *et al.*, 1994) to support glucose oxidation. Acetyl-CoA generated from pyruvate enters the TCA cycle in the mitochondria and produces $NADH+H^+$ and FADH2. These reducing equivalents fuel oxidative phosphorylation via ETC to produce ATP (Figure 1.2).

Since the proper function of FA and glucose metabolism and its flexibility are crucial to maintain cardiac performance, it is not only regulated by intrinsic regulatory mechanisms

but also by hormones and signaling molecules secreted by other organs such as insulin released by the endocrine pancreas.

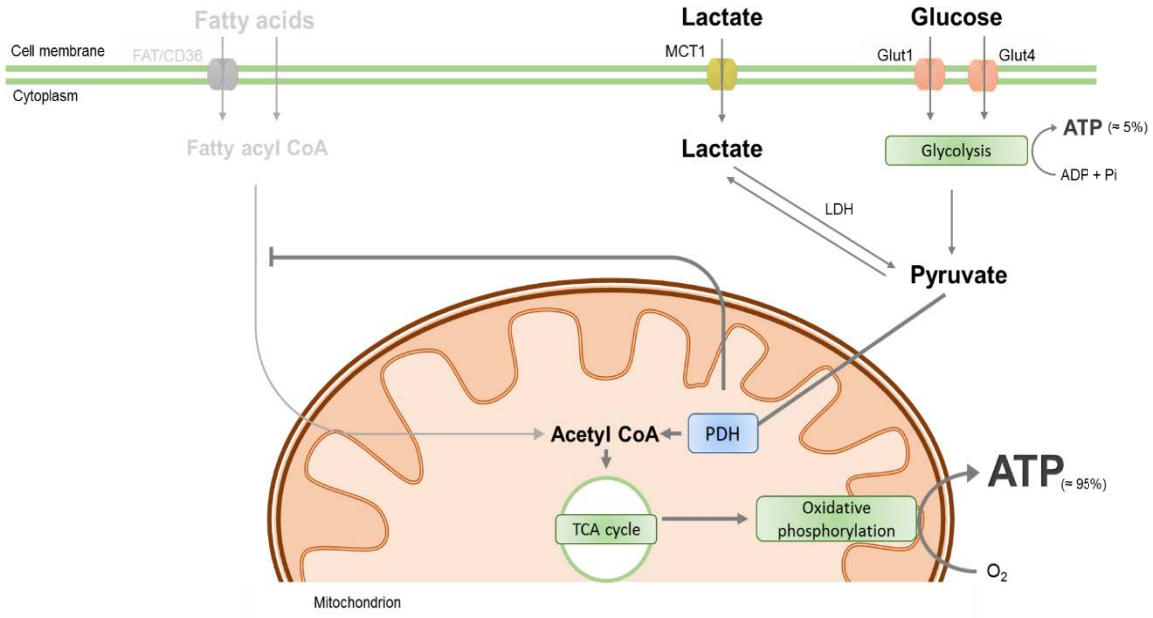

Figure 1.2: Overview of glucose metabolism in cardiomyocytes

To fuel TCA cycle, acetyl-CoA can be generated from carbohydrate sources such as lactate and glucose. Whilst lactate enters the cell via monocarboxylate transporter 1(MCT1), glucose transport is performed by glucose transporter 1 (Glut1) and 4 (Glut4). Both substrates are converted into pyruvate by lactate dehydrogenase (LDH) or glycolysis. Pyruvate then is transported into the mitochondria and transformed to acyl-CoA by pyruvate dehydrogenase (PDH) to fuel TCA cycle.

1.3 Regulation of blood glucose levels by the endocrine pancreas

The pancreas is the major organ regulating blood glucose levels by secreting hormones such as glucagon and insulin. The pancreas secretes a variety of digestive enzymes (exocrine pancreas) and releases blood glucose-regulating hormones to the circulation (endocrine pancreas). The cells regulating blood glucose levels are clustered to so-called pancreatic islets or islets of Langerhans and show an even distribution over the whole pancreas (Ionescu-Tirgoviste *et al.*, 2015). The pancreatic islets mainly consist of alpha-cells (approximately 20%) and beta-cells (approximately 75%), and to a lesser extent of delta-cells (approximately 4%) and PP cells (approximately 1%) (Da Silva Xavier, 2018).

The alpha-cells produce the hormone glucagon for the regulation of glucose storage. Glucagon release is stimulated by a decline in blood glucose, to increase blood glucose levels. The glucagon antagonist insulin is a hormone produced and secreted by beta-cells. It regulates glucose utilization in insulin-dependent tissues such as skeletal muscle, adipose tissue, and the heart. The secretion of insulin is stimulated by a variety of stimuli such as glucose (Grodsky *et al.*, 1963), extracellular Ca^{2+} (Milner *et al.*, 1967), but also cytokines (Nunemaker *et al.*, 2014), and hormones (Drucker, 2013). The released insulin triggers a decrease in blood glucose levels by mediating glucose uptake into the tissue requiring glucose (Betts *et al.*, 2014).

Glucose metabolism is the most important physiological regulator of insulin secretion, gene expression and synthesis. To sense circulating glucose molecules, beta-cells constitutively express the glucose transporter 2 (Glut2) (Guillemain *et al.*, 2000). The absence of Glut2 leads to dysregulated insulin gene expression and secretion (Guillam *et al.*, 1997). Independent of its role in glucose sensing, Glut2 also mediates glucose influx into beta-cells by facilitated diffusion and is the only glucose transporter expressed in beta-cells (Heimberg *et al.*, 1995). The presence of glucose inside beta-cells is the major stimulus for controlling transcription, translation, posttranslational processing and secretion of insulin (Poitout *et al.*, 2006). Rodents have two nonallelic insulin genes (*Ins1* and *Ins2*), which encode for functional insulin proteins (Duvillie *et al.*, 1997; Soares *et al.*, 1985). The *Ins1* gene can compensate for the absence of *Ins2* gene, however not the other way around. Under normal conditions, the Ins2 protein represents the majority of total insulin amount in mice (Leroux *et al.*, 2001).

1.3.1 Regulation of insulin biosynthesis and secretion

Insulin is exclusively expressed in pancreatic beta-cells (Melloul *et al.*, 2002). Its transcriptional regulation gives beta-cells the ability to quickly respond to cellular stimuli. A unique combination of transcription factors synergistically activates insulin transcription. This allows beta-cells to respond to external stimuli by regulating the transcriptional response through more than one pathway (Hay *et al.*, 2006). The transcription factor pancreatic duodenal homeobox-1 (PDX1) was described to be a key player in regulating insulin gene transcription (Wright *et al.*, 1989) whose activity is modulated by several

external stimuli including glucose. Additionally, expression level of the co-transcription factor Pgc1-α has also been linked to efficient insulin secretion (Oropeza *et al.*, 2015).

In response to glucose, beta-cells increase their rate of insulin translation, which is at least partly controlled by dephosphorylation of the eukaryotic initiation factor 2a (eIF2a) mediated by protein phosphatase 1 (PP1) (Vander Mierde *et al.*, 2007). In turn, downregulation of insulin synthesis was described to be mediated by phosphorylation of eIF2a via pancreatic ER kinase (PERK) (Shi *et al.*, 1998).

Additionally, insulin is also known to undergo a number of posttranslational modifications. The insulin gene encodes for a precursor protein known as preproinsulin, which is translocated across the rough endoplasmic reticulum (ER) membrane into the lumen, where it is cleaved to generate proinsulin (Patzelt *et al.*, 1978). Proinsulin then is folded and transported from ER to the golgi apparatus, where it enters immature secretory vesicles and is then cleaved to insulin and C-peptide ready for secretion when required (Steiner, 2008). Glucose-triggered insulin secretion is induced by a closure of K_{ATP} channels. This results in an opening of plasma membrane Ca^{2+} channels leading to an elevation of intracellular Ca^{2+} mediating exocytosis of insulin vesicles. Also other activators such as the signaling molecule cAMP are important for potentiating insulin secretion (Prentki *et al.*, 1987). Insulin release is also modified by additional regulatory mechanisms mediated via circulating cytokines or hormones. Gastrointestinal cells for example release circulating peptide hormones following ingestion of a meal and thereby stimulate insulin secretion (Drucker, 2013). Additionally, various proinflammatory cytokines such as interleukin -1β (IL-1β), interleukin-6 (IL-6) (O'Neill *et al.*, 2013), C-X-C ligand motif 1 (Cxcl1) and C-X-C ligand motif 5 (Cxcl5) promote insulin secretion in beta-cells (Nunemaker *et al.*, 2014). However, these cytokines were also described to promote beta-cell dysfunction in connection with an insulin resistance in patients establishing type 2 diabetes (T2D).

Insulin itself has also been reported to have a negative regulatory feedback on its own secretion (Ammon *et al.*, 1991), expression (Koranyi *et al.*, 1992) and synthesis (Rutter, 1999).

Taken together, insulin is widely regulated on all levels, but many regulating mechanisms are still unclear. The complexity of how regulating factors interact with beta-cells makes it difficult to understand which parameters determine their action (Fridlyand *et al.*, 2016).

1.4 Insulin signaling pathways in the heart

Secreted insulin is transported by the circulation to reach insulin-responsive tissues. It increases glucose uptake in various organs including the heart. Insulin mediates its action by binding to the insulin receptor (IR). IR is a transmembrane receptor present on the surface of insulin-responsive cells such as cardiomyocytes, and belongs to the family of tyrosine kinase receptors (Ward *et al.*, 2009). Upon ligand binding insulin receptor undergoes conformational change leading to autophosphorylation at tyrosine residues of IR. This activation then triggers autophosphorylation leading to recruitment and phosphorylation of the insulin receptor substrate (IRS) on serine residues. There are two abundant isoforms expressed in the heart: IRS1 and IRS2. Both are major mediators of insulin action in the heart (Qi *et al.*, 2013). An important downstream signaling cascade of IRS1 and 2 includes the activation of phosphoinositide 3-kinase (PI3K). This results in 3-phosphoinositide-dependent protein kinase 1 (PDK1)-mediated phosphorylation of Akt (or protein kinase B (PKB)) at threonine 308 (Alessi *et al.*, 1997) and mTOR complex 2 (mTORC2)-mediated phosphorylation of Akt at serine 473 (Sarbassov *et al.*, 2005). The heart is known to express two isoforms of Akt: 1 and 2 (for detailed information on Akt signaling in the heart see section 1.5). Most likely, the Akt2 isoform phosphorylates the Akt substrate 160 (AS160) at threonine 642 (Peck *et al.*, 2009) mediating glucose transporter 4 (Glut4) translocation to the plasma membrane to increase glucose uptake (Figure 1.3). In addition, insulin also initiates the activation of mitogen-activated protein kinase (MAPK) and extracellular regulated kinase (ERK) signaling to mediate transcriptional regulation of genes involved in cellular differentiation and proliferation (Boulton *et al.*, 1991). Besides reducing blood glucose levels insulin is also important to stimulate glycolysis by increasing hexokinase and PFK-2 activity and thus, the breakdown of carbon sources to generate ATP (Wu *et al.*, 2004). Additionally, insulin also promotes glycogen synthesis by inactivating the inhibitory effect of Gsk3-β on glycogen synthase, which then catalyzes conversion of glucose into glycogen (Embi *et al.*, 1980). Moreover, insulin promotes the transport of FAs from the circulation into the cytosol by mediating increased presence of FAT/CD36 in the plasma membrane (Figure 1.3) and stimulating triacylglycerol synthesis. Insulin also increases protein synthesis and in turn decreases protein degradation.

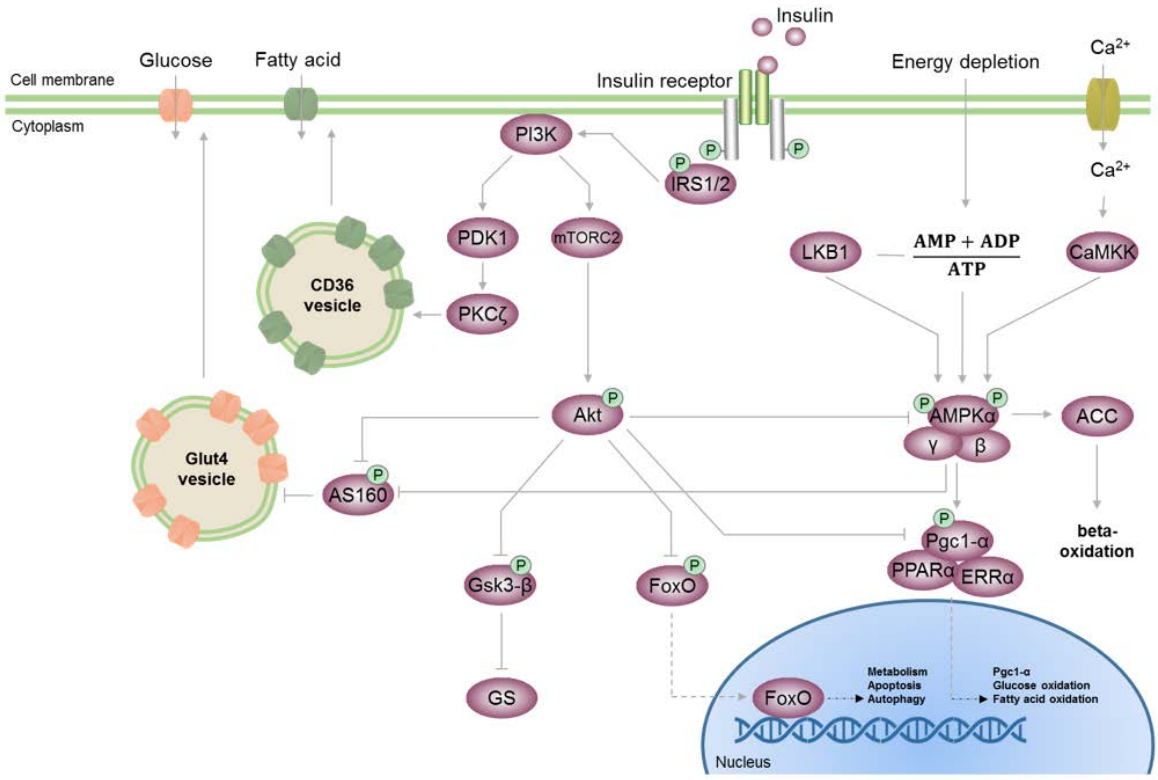

Figure 1.3: Schematic of insulin, Akt and AMPKα signaling pathway in metabolic regulations

Insulin mediates its action through insulin receptor substrates 1 and 2 (IRS1/2) and phosphoinositide 3-kinase (PI3K). PI3K mediates activation of PI3K-dependent kinase 1 (PDK1) and mTOR complex 2 (mTORC2). Subsequently, PDK1 initiates fatty acid translocase (FAT/CD36) and mTORC2 mediates glucose transporter 4 (Glut4) translocation by inhibition of Akt substrate 160 (AS160). Akt inhibits glycogen synthase kinase 3-β (Gsk3-β) to activate the glycogen synthases (GS) and the transcription factor forkhead box protein O (FoxO). The activation of AMP-mediated protein kinase α (AMPKα) is mediated by ATP or AMP/ATP ratio or two upstream kinases: Liver kinase b1 (LKB1) and Ca^{2+}/Calmodulin-dependent protein kinase kinase (CaMKK). AMPKα signaling can be inhibited by Akt activation. CaMKK activates AMPKα in response to increased intracellular Ca^{2+} concentrations. AMPKα mediates Glut4 translocation via inhibition of AS160 and also promotes beta-oxidation by inhibiting Actyl-CoA carboxylase (ACC). AMPKα activity also activates peroxisome proliferator-activated receptor gamma coactivator 1-α (Pgc1-α), which together with peroxisome proliferator-activated receptors (PPARγ) and estrogen related receptor α (ERRα) increases transcription of genes involved in glucose and FA oxidation.

1.4.1 Role of insulin signaling in the regulation of substrate uptake in cardiomyocytes

As described earlier, insulin plays a key role in cardiac glucose homeostasis by mediating translocation of Glut4 from storage vesicles to the plasma membrane to promote glucose uptake. Cardiomyocytes also express the insulin independent Glut1 (Kraegen *et al.*, 1993), which is required for basal glucose uptake. Under non-stressed conditions, glucose transport

proteins are slowly recycled between the plasma membrane and the cytosol. Under stress conditions insulin rapidly mediates translocation of intracellular Glut4 containing vesicles to the plasma membrane. This transportation was described as a multiple-step process. The primary recruitment of Glut4 is mediated via PI3K/Akt2 signaling and AS160 phosphorylation (Peck *et al.*, 2009). Insulin-stimulated Akt2 suppresses the Rab-GAP activity of AS160 localized at the storage vesicles by phosphorylating threonine 642 and thus promoting exocytosis (Figure 1.3) (Ramm *et al.*, 2006). The following trafficking and docking are influenced by insulin-regulated proteins, which control the actin dynamics to regulate Glut4 translocation (Hoffman *et al.*, 2011). This process also involves the modulation of actin filaments and snap receptor (SNARE) proteins to guide vesicles to the plasma membrane, known as vesicle- and target- SNAREs (vSNARE and tSNARE respectively) and small GTPases of the Rab family. The SNARE-mediated docking machinery for insulin-mediated Glut4 translocation involves tSNARES such as syntaxin 4 and synaptosomal-associated protein 23 (SNAP 23) and vSNARES such as vesicle-associated membrane protein 2 (VAMP2) (Bryant *et al.*, 2011). All SNARE complexes are highly regulated by members of the Sec1/Munc18-like (SM) family. It has been recently shown that insulin dependent Glut4 vesicle fusion with the plasma membrane is mediated by Munc18c (Oh *et al.*, 2005). Munc18c binds syntaxin4, and upon insulin dependent tyrosine phosphorylation of Munc18c the Munc18c/syntaxin4 complex dissociates. This promotes vesicle fusion with the plasma membrane (Ke *et al.*, 2007). Moreover, also insulin-independent Akt phosphorylation may be sufficient to stimulate Glut4 translocation (Ng *et al.*, 2008). However, the exact regulation of Glut4 translocation has not been fully described.

FA metabolism is also acutely modified by insulin signaling. The transmembrane uptake of FAs is mediated at least in part by the membrane translocation of fatty acid translocase (FAT/CD36), which shows similarities to the translocation of Glut4. Translocation of FAT/CD36 initiates increased FA uptake to fuel FA oxidation, but also lipid synthesis and storage (Glatz *et al.*, 2010). Insulin mediates PI3K activation resulting in increased FAT/CD36 exposure on the cell surface (Luiken *et al.*, 2002). Furthermore, it also rapidly upregulates FAT/CD36 expression in the heart in time- and dose- dependent manner via PI3K signaling pathway (Chabowski *et al.*, 2004). However, downstream of PI3K, PKC-ζ but not Akt activation drives translocation of FAT/CD36 (Luiken *et al.*, 2009) (Figure 1.3).

1.5 AKT signaling in the heart

As mentioned in section 1.4, insulin and Akt signaling are tightly connected. Akt is a serine/threonine kinase and gets activated in response to insulin binding to the insulin receptor via activation of PI3K. There are two isoforms of Akt (Akt1 and Akt2) expressed in the heart mediating a variety of cellular processes by phosphorylating proteins. Akt1 is the most important isoform in the heart which regulates somatic growth (Cho *et al.*, 2001b). Its short-term activation is cardio protective by promoting physiological hypertrophy (Shiojima *et al.*, 2002). However, long term activation was described to induce pathological hypertrophy (Kemi *et al.*, 2008). Akt2 is required for mediating insulin-stimulated glucose uptake and oxidation, independent of Akt1 (DeBosch *et al.*, 2006). Mice lacking Akt2 exhibit a reduced ability to respond to insulin, showing its essential role in maintaining normal glucose homeostasis (Cho *et al.*, 2001a).

One downstream target of Akt is AS160, which is involved in Glut4 translocation (see section 1.4.1). Other actions of Akt involves phosphorylation of inhibitors mediating autophagy and phosphorylation of members of the forkhead transcription factor (FoxO) family. FoxO activation leads to inhibition of promotors expressing pro-apoptotic signaling molecules. Akt mediates phosphorylation of FoxO1 at serine 253, inhibits its nuclear translocation and therefore its transcriptional activity (Riehle *et al.*, 2014). Additionally, Akt also phosphorylates and thus inhibits Gsk3-β at serine 9 to promote glycogen synthesis. Interestingly, Akt-mediated inhibition of Gsk3-β was shown to promote cardiac hypertrophy (Hardt *et al.*, 2002). Akt signaling may also promote attenuation of FA oxidation through the reduced activity of peroxisome proliferator-activated receptor γ (PPARγ) and the peroxisome proliferator-activated receptor γ coactivator- α (Pgc1-α) (Li *et al.*, 2007) (Figure 1.3).

1.6 AMP-activated kinase (AMPK) signaling in the heart

The AMP-activated kinase (AMPK) is another protein kinase that plays a crucial role in maintaining cellular energy homeostasis. It acts as a cellular energy sensor and thus, is activated in response to energy depletion. AMPK is a ubiquitously expressed serine/threonine kinase consisting of three subunits: a catalytic α-subunit, a scaffolding β-subunit and a regulatory γ-subunit. A reduced ratio of cellular ATP/AMP or ATP/ADP is a

signal for metabolic stress and low energy levels, and therefore initiates the allosteric activation of AMPKα. Binding of cellular AMP or ADP at the AMPKγ subunit triggers a conformational change (Xiao *et al.*, 2013) and facilitates the phosphorylation at threonine 172 within the AMPKα subunit (Gowans *et al.*, 2013; Hawley *et al.*, 1996). Phosphorylation of AMPKα at threonine 172, and therefore its activation, can also be mediated by two upstream kinases: the liver kinase b1 (LKB1) and the Ca^{2+}/Calmodulin-dependent protein kinase β (CaMKKβ); with LKB1 as the main upstream kinase in cardiomyocytes (Li *et al.*, 2019). Activation of LKB1 is controlled by a phosphorylation-independent allosteric process in response to cellular energy stress (Zeqiraj *et al.*, 2009). CaMKKβ activates AMPKα in response to increased intracellular Ca^{2+} and without any dependence on ATP/AMP or ATP/ADP levels (Woods *et al.*, 2005). Once activated, AMPKα rapidly promotes glucose uptake by mediating Glut4 translocation via AS160 phosphorylation (Kramer *et al.*, 2006), and slows down the endocytosis of Glut4 to keep the transporter exposed on the cell surface (Yang *et al.*, 2005). In addition, AMPK activates catabolic reactions such as glycolysis and oxidative phosphorylation to produce ATP, and attenuates biosynthetic pathways consuming ATP (Hardie *et al.*, 2003). Activation of AMPK also promotes FA uptake by an increased rate of FAT/CD36 translocation. Furthermore, it inhibits acetyl-CoA carboxylase (ACC) by phosphorylation. ACC catalyzes the production of malonyl-CoA, which is an inhibitor of CPTI. As mentioned above, CPTI catalyzes an essential step in the movement of FAs from the cytosol into the intermembrane space of mitochondria. Hence, AMPK-mediated ACC inhibition increases CPTI activity and the translocation of FAs across the mitochondrial membrane to fuel beta-oxidation (Dyck *et al.*, 2006). AMPK also directly phosphorylates the co-transcription factor Pgc1-α at serine residue 538 and threonine residue 177 (Fernandez-Marcos *et al.*, 2011), which activates PPARγ and ERRα and thus their transcriptional activation (Handschin *et al.*, 2006). Importantly, the activation of AMPK under stress conditions has been described to have a protective function in the cardiovascular system (Kim *et al.*, 2011; Miller *et al.*, 2008; Russell *et al.*, 2004) and might attenuate the progression of HF (Shibata *et al.*, 2004).

1.7 Cardiovascular disease and the development of heart failure (HF)

Cardiovascular diseases (CVD) including heart failure are the leading cause of death worldwide. Mortality connected to heart failure has risen and heart failure rates are predicted to increase even more in the future, since the survival rates from other types of CVDs, such as myocardial infarction, improved over the last decades (Metra *et al.*, 2017). The underlying mechanisms for the development of heart failure are diverse and include hypertension, hyperlipidemia, pre-existing or acute events such as coronary artery disease or cardiomyopathies (Mendis *et al.*, 2011). Typical risk factors for heart failure include smoking, diabetes mellitus or lack of exercise. These factors cause a variety of cardiac impairments such as mitochondrial dysfunction or abnormal adrenergic signal transduction (Stanley *et al.*, 2005). These alterations are initially asymptomatic but lead to further worsening of symptoms until patients develop end-stage heart failure. Patients with heart failure have a poor prognosis (Metra *et al.*, 2017). Depending on the study, the 1-year mortality is around 20-30% and 5-year mortality is 45-75% (Bui *et al.*, 2011).

The onset of heart failure is typically preceded by the development of cardiac hypertrophy, which is a **compensatory** response to various stimuli and causes an increased cardiac workload (Figure 1.4). Depending on the strength and duration of the stimuli, cardiac hypertrophy can be classified in physiological and pathological hypertrophy (Shimizu *et al.*, 2016). In general, hypertrophy is characterized by an increased cardiomyocyte size without increasing cell number, leading to thickening of the ventricular wall to maintain cardiac contractility (Grossman *et al.*, 1975).

Physiological hypertrophy is characterized as a reversible process with normal or enhanced contractile function and normal cardiac architecture (Weeks *et al.*, 2011). Pathological hypertrophy, however, is associated with increased cardiomyocyte death and metabolic remodeling, and is characterized by a reduced cardiac function (Lyon *et al.*, 2015). If the initial cardiac stress constantly continues, the compensatory state develops into a **decompensatory** state connected to severely impaired heart function (Figure 1.4). Hallmarks of this state are ventricular dilation and a fall in contractile force, defined by ejection fractions of < 40% (Yancy *et al.*, 2013). This condition is called heart failure with reduced ejection fraction (HFrEF, also referred to as systolic heart failure). This form of heart failure is defined by an enlarged EDV relative to the SV indicating that the LV is dilated. However, nearly half of the patient with heart failure show no changes in ejection

fraction (EF > 50%), which is referred to as heart failure with preserved ejection fraction (HFpEF or diastolic heart failure). In this case, EDV is appropriate for the SV and the LV is not dilated (Borlaug *et al.*, 2011; Iwano *et al.*, 2013).

At the end stage of heart failure, the heart is not able to sufficiently supply organs and tissues with oxygen. The cardiac muscle itself has a low ATP content due to a decreased ability to generate ATP by oxidative metabolism and thus is unable to fuel the contractile work (Ashrafian, 2002; Dzeja *et al.*, 2000).

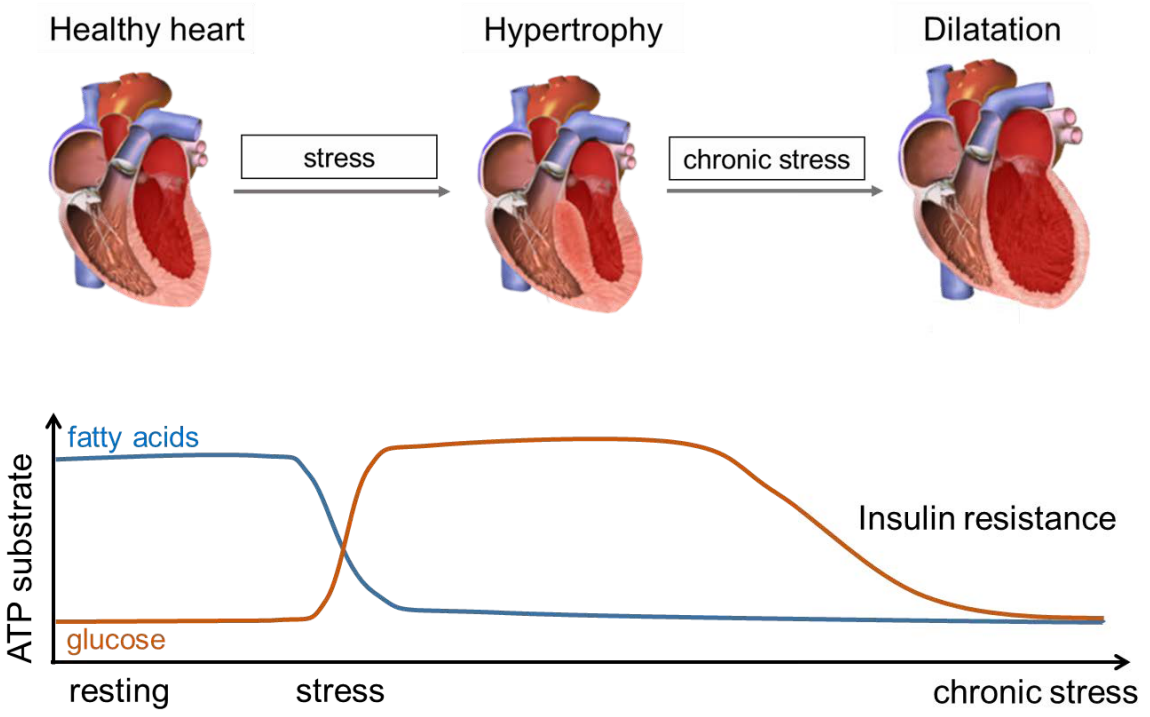

Figure 1.4: Changes in cardiac structure associated with altered substrate utilization in the heart

The upper part shows the progression of a cardiac dilative phenotype. Under stress conditions the heart is capable to thicken the heart muscle compensating for the enhanced workload (cardiac hypertrophy). If the increased workload evolves into chronic stress, the heart develops a left ventricular dilation (decompensatory state), subsequently leading to heart failure. In connection to structural changes the lower part shows substrate preference to generate ATP. The healthy heart prefers fatty acids (FAs) as main substrate under resting conditions. Under stressed conditions, the heart shifts it substrate preference towards glucose. The dilative and decompensatory state is characterized by a permanent shift in metabolism resulting in metabolic inflexibility and energy insufficiency, and is associated with a cardiac insulin resistance.

1.7.1 Metabolic alterations in the failing heart

The early stage of acute heart failure is characterized as compensated hypertrophy with altered cardiac metabolism. One observation is a permanent shift from FA oxidation to glucose utilization (Taegtmeyer, 2002), which is referred to as 'substrate switch'. This was described to cause increased glucose uptake and glycolytic rate and no changes or decreased glucose oxidation. Additionally, the overall FA oxidation is reduced (Allard *et al.*, 1994), possibly resulting in a metabolic inflexibility (Figure 1.5). In addition, massive changes in expression patterns and activities of transcriptional proteins regulating glucose uptake, glycolysis and FA oxidation occur. This, however, leads to strong limitations in acetyl-CoA availability to fuel TCA cycle. In the long run, a reduced mitochondrial oxidative metabolism results in a depletion of energy in the heart (Sorokina *et al.*, 2007). The substrate switch to glucose intends to generate more ATP through oxygen efficient pathways (protective mechanism) but results in an overall lack of ATP (Beer *et al.*, 2002), which is also referred to as metabolic inflexibility (Stanley *et al.*, 2005). This phenotype shows similarities to a fetal like metabolic profile, where glucose is the primary substrate because FA transport is underdeveloped (Bernardo *et al.*, 2010).

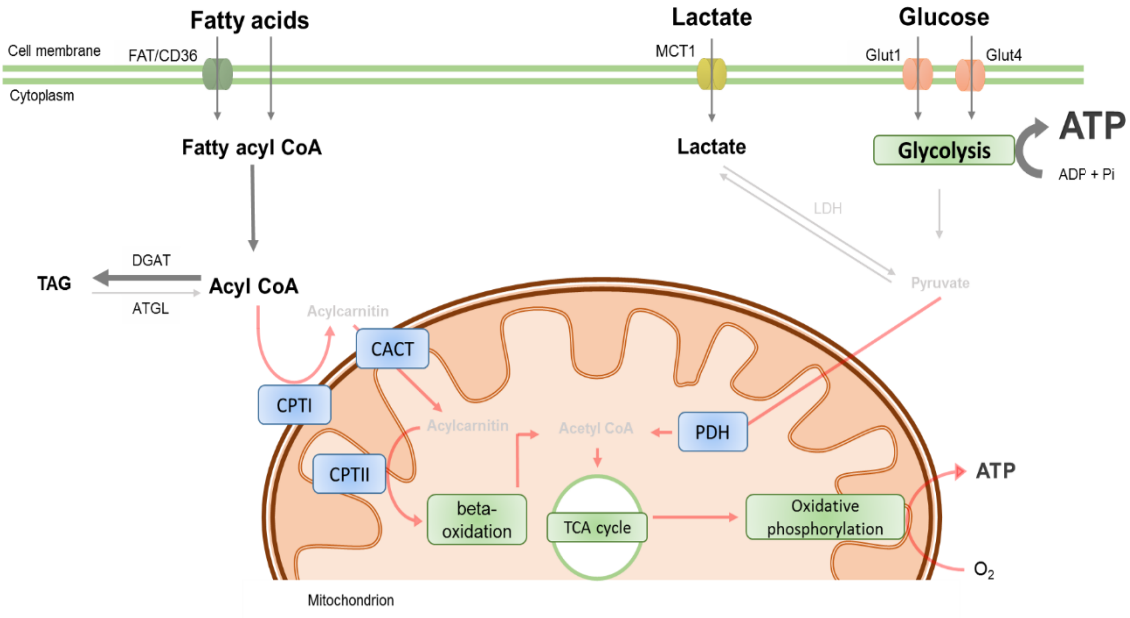

Figure 1.5: Overview of metabolic remodeling in heart failure

During the establishment of heart failure, fatty acid (FA) and glucose oxidation within the mitochondria is disrupted causing a reduced ATP production by oxidative phosphorylation. This is caused by a general lack of the tricarboxylic acid (TCA) cycle substrate acetyl-CoA. Acyl-CoA is

primary converted to triacylglycerol (TAG) catalyzed by diglyceride acyltransferase (DGAT). Glycolysis rate is increased to compensatory produce more ATP. Bold lines represent pathways which are increased in their activity. Thin and red lines indicate for a reduced activity of pathways. Fatty acid translocase (FAT/CD36), monocarboxylate transporter 1 (MCT1), glucose transporter 1 (Glut1) and 4 (Glut4), adipose triglyceride lipase (ATGL), lactate dehydrogenase (LDH), pyruvate dehydrogenase (PDH), carnitine-acylcarnitine translocase (CACT), carnitine palmitoyltransferase I (CPTI) and II (CPTII)

One of the crucial regulators of oxidative metabolism in the heart is the transcriptional co-activator peroxisome proliferator-activated receptor-γ coactivator1-α (Pgc1-α) that mediates the activity of multiple transcription factors (Lehman *et al.*, 2002). Pgc1-α forms a complex with estrogen related receptor α (ERRα) and peroxisome proliferator-activated receptor-γ (PPARγ) to amplify the expression of genes providing mitochondrial function (Liu *et al.*, 2011). In several animal models of cardiac dysfunction reduced *Pgc1*-α expression has been shown to be associated with a metabolic switch from FA oxidation to glycolysis (Arany *et al.*, 2005; Arany *et al.*, 2006; Garnier *et al.*, 2003; Huss *et al.*, 2007; Huss *et al.*, 2005). Additionally, the lack of Pgc1-α specifically in rodents can cause insulin resistance and glucose intolerance in liver (Estall *et al.*, 2009), skeletal muscle (Handschin *et al.*, 2007) or adipose tissue (Kleiner *et al.*, 2012).

Other characteristics of heart failure are insulin resistance, hyperglycemia and hyperinsulinemia, which contribute to cardiac dysfunction. This condition often has been referred to as ‘diabetic cardiomyopathy’ (Rubler *et al.*, 1972). It is associated with impaired mitochondrial oxidative capacity, mitochondrial dysfunction and inflammation (Boudina *et al.*, 2007; Jia *et al.*, 2016). Insulin resistance has often been defined as a reduction in insulin-mediated myocardial glucose uptake. However, the underlying mechanism has not been investigated in detail and is still incompletely understood. One of the key factors of metabolic homeostasis, AMPK, was described to play a protective role in the pathogenesis of heart failure (Li *et al.*, 2019). It helps restoring energy supply by increasing glucose and FA uptake and promoting mitochondrial biogenesis (Handschin *et al.*, 2006; Kramer *et al.*, 2006). Thereby, AMPK activity promotes ATP generation and cardiac contractility. Another group of stress-activated kinases, which are involved in regulating metabolic processes are p38 mitogen-activated protein kinases (MAPK).

1.8 The role of p38 mitogen-activated protein kinase (MAPK) in the heart

Members of the p38 mitogen-activated protein kinases (MAPK) family are stress activated kinases. Four p38 MAPK isoforms have been described: MAPKα (MAPK14), MAPKβ (MAPK11), MAPKγ (MAPK12), MAPKδ (MAPK13). Each isoform has a tissue-specific expression pattern: p38 MAPKα is ubiquitously expressed in many cell types and is highly abundant in the heart (Martin *et al.*, 2015), p38 MAPKβ is highly expressed in brain and lung, p38 MAPKγ is mostly detected in skeletal muscle and cells of the nerve system, and p38 MAPKδ is enriched in uterus and pancreas (Ono *et al.*, 2000). Canonical activation of p38 MAPK isoforms is triggered by different extracellular stimuli such as inflammatory cytokines, TGFβ, heat shock, osmotic shock, and oxidative stress (Martin *et al.*, 2015; Ono *et al.*, 2000). Ligand binding to G-protein-coupled receptors activates MAPK kinase kinases (MKKK) and downstream MAPK kinases (MKK) (Han *et al.*, 1994), such as MKK3, MKK4 and MKK6 (Derijard *et al.*, 1995; Raingeaud *et al.*, 1996). The specific activator of the p38 MAPK isoform depends on the stimulus (Remy *et al.*, 2010). MKKs mediate a dual phosphorylation at threonine 180/tyrosine 182 residues, which triggers a translocation into the nucleus, resulting in activation of transcription factors and subsequently in altered expression of target genes (Figure 1.6). p38 MAPK is inactivated by dephosphorylation and its export to the cytoplasm (Zarubin *et al.*, 2005). Transcription factors targeted by p38 MAPK signaling are for example activating transcription factor 2 (ATF2), myocyte enhancer factor 2 (MEF2), signal transducer and activator of transcription 1 (STAT1) and ETS-like 1 (Elk1) protein regulating diverse functions.

From knockout studies it is known that deficiency of p38 MAPKα isoform in the mouse leads to embryonic death due to impaired placental development (Adams *et al.*, 2000; Allen *et al.*, 2000). *In vitro* inhibition of p38 MAPK or expression of dominant negative mutant p38 MAPK can attenuate cardiomyocyte growth in response to hypertrophic stimuli (Liang *et al.*, 2003). Also, p38 MAPKα activation in cultured cardiomyocytes was shown to be sufficient to induce a hypertrophic response (Nemoto *et al.*, 1998). However, *in vitro* and *in vivo* studies showed different results. Cardiomyocyte specific p38 MAPKα KO mice showed an elevated cardiac hypertrophy in response to pressure overload (Nishida *et al.*, 2004; Zhang *et al.*, 2003). Furthermore, specific deletion of p38 MAPKα in the cardiomyocytes results in enhanced physiological hypertrophy by upregulated Akt activity in response to exercise (Taniike *et al.*, 2008). p38 MAPKα inhibitors have been used in cardiac ischemic

animal models promoting reduction in cardiac injury after myocardial infarction (Behr *et al.*, 2001; Liu *et al.*, 2005; See *et al.*, 2004). This is possibly due to a protective function in the context of fibrosis, because p38 MAPKα KO in cardiac fibroblasts had a positive effect on the outcome after myocardial infarction (Liu *et al.*, 2020; Molkentin *et al.*, 2017). These results show that the role of p38 MAPKα in the heart is still controversially discussed and by far not clear.

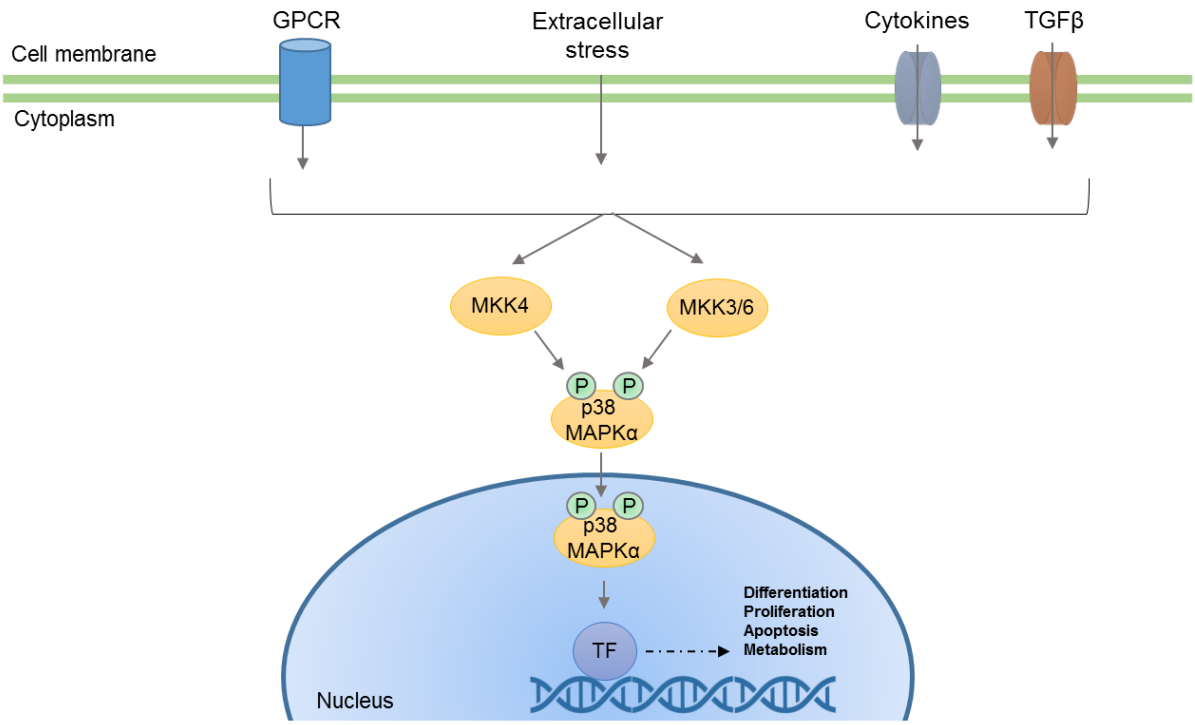

Figure 1.6: Signaling pathways of p38 MAPKα in the heart

The p38 mitogen-activated protein kinase α (MAPKα) signal transduction is triggered by a variety of signals such as extracellular stress, cytokines such as transforming growth factor β (TGFβ) or molecules binding G protein-coupled receptors (GPCR). This leads to the activation of a three-tiered MAPK phosphorylation cascade in which MAPK kinase kinases (MAPKKKs) phosphorylate the p38 MAPK specific MAPK kinase (MKK) 3, MKK4 or MKK6. The dual phosphorylation triggers p38 MAPKα translocation into the nucleus initiating expression of transcription factors involved in differentiation, proliferation, apoptosis and metabolism.

1.8.1 Mouse model of pressure overload-induced heart failure: cardiac specific deletion of p38 MAPKα

The p38 MAPKα is known to be involved in pressure overload induced cardiac reorganization (Bao *et al.*, 2007). However, it still remains unclear if the activity of p38 MAPKα in the heart in response to stress stimuli is beneficial or detrimental in the process of cardiac remodeling. Investigation of the cardiac specific influence of p38 MAPKα signaling under stress conditions was performed by using a mouse model with an inducible cardiomyocyte-specific p38 MAPKα knockout (KO). This mouse model was previously established in our laboratory and is hereafter referred to as iCMp38 MAPKα. To induce the KO, 6-8 week old mice with floxed p38 MAPKα (p38 MAPKα$^{flox/flox}$) gene and expressing the merCremer recombinase under the control of a α-MHC promotor exclusively in cardiomyocytes were injected intraperitoneally for 10 days with tamoxifen. As control (Ctrl), p38 MAPKα$^{flox/flox}$ litter mates without delete were used (see section 3.2). To study the influence of p38 MAPKα deletion under conditions of cardiac pressure overload, mice were exposed to the vasoconstrictor AngII (by osmotic mini pumps). The studies exhibited that within 48 hours of AngII-induced pressure overload, mice developed a strong dilative phenotype with severely impaired cardiac function (Bottermann *et al.*, submitted), without a hypertrophic state in between. This rapidly induced cardiac phenotype suggests a protective role of cardiac p38 MAPKα. Initial analyses of the cardiac tissue showed strong lipid droplet accumulation 48 hours after the onset of AngII treatment, indicating metabolic dysfunction (Figure 1.7).

Furthermore, this mouse model was also used to investigate interorgan communication between the failing heart and skeletal muscle (Leitner *et al.*, 2017) as well as adipose tissue (Bottermann *et al*., submitted). In these studies, iCMp38 MAPKα KO mice were described to induce a skeletal muscle wasting program and increase adipose tissue lipolysis during the establishment of HF.

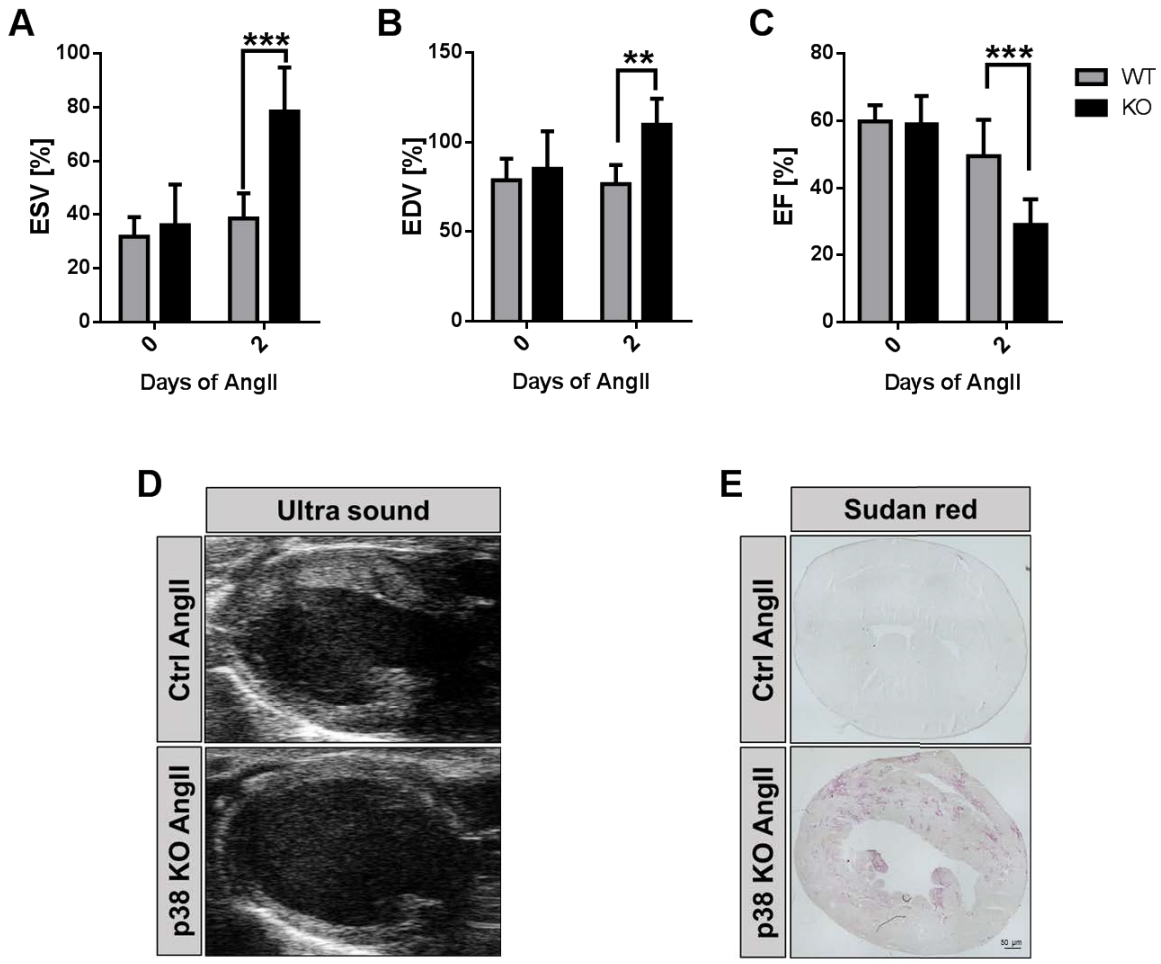

Figure 1.7: Characterization of the AngII-induced pressure overload iCMp38 MAPKα KO mouse model

The cardiac dysfunction was defined by (A) an increased end systolic volume (ESV), (B) an increased end diastolic volume (EDV), and (C) a decreased ejection fraction (EF) in iCMp38 MAPKα KO (black) compared to control (grey) hearts after 48 hours of AngII treatment. Data are presented as mean ±SD, n = 5-15. Statistical significance was calculated using Two-way ANOVA (** p <0.001, *** p <0.001). (D) High resolution ultrasound images of control (upper panel) and iCMp38 MAPKα KO (lower panel) hearts after 48 hours of AngII administration exhibiting left ventricular dilation in iCMp38 MAPKα KO hearts. (E) Histological sections of control (upper panel) and iCMp38 MAPKα KO (lower panel) hearts 48 hours after the onset of AngII exposure showing lipid droplet accumulation within the cardiac muscle of iCMp38 MAPKα KO (stained with sudan red to visualize lipids). Experiments and analysis were performed by Dr. L. Leitner, Dr. K. Bottermann and Dr. V. Oenarto.

1.9 Aim of the project

Heart failure is a complex clinical syndrome and known to be associated with cardiac metabolic remodeling. In patients with heart failure, the hearts show rearrangements in

metabolism which promote metabolic inflexibility promoting resulting in an energy deficit. However, the underlying molecular mechanisms still remain unclear. The cardiomyocyte specific p38 MAPKα KO mouse model described in section 1.8.1 is an interesting, inducible model of heart failure, which was used to investigate metabolic alterations in the early response to pressure overload eventually causing heart failure. The present study analyzed the tasks below.

- Confirmation of the reproducibility and replicability of the iCMp38 MAPKα model was the first task of this thesis. This included the specific induction of the KO in cardiomyocytes and the pressure overload induced dilative cardiac phenotype after 48 hours of AngII treatment.

- The deletion of p38 MAPKα in the heart itself does not exhibit a cardiac dilative phenotype under baseline conditions and metabolic remodeling was hypothesized to occur without primarily affecting cardiac function. Thus, the second task of this work was to investigate metabolic processes in iCMp38 MAPKα focusing on both baseline and AngII treated condition. This included analyses of substrate preference and insulin sensitivity. To further investigate the underlying mechanisms, signaling transduction pathways such as insulin, Akt and AMPK signaling which could be influenced by the loss of p38 MAPKα were analyzed.

- The third task was to characterize cardiac proteins involved in metabolic processes on transcriptional and translational levels under baseline conditions and AngII conditions and to analyze alterations in protein levels or activity.

- Lastly, not only the heart itself but also the interorgan communication is an important feature during the establishment of heart failure. Since iCMp38 MAPKα KO mice already showed cross organ communication with adipose tissue and skeletal muscle, relevant tissues associated with metabolic homeostasis should also be analyzed. Regarding this, the pancreas, as an important regulator of maintaining metabolic processes, was also be investigated in this work.

In summary, in this study a better understanding of the different regulatory mechanisms controlling p38 MAPKα under conditions of AngII-induced pressure overload should be investigated. This could be helpful to target metabolic alteration to attenuate heart failure development in animal models and offers the opportunity to translate these approaches to patients suffering from heart failure.

2 Materials

2.1 Laboratory equipment

Device	**Manufacturer (*Product name*)**
Autoclave maschine	Systec (*Vx-100*)
Centrifuges	Eppendorf (*5415R*), Eppendorf (*5402*), VWR (*Mega Star 1.6R*), Labnet (*Spectrafuge Mini Centrifuge*), Roth (*Rotilabo*)
Fluoresence microscope	Keyence (*BZ 9000*)
Freezer (-20°C)	Liebherr (*GN 5215*)
Freezer (ultra-low temperature)	Thermo Scientific (*Revco UxF*)
Fridge	Liebherr (*Gkv 4310*)
Homogenizer	Qiagen (*TissueRuptor II*)
Ice Maschine	Ziegra (*ZBE 110-35P*)
Incubator	Heraeus (*B6120*), Infors HAT (*Ecotron*)
Light microscope	Leica (*M60*)
Liquid nitrogen tanks	Cryothem (*Apollo*)
Magnetic stirrer	Heidolph (*MR3001*)
PCR plate centrifuge	VWR (*521-1648E*)
Photometer	Bio-Rad (*iMark, Microplate Absorbance Reader*)
Pipettes	Gilson (*Pipetman 10-1000 µL*)
Power Blotter	Thermo Scientific (*Pierce^{TM} G2 Fast Blotter*)
Real Time PCR System	Applied Biosystems (*StepOnePlus*)
Scintillation counter	Beckman Coulter (*LS6500*)
Spectrophotometer	Peqlab (*Nanodrop ND-1000 Spectrometer*)

Test Tube shaker	Heidolph (*Relax top*)
Thermomixer	Eppendorf (*Thermomixer comfort*)
Ultracentrifuge	Thermo Scientific (*Mx120*)
Ultrasound bath	Elma Transsonic (*TS540*)
Ultrasound device	VisualSonic (*Vevo 2100 Imaging System*)
Vaporizer	VetEquip (*Isofluorane vaporizer*)
Water purification system	Merck Millipore (*MilliQ*)

2.2 General chemicals, enzymes and buffer

Chemical	**Manufacturer (*Cat No.*)**
2-propanol	Merck (*#101040*)
4-OH Tamoxifen	Sigma (*#H6278*)
Angiotensin II, human	Sigma (*#A9525*)
β-Mercaptoethanol	Sigma (*#M7522*)
Bromphenol blue	Roth (*#A5121*)
Butanol	Roth (*#7724*)
D-Glucose	Sigma (*#G7528*)
Ethanol, 99%	Roth (*#9065.3*)
Insulin, human	Lilly France S.A.S. (*40 i.E./mL*)
Isoflurane	Piramal (*#66794-017-25*)
Magnesium chloride	Roth (*#2189.2*)
Phosphatase Protease Inhibitor Cocktail	Thermo Scientific (*#78442*)
Peanut oil	Sigma (*#P2144*)
Perchloric acid	Sigma (*#311521*)
Triton X-100	Sigma (*#T8787*)
Tween 20	Merck (*#822.184*)

Enzyme	**Manufacturer (*Cat No.*)**
DNAse (RNAse free Set)	Qiagen (*#79254*)
Liberase	Sigma (*#5401020001*)
Proteinase K	Sigma (*#P6556*)
Restriction Enzymes	New England Biolabs
Taq DNA Polymerase	Qiagen (*#201203*)

Buffer	**Ingredients (*Concentration*)**
Phosphate-buffered saline (PBS), pH 7.4	NaCl (*137 mM*), KCl (*2.7 mM*), Na_2PO_4*$2H_2O$ (*8.1 mM*), KH_2PO_4 (*1.76 mM*)
Lysis buffer, pH 7.4	Tris HCl pH 7.4 (*10 mM*), NaCl (*100 mM*), IGEPAL (*1%*), Phosphatase/protease inhibitor (1:100)
Fractionation buffer	Tris HCl (*10 mM*), NaCl (*10 mM*), $MgCl_2$ (*0.5 mM*), Phosphatase/protease inhibitor (1:100)
4x Lämmli buffer	Tris-HCl pH 6.8 (*250 mM*), Glycerol (*25% v/v*), SDS (*8% w/v*), Bromphenol blue (*0.005% w/v*), DTT (*100 mM*)
SDS running buffer	Tris (*25 mM*), Glycin (*250 mM*), SDS (*0.1% w/v*)
Anode buffer, pH 8.8	Tris HCl (*300 mM*), Tricine (*100 mM*)
Cathode buffer, pH 8.7	Tris HCl (*30 mM*), Aminocaproic acid (*300 mM*)
Tris-buffered saline (TBS), pH 7.5	Tris-Cl (*50 mM*), NaCl (*150 mM*)
Tris-buffered saline +Tween (TBS-T)	Tris-Cl (*50 mM*), NaCl (*150 mM*), Tween 20 (*0.1%*)

2.3 Antibodies

Primary antibodies	**Manufacturer (*Cat No.*)**
Mouse anti-Akt(pan)	Cell signaling (*2966*)
Mouse anti-Akt1	Cell signaling (*2967*)
Rabbit anti-Akt1^{S473}	Cell signaling (*9018*)
Mouse anti-Akt2	Cell signaling (*5239*)
Rabbit anti-Akt2^{S474}	Cell signaling (*8599*)
Rabbit anti-Akt^{S473}	Cell signaling (*4060*)
Rabbit anti-Akt^{T308}	Cell signaling (*4056*)
Mouse anti-AMPKα	Cell signaling (*2793*)
Rabbit anti-AMPKα^{S485}	Cell signaling (*4184*)
Rabbit anti-AMPKα^{T172}	Cell signaling (*2535*)
Rabbit anti-AS160	Millipore (*07-741*)
Rabbit anti-AS160^{T642}	Cell signaling (*4288*)
Rabbit anti-ATP-Synthase	Proteintech (*14676*)
Mouse anti-Caveolin3	BD (*610420*)
Rabbit anti-Glut1	Abcam (*ab652*)
Rabbit anti-Glut2	Abcam (*ab192599*)
Rabbit anti-Glut4	Abcam (*ab654*)
Rabbit anti-Gsk3-β	Cell signaling (*9315*)
Mouse anti-Gsk3-β^{S9}	Cell Signaling (*14630*)
Mouse anti-Insulin	Cell signaling (*8138*)
Rabbit anti-Na^+/K^+-ATPase	Cell signaling (*3010*)
Mouse anti-p38 MAPKα	Cell signaling (*9212*)
Rabbit anti-p38 MAPKα$^{T180/Y182}$	Cell signaling (*9216*)
Rabbit anti-Pgc1-α	Proteintech (*20658*)

Secondary antibodies	**Manufacturer (*Cat No.)***
IRDye 800CW Goat anti-Mouse IgG	LI-COR (*925-32210*)
IRDye 800CW Goat anti-Rabbit IgG	LI-COR (*925-32211*)
IRDye 680RD Goat anti-Mouse IgG	Li-COR (*925-68070*)
IRDye 680RD Goat anti-Rabbit IgG	LI-COR (*925-68071*)

2.4 Kits

Name	**Manufacturer (*Cat No.*)**
Insulin (Mouse) ELISA	DRG (*EIA-3439*)
Insulin (Mouse) ELISA ultrasensitive	DRG (*EIA-3440*)
Maxima SYBR Green/ROX qPCR	Thermo Scientific (*K0221*)
Pierce BCA Protein Assay Kit	Thermo Scientific (*23225*)
QuantiTect Reverse Transcription Kit	Qiagen (*205311*)
RNeasy Fibrous Tissue Kit	Qiagen (*74704*)
RNeasy Lipid Tissue Kit	Qiagen (*74804*)
Ultra-Sensitive Mouse Insulin ELISA Kit	Crystal Chem (*90080*)

2.5 qRT-PCR Primers

All primers for gene expression analysis were predesigned by *Sigma-Aldrich* and primer pairs were ordered from *KiCqStart Primers*.

Gene name	**Sequence**
ACC	Forward 5‘-CTGTATGAGAAAGGCTATGTG-3‘ Reverse 5‘-AACCTGTCTGAAGAGGTTAG-3
Acsl1	Forward 5‘-GGAAATCATCAGCCTCAAAG-3‘

	Reverse 5‘-GATGAATGCACTCTCTGTTG-3
CD36	Forward 5‘-GACATTTGCAGGTCTATCTAC-3‘
	Reverse 5‘-TTTCAGTGCAGAAACAATGG-3
CPTIb	Forward 5‘-ACTAACTATGTGAGTGACTGG-3‘
	Reverse 5‘-TGGCATAATAGTTGCTGTTC-3
CPTIc	Forward 5‘-CAAATGACTTCCTGAGGTTG-3‘
	Reverse 5‘-GTGACGTACAGAAAATCCATC-3
CPTII	Forward 5‘-ACCATGAAGAGATACCTCAG-3‘
	Reverse 5‘-CTTACACAACACTTCTGTCTTC-3
DGAT1	Forward 5‘-ACCTACCGAGATCTCTATTAC-3‘
	Reverse 5‘-CATGGAGTTCTGGATAGTAGG-3
Ins1	Forward 5‘-GAGGTACTTTGGACTATAAAGC-3‘
	Reverse 5‘-TTGAAACAATGACCTGCTTG-3‘
Ins2	Forward 5‘-AGCAGGAAGGTTATTGTTTC-3‘
	Reverse 5‘-ACATGGGTGTGTAGAAGAAG-3‘
PDK4	Forward 5‘-ACAATCAAGATTTCTGACCG-3‘
	Reverse 5‘-TCTCCTTGAAAATACTTGGC-3
Pgc1-α	Forward 5‘-TCCTCTTCAAGATCCTGTTAC-3‘
	Reverse 5‘-CACATACAAGGGAGAATTGC-3‘
PPARγ	Forward 5‘-GATGTCACACAATGCAATTC-3‘
	Reverse 5‘-CAGTTTCCGAATCTTTCAGG-3
Slc2a1	Forward 5‘-AAGTCCAGGAGGATATTCAG-3‘
	Reverse 5‘-CTACAGTGTGGAGATAGGAG-3‘
Slc2a4	Forward 5‘-CAATGGTTGGGAAGGAAAAG-3‘
	Reverse 5‘-AATGAGTATCTCAGGAGGC-3‘

3 Methods

3.1 Animal husbandry

All mice (*Mus musculus*) used in this study were housed under controlled temperature (22°C) and lighting (12 h/12 h dark-light cycle) with free access to water and standard mouse diet. All animal experiments followed the guidelines of National Institutes of Health (NIH) and were performed in accordance to national statutory regulations for animal research. All procedures were approved by the local animal care and use committee (LANUV, Recklinghausen, Licence no. AZ: 84-02.04.2014.A220 and 84-02.04.2014.A308).

3.2 Mouse strains and inducible gene knockouts

All used mice were male and of an inbred C57BL/6J mouse line background. Mutant mice were generated by crossbreeding C57BL/6J mice homozygously expressing floxed target gene with C57BL/6J mouse line expressing tamoxifen-inducible Cre-recombinase (merCremer) specifically in cardiomyocytes under the control of α-MHC promotor (Sohal *et al.*, 2001; Verrou *et al.*, 1999). The Cre-Lox recombination has been used to generate targeted DNA rearrangements in mice for decades. Therefore, transgenic mice expressing a fusion protein consisting of the Cre recombinase and a mutant of the human estrogen receptor ligand binding domain (merCremer) were used (Feil *et al.*, 1996). The expression of the Cre-fusion protein is controlled by the α-MHC promotor which is exclusively active in cardiomyocytes (Sohal *et al.*, 2001). Nuclear localization of Cre was induced by 4-hydroxytamoxifen (OH-Tx), which functions as a ligand of the merCremer. Subsequently, Cre recombinase efficiently excises DNA section flanked by loxP recognition sites (Feil *et al.*, 1997; Lakso *et al.*, 1992; Orban *et al.*, 1992). In the present study mice were injected intraperitoneally (i.p.) with 500 µg OH-Tx (5 mg/mL in peanut oil) with a 23 G needle (*B. Braun Melsungen AG*, Cat No. #4657640) followed by a prior defined recovery time, to

ensure a successful knockout and to exclude side effects of OH-Tx injections. As control animals (Ctrl) floxed littermates equally injected with OH-Tx were used.

Mutant mouse lines:

3.2.1 $p38^{flox/flox}$ male mice (exon 2 and 3) (Ventura *et al.*, 2007) were crossbred with α-MHC merCremer deleter mice. 6-8 week old mice were injected (i.p.) 10 consecutive days with OH-Tx to generate cardiomyocyte specific p38 MAPKα knockout (iCMp38 MAPKα KO) followed by 4 weeks of recovery time.

3.2.2 $Akt1^{flox/flox}$ and $Akt2^{flox/flox}$ male mice (Akt1 exon 6 and 7, Akt2 exon 5 and 6) were crossbred with α-MHC merCremer deleter mice. 12 week old mice were injected i.p. 5 consecutive days with OH-Tx to generate cardiomyocyte specific Akt1 and Akt2 double knockout (iCMAkt1/2 KO) followed by 7 days of recovery time

The genotypes of the mice were determined by tissue biopsies (about 3 weeks after birth, after separated from mother) and subsequent DNA analysis by PCR using different allele specific primers.

3.3 DNA analysis and genotyping

3.3.1 DNA isolation

Genomic DNA was isolated from tail tips (three weeks old mice). Tissues were digested using Phire Animal Tissue Direct PCR Kit (Thermo Scientific *#F-140WH*) according to the manufacturer's protocol. Purified DNA can be stored up to 4 weeks at 4°C or longer at -20°C.

3.3.2 Polymerase chain reaction (PCR)

PCR was performed using qTower from Analytik Jena and processed with Maxima SYBR Green/Rox qPCR Master Mix (2x) in accordance with manufacturer's protocol. The reaction master mix was prepared by adding the components (except template DNA, see Table 3.1) at room temperature, mixed thoroughly and dispensed appropriate volume into 96-well plate (Thermo Scientific *#AB0800*). Next, template DNA was added to wells containing master mix and plate was covered with sealing film (BioRad *#MSB1001*).

Table 3.1: List of content (per reaction) and primers used for PCR experiments determine the genotype of the mice

Reagents	**Volume (*Concentration*)**
PCR master mix:	
Maxima SYBR Green Mix (2x)	12.5 µL
Primer (Fwd)	0.13 µL (10 µM)
Primer (Rev)	0.13 µL (10 µM)
ddH_2O	11.3 µL
template DNA	1 µL (≤ 500 ng per reaction)
	reaction volume: 25 µL
Primers	
p38 MAPKα	Forward 5‘-CTACAGAATGCACCTCGGATG-3‘ Reverse 5‘-AGAAGGCTGGATTTGCACAAG-3‘
Akt1	Forward 5‘-CTGGCTTCCTGTATGGGTCTGGGTAC-3‘ Reverse 5‘-CCAACAGCAAGAGAGCTGGCCACAA-3‘
Akt2	Forward 5‘-TGGCTTCTCCAGCAGCACCTCTT-3‘ Reverse 5‘-GAAGATTTGTTTAAGGCTCTTGAGACT-3‘
merCremer	Forward 5‘-CCCACCAGCCTTGTCCTAAT-3‘ Reverse 5‘-ATGAGAGGACAGTGCCAAGC-3‘

Thermal cycling conditions:

1) Initial denaturation: 98ºC – 10 minutes
2) Denaturation: 98ºC – 15 seconds
3) Annealing: temperature adjusted to primers – 30 seconds
4) Extension: 72ºC – 30 seconds
5) Go back to step 2) 40 times

To visualize and analyze the amplification company software qPCRsoft (Analystik Jena) was used. Detection of amplification showed the existence of the target sequence (floxed

genes or merCremer) whereas no amplification indicated for the absence of the target sequence.

3.4 *In vivo* methods

All in vivo experiments were performed using isoflurane inhalation anesthetic, isoflurane vaporizer (*VetEquip*), surgery tools (*F.S.T.*) and a thermometer, heating platform and heater lamp to control and maintain body temperature of the mice. All mice were prepared for surgery with a shaver (*Contura*) and hair remover lotion (*Veet*) to remove hair at surgery spot and were treated with eye ointment (*Bayer #81552983*) to avoid eye injury during the procedures.

3.4.1 Echocardiography

Heart function was measured for assessment of left ventricular size and function to investigate the influence of genetic modifications or treatments on cardiac performance. All recordings were taken with *Vevo 2100 High Frequency Ultrasound System*. Mice were anesthetized in an induction chamber with an inflow of isoflurane at flow rate of 3-4% (v/w). Echocardiography measurements were performed with continuously delivered gas inhalation agent isoflurane (1-3%). The mice were placed with the back on a warm pad (platform temperature of the equipment set at 40 – 42°C) to keep the animal core temperature at 37°C and a rectal thermometer was inserted for monitoring the body temperature. The limbs were taped onto the metal ECG allowing to monitor heart and breathing frequency (heart rate was maintained at 400-500 beats per minute). Chest hair was removed by shaving followed by application of hair remover lotion. Pre-warmed echo gel (*Parker Laboratories*) was placed on the chest and the mouse heart was imaged using an echo transducer MS400 (18-38 mHz). By placing the transducer along the long-axis, two dimensional left ventricular parasternal long-axis was obtained. By rotating the transducer clockwise by 90° the short-axis of the left ventricle was visualized and m-mode und b-mode was imaged, respectively. In addition, pulmonary vein diameter and pulmonary vein pulsed wave (to assess the flow in the pulmonary vein) were measured. After scanning, the echo gel was removed, and the mouse was placed back in the cage for recovery. For analyzing the data Vevo Lab 1.7.1

software was used. At least three beats were measured and averaged for the interpretation of any given measurement.

Based on these two-dimensional images ejection fraction (EF), left ventricular end diastolic volume (LVEDV), and left ventricular end systolic volume (LVESV) were calculated using the biplane Simpson method.

3.4.2 Osmotic mini pump implantation

To induce hypertension and increase cardiac workload we used angiotensin II (AngII) as a potent vasoconstrictor. Continuous AngII-application was implemented using osmotic mini pumps (*Alzet* model 1003D). Pumps were filled 12-16 hours before use with AngII (*Sigma-Aldrich* #A9525) or PBS according to manufacturer's recommendation and stored over night at 37°C in PBS. Mice were anesthetized in an induction chamber with an inflow of isoflurane at a flow rate of 3-4% (v/w) and the implantation was performed with continuously delivered isoflurane inhalation (1-3%). An incision at the back was made to subcutaneously insert the osmotic pump. After 4-6 hours pumps reach a constant pump performance of 1.5 mg/kg/day AngII.

3.4.3 *In vivo* intraperitoneal insulin stimulation

Mice were stimulated with intraperitoneal injection of insulin to analyze phosphorylation levels of proteins mediating insulin signaling and the influence of protein absence on insulin signal transduction. 12 week old mice were fasted 4-5 hours pre stimulation, 1 mg/kg body weight insulin (*Lilly France*) was intraperitoneally injected with a 30 G needle (*B. Braun Melsungen AG* #4656300). Control groups were injected equally with PBS. After 10 minutes mice were sacrificed by cervical dislocation and harvested organs were immediately frozen in liquid nitrogen. Proteins were extracted (described in section 3.7.1) and phosphorylation levels were analyzed via western blotting (described in section 3.7.2).

3.4.4 *In vivo* glucose tolerance test and plasma insulin measurement

Measurements of blood glucose and plasma insulin levels were performed to define how quickly glucose was cleared from the blood and insulin was secreted from pancreatic beta-

cells. These results were used to determine an insulin resistance. 12 week-old mice (treated with and without AngII) were starved for 4 hours and baseline blood glucose levels were measured from tail vein using a handheld blood glucose monitor (*Nova Biomedical* StatStrip Xpress2). Mice then received i.p. injections of 1 g/kg body weight D-glucose (*Sigma* #G7528). Blood glucose levels were measured, at times 5, 15, 30, and 60 minutes. In addition, 30 µL of blood was sampled at times 0, 15 and 30 minutes. Afterwards, blood samples were spun for 15 minutes at 1,500 g and 4°C and plasma was stored at -80°C for further analysis. Plasma insulin levels were measured using Ultra-Sensitive Mouse Insulin ELISA Kit (*Crystal Chem* #90080) in accordance to manufacturer's protocol.

3.4.5 *In vivo* tissue [^{3}H]-2-DG transport during glucose tolerance test

Organ specific glucose uptake was analyzed as described before (Gaykema *et al.*, 2017; Zisman *et al.*, 2000). 12 week old animals were starved for 4 hours and 2-deoxy-D-[1,2-^{3}H]-glucose (*PerkinElmer* #NET328A250UC) was mixed with 20% glucose and injected intraperitoneally (1 g/kg body weight; 10 µCi/mouse). Blood was sampled from tail vein at 0, 15, 30, 60, and 120 minutes and blood glucose levels were measured using a glucometer (*OneTouch* Ultra2 meter). Blood samples were spun for 5 minutes at 13,000 g and 1 µL of plasma was mixed with scintillation fluid (*PerkinElmer* #1200.437). Afterwards, tracer amount was measured at different time points using a scintillation counter. These results were used to calculate plasma glucose-specific activity. To determine the organ specific uptake of 2-deoxy-D-[1,2-^{3}H]-glucose-6-phosphate mice were sacrificed at 120 minutes and tissues were extracted and homogenized in 1.6 mL distilled water. Homogenates were spun at 13,000 g for 5 minutes and supernatants were passed through an ion exchange column to extract labeled 2-deoxy-D-[1,2-^{3}H]-glucose-6-phosphate. The amount of accumulated 2-deoxy-D-[1,2-^{3}H]-glucose-6-phosphate was calculated by the difference between total and eluted ^{3}H radioactivity in supernatants determined by using scintillation counter. Values were normalized to plasma glucose-specific activity area under the curve defined by scintillation counting.

3.5 *Ex vivo* methods

The Langendorff preparation (Langendorff, 1895) was used to investigate the effect of insulin exclusively on the isolated heart without any influence of other tissues and to analyze single gene alterations on heart physiology and function.

The heart was rapidly removed from the sacrificed mouse and a balloon connected with a blunt end cannula was inserted into the left ventricular cavity via the mitral valves. Usage of this balloon allows to continuously monitor left ventricular pressure. Once in position the balloon was fixed to avoid movement of the balloon during subsequent perfusion and connected to LV pressure transducer. Next the opened aortic root was slipped over and fixed at a blunt-end 21 G cannula. The cannulated heart was placed in the perfusion apparatus and continuously infused with oxygenated Krebs-Henseleit buffer (KHB, continuously gassed with 95% O_2, 5% CO_2) (Table 3.2) and maintained at 37°C using a water tempered glass jacket. The perfusion solution is delivered in the retrograde direction down the aorta at constant pressure of 80 mmHg (recommended flow rates of 1 -2 mL per minute) (Broadley, 1979; Sutherland *et al.*, 2003).

Table 3.2: List of solutions used for Krebs-Henseleit buffer to perform Langendorff perfusion experiments

Ingredients (*Concentration*)	**Manufacturer (*Cat No.*)**
NaCl (*118 mM*)	Sigma-Aldrich (*#S5886-500G*)
KCl (*4.7 mM*)	Sigma-Aldrich (*#P5405-250G*)
$MgSO_4$ (*1.2 mM*)	Sigma-Aldrich (*#M1880-500G*)
$CaCl_2$ (*1.25 mM*)	Sigma-Aldrich (*#C3306-250G*)
KH_2PO_4 (*1.2 mM*)	Sigma-Aldrich (*#P5655-100G*)
$NaHCO_3$ (*25 mM*)	Roth (*#8551.1*)
D-(+)-Glucose	Sigma-Aldrich (*#16301-250G*)

For ex vivo insulin stimulation hearts were placed at the perfusion apparatus and perfused with a constant pressure of 80 mmHg. After 20 minutes of equilibration hearts were perfused for another 30 minutes with KHB. Subsequently hearts were stimulated with insulin (6 nM) for 10 minutes. Insulin was added to KHB using a syringe pump right before entering left

ventricle. After the procedure the hearts were immediately frozen in liquid nitrogen and stored at -80°C for further investigations using western blotting (described in section 3.7.2).

For *ex vivo* insulin stimulation and perfusion with ^{13}C-labeled palmitate and ^{13}C-glucose (both from Cambridge Isotope Laboratories) the hearts were processed basically as described before (Flogel *et al.*, 1999). After placing hearts at the perfusion apparatus they were perfused at constant pressure (80 mmHg) with KHB for 20 minutes. After the hearts had stabilized, cardiac perfusion was continued for a 20 minutes' equilibration phase with a fixed perfusion rate in accordance with the steady flow rate. Subsequently, the buffer was switched to a buffer containing 5 mM [1,6-$^{13}C_2$]glucose and 0.5 mM [U-$^{13}C_{16}$]palmitate and supplemented with either 0.6 µM or 6 µM insulin for 30 minutes at constant substrate perfusion flow rate using a roller pump (Flogel *et al.*, 2005). Finally, the hearts were freeze clamped and stored at -80°C. To investigate the substrate utilization, proteins were extracted with 1 M perchloric acid, neutralized using KOH, lyophilized and measured using NMR spectroscopy (described in section 3.9).

3.6 Islet isolation

To isolate pancreatic islets, an already described and modified protocols was used (Nikolova *et al.*, 2006; Yesil *et al.*, 2009). 12 week old mice were sacrificed by cervical dislocation and the bile duct was clamped off at the duodenal insertion. Then low glucose DMEM (*Thermofisher* #21885025) with freshly added Liberase TL (*Roche* #5401020001) was injected into the bile duct to efficiently perfuse the whole pancreatic tissue. Afterwards tissues were digested at 37°C for 17.5 minutes and the enzymatic reaction was stopped using DMEM containing 15% FCS. Samples were vigorously shaken, washed with DMEM and filtered through a 400 µm mesh sieve. Filtered DMEM containing the islets was carefully placed on 7 mL histopaque (*Sigma* #10771). After centrifugation for 25 minutes at 1,200 rpm the islets were collected from the interphase between histopaque and DMEM, pelleted and resuspended in 1 mL TRIzol reagent (*Invitrogen* #15596-026) to extract RNA. Expression levels were then measured using quantitative RT-PCR (described in section 3.8.3).

3.7 Protein analysis

3.7.1 Tissue preparation

All samples were stored at -80°C and were kept on dry ice during transportation to avoid degradation of proteins. For approximately 90 mg tissue 500 µL lysis buffer freshly supplemented with Phosphatase & Protease Inhibitor Cocktail (1:100 *Thermo Scientific*) was used. Tissue was immediately homogenized with TissueRuptor (*Qiagen*) and lysates were centrifuged for 5 minutes at 13,000 g and 4°C. Supernatants were transferred to fresh tubes kept on ice and protein concentrations were determined using BCA Assay Kit (*Pierce*™ #23225) due to manufacturer's protocol. Protein extract concentrations were set to 2 µg/µL with lysis buffer and 4x laemmli buffer and were heated at 95°C for 5 minutes. Samples were aliquoted and immediately loaded to a SDS-PAGE gel or stored at -80°C for future use.

3.7.2 Western blotting

Western blot analysis was used to qualitatively detect specific proteins and their phosphorylation level in tissue homogenates.

Before proteins could be transferred to a membrane, they had to be separated using polyacrylamide gel electrophoresis. Therefore 20 µL of protein lysates (40 µg of total protein) and molecular weight marker (see Table 3.5) were loaded on a SDS-PAGE gel (consisting of a separation and a stacking gel, see Table 3.3 and 3.4). Electrophoretic separation of proteins according to their molecular size was performed using Hoefer-electrophoresis tanks filled with SDS running buffer. The gel was run for approximately 1 hour at 150 – 200 V (running time and voltage was adapted to size of protein of interest).

Table 3.3: List of solutions used to pour 2 separation gels: Ingredients required to reach specific percentage dependent on the size of protein of interest.

Protein size	**100 – 180 kDa**	**40 – 100 kDa**	**10 – 40 kDa**	**3 – 10 kDa**
Gel percentage	7.5%	10%	12.5%	15%
Reagent	**Amount for 2 gels (1 mm thick)**			
ddH_2O	5.625 mL	5 mL	4.375 mL	3.75 mL
1 M Tris HCl pH 8.8	2.5 mL	2.5 mL	3.125 mL	3.75 mL
40% Acrylamid	1.875 mL	2.5 mL	2.5 mL	2.5 mL
10% SDS	100 µL	100 µL	100 µL	100 µL
10% APS	20 µL	20 µL	20 µL	20 µL
TEMED	25 µL	25 µL	25 µL	25 µL

Table 3.4: List of solutions used to pour 2 stacking gel: Ingredients required for a 2.5% gel

Reagent	**Amount for 2 gels (1 mm thick)**
ddH_2O	3.7 mL
1 M Tris HCl pH 6.8	625 µL
40% Acrylamid	625 µL
10% SDS	50 µL
10% APS	10 µL
TEMED	15 µL

Table 3.5: List of Protein Ladder used in the western blot protocol

Reagents	**Company (*Cat No.*)**
PageRuler™ Prestained Protein Ladder, 10 to 180 kDa	ThermoFisher (*26616*)
PageRuler™ Plus Prestained Protein Ladder, 10 to 250 kDa	ThermoFisher (*26619*)

Following electrophoresis proteins were transferred to a nitrocellulose membrane (*GE Healthcare* #10600002) using Pierce G2 Fast Blotter (*Thermo Scientific*). The transfer was performed with settings regarding time, ampere and voltage dependent on protein sizes and was chosen in accordance to manufacturer's manual (see Figure 3.1). Non-specific binding sites on the membrane were blocked using blocking buffer (TBS 1:1 Odyssey solution) for 1 hour at room temperature.

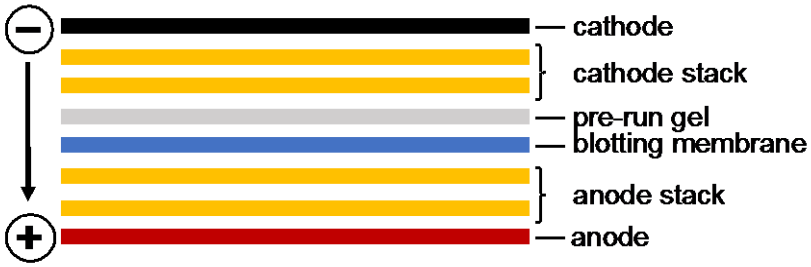

Figure 3.1: Orientation of filter paper, membrane and gel for transferring proteins

By applying a voltage, negatively charged proteins move away from the cathode (negatively charged pole) towards the anode (positively charged pole). The transfer stack contains from the bottom: two sheets of pre-wet filter paper and the blotting membrane equilibrated in anode buffer, pre-run gel and two sheets of filter paper equilibrated in cathode buffer.

Afterwards membranes were incubated in 2 mL of primary antibody solution (diluted in TBS 5% Albumin) over night at 4°C. The following primary antibodies were used (see section 2.3): anti-p38MAPKα (*Cell Signaling*), anti-phosphop38MAPKα$^{T180/Y182}$ (*Cell Signaling*), anti-Glut1 (*Abcam*), anti-Glut2 (*Abcam*), anti-Glut4 (*Abcam*), anti-AMPKα (*Cell Signaling*), anti-pAMPKα^{T172} (*Cell Signaling*), anti-pAMPKα^{485} (*Cell Signaling*), anti-Akt (*Cell Signaling*), anti-pAkt^{S473} (*Cell Signaling*), anti-AS160 (*Millipore*), anti-pAS160^{T642} (*Cell Signaling*), anti-Insulin (*Cell Signaling*). The next day membranes were washed 3 times for 10 minutes with TBST. Secondary antibodies (*LI-COR,* see section 2.3) were diluted 1:10,000 (in TBST 1:1 blocking buffer) and blots were incubated in 2 mL secondary antibody solution for 50 minutes at room temperature. Before scanning membranes were washed again two times for 10 minutes in TBST and once for 10 minutes in TBS. Proteins were visualized using Odyssey 9120 Imaging Systems (*LI-COR*). Quantification and normalization was performed using REVERT Total Protein Stain (*LICOR*) due to manufacturer's recommendation.

3.7.3 Subcellular fractionation

A fractionation protocol was established to separate different cellular organelles in accordance to their density. It was used to analyze glucose transporter 4 (Glut4) translocation from storage vesicles located in cytoplasm to the plasma membrane in an insulin dependent manner.

Mouse hearts were isolated and stimulated with insulin in a Langendorff setup (described in section 3.5). Frozen tissues were homogenized using TissueRuptor (*Qiagen*) in 1 mL fractionation buffer (freshly supplemented with Protease & Phosphatase Inhibitor). The lysed tissues were processed to differential centrifugation modified from the protocol published by Taha and colleagues (Taha *et al.*, 2014) consisting of a sequential increasing gravitational force (Figure 3.2). Low-speed centrifugation steps (up to 2,000 g) were performed using a table centrifuge and high-speed centrifugation steps (up to 135,000 g) were conducted with an ultracentrifuge. For further analysis of specific protein amount, fractions were diluted in defined volumes of fractionation buffer (FB) and 4x laemmli (4xL) (see Table 3.6).

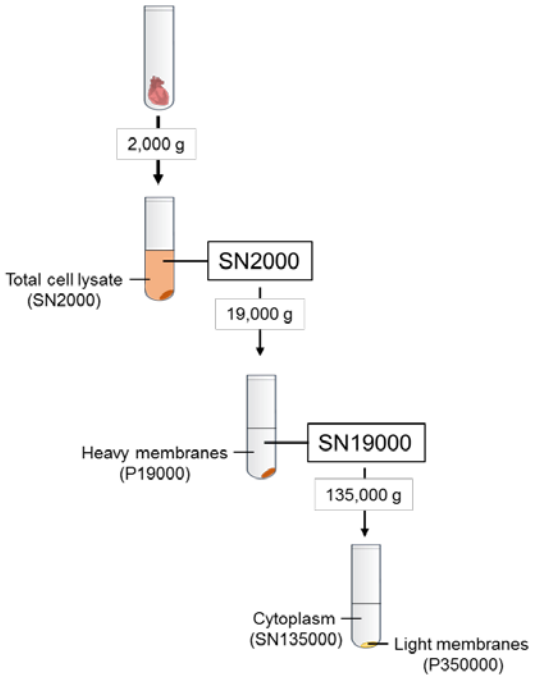

Figure 3.2: Flow diagram of subcellular fractionation procedure with centrifugation steps and the separation of cellular components in different fractions. supernatant (SN), pellet (P)

Table 3.6: Fractions obtained from subcellular fractionation, volumes for sample dilution with fractionation buffer (FB) and 4x laemmli buffer (4xL) to reach comparable protein amounts and marker used to identify cellular components of different fractions.

Fractions	Labeling	Dilution	Marker
Fraction 1: total cell lysate (TCL)	SN2000	100 µL + 1,675 mL FB + 4xL (0.25 mL per 1 mL)	Na^+/K^+-ATPase, ATP-Synthase, Glut4, Caveolin3
Fraction 2: heavy membranes (HM)	P19000	Dissolve in 1.775 mL FB + 4xL (0.25 mL per 1 mL)	Na^+/K^+-ATPase, ATP-Synthase, Glut4, Caveolin3
Fraction 3: light membranes (LM)	P135000	Dissolve in 1.775 mL FB + 4xL (0.25 mL per 1 mL)	Glut4
Fraction 4: cytoplasm (CP)	SN135000	1.775 mL + 4xL (0.25 mL per 1 mL)	PDI

Samples were analyzed using western blotting (described in section 3.7.2). Detection of single proteins in the different fractions was analyzed using anti-Glut4 antibody (*Abcam*), anti-Na^+/K^+-ATPase antibody (*Cell signaling*), anti-ATP-Synthase antibody (*Proteintech*), anti-caveolin3 antibody (*BD*), and anti-PDI antibody (*Cell signaling*) in western blot experiments.

3.7.4 Insulin enzyme-linked immunosorbent assay

Plasma was isolated from whole blood sampled from the right ventricle right after mice were euthanized. Blood was spun for 15 minutes at 1,500 g and 4°C and plasma supernatant was transferred into a new Eppendorf tube. Plasma insulin levels were measured with enzyme-linked immunosorbent assay (ELISA) Kit (*DRG Diagnostics*) according to the manufacturer's instructions. Absorbance was measured with a microplate reader (*Bio-Rad*).

3.8 Gene expression analysis

3.8.1 RNA isolation

Isolated RNA was used for array analyses and real time-PCR to get information about altered expression levels causing altered phenotype.

RNA was isolated from harvested tissues snap-frozen in liquid nitrogen immediately after harvesting and stored at -80°C. Tissues were homogenized with Tissue Ruptor (*Qiagen*) and RNA was prepared using RNeasy Fibrous Tissue Mini Kit for heart tissue and RNeasy Lipid Tissue Mini Kit (both from *Qiagen*) for pancreatic tissue in accordance to manufacturer's recommendation. Purified RNA was diluted in RNAse free water (*Thermofisher*) and concentration was measured with Nanodrop spectrophotometer (*Peqlab*) and stored at -20°C for further analysis.

3.8.2 Gene expression profiling (Microarray analysis)

Microarray analysis allows genome wide measurement of expression levels to identify genes as potential candidate contributing to characterized phenotype in transgenic mice.

Isolated RNA from heart tissue (described in section 3.8.1) was first analyzed for quality by the 'Biologisch-Medizinisches Forschungszentrum (BMFZ)' of the Heinrich-Heine University to determine RNA integrity number (RIN). This value ranks from 1 to 10 with 10 being the most intact and the least degraded (Schroeder *et al.*, 2006). For further measurements only samples with a RIN of 8-10 were used for microarray transcript analysis also performed by BMFZ. Data of significantly altered transcripts were analyzed using Ingenuity Pathway Analysis (IPA) software (*Qiagen*)

3.8.3 Real-time quantitative polymerase chain reaction (qRT-PCR)

qRT-PCR amplification of specific DNA segments can be monitored to investigate expression levels of specific genes.

First 1 µg of total RNA was transcribed into complementary DNA (cDNA) using QuantiTech Reverse Transcription Kit (*Qiagen*). The synthesized cDNA could be directly used for qRT-PCR experiments or stored at -20°C for later usage. For performing transcript expression measurement, the Maxima SYBR Green/ROX qPCR Master Mix (*Thermo Scientific*) was used as indicated in Table 3.7.

Table 3.7: List of content per reaction well for transcript detection using SybrGreen.

Reagents	**Volume (Concentration)**
SybrGreen MM (2x)	10.0 µL
ddH2O	7.2 µL
cDNA	1.0 µL (20 ng)
Primer (Forward)	0.9 µL (1 µM)
Primer (reverse)	0.9 µL (1 µM)
	reaction volume: 20.0 µL

qRT-PCR was performed with a total reaction volume of 20 µL in 96 well reaction plates (*Applied Biosystems*). Specific primer sequences used for measurement are listed in section 2.5, whereas Nudc was used as housekeeping gene for normalizing expression of individual genes. Each gene was measured in two technical replicates. qRT-PCR was performed using Step One Real-Time PCR System (*Thermo Scientific*). The following setting was used to amplify single genes: First cycle at 95°C for 10 minutes followed by 40 cycles at 95°C for 15 seconds and at 60°C for 60 seconds. Afterwards the specificity of amplicons was verified by a melting curve analysis, which starts at 95°C for 15 seconds followed by a time period of 60 seconds at 60°C and then the temperature was again increased every 15 seconds by 0.3°C until the final temperature of 90°C was reached. Quantification of expression levels was performed using the X_0 method which provides information about expression levels, including procedures to calculate standard deviations. This method based on the equation described by Thomsen an colleagues (Thomsen *et al.*, 2010):

$$X_n = X_0(1 + E)^n$$

Where E is equal the efficiency of amplification (whereby it is assumed that E is perfect (meaning equal 1 or 100% efficiency of the qPCR), X_n is equal the target quantity at cycle n and n is equal the number of cycles detected by manual setting threshold in the linear phase of gene expression. X_0 is equal the initial amount of cDNA in a sample and can be calculated with the equation solved after X_0:

$$X_0 = \frac{X_n}{2^n}$$

Afterwards genes of interest were divided by the reference gene of the same sample to statistically analyze differences between two groups (e.g. varying in treatment of genotype).

3.9 Nuclear magnetic resonance (NMR) measurements

Substrate utilization from isolated hearts perfused with [1,6-$^{13}C_2$]glucose and [U-$^{13}C_{16}$]palmitate (described in section 3.5) was determined on a Bruker DRX 9.4 Tesla WB NMR spectrometer (frequencies: 400.1 MHz for ^{1}H and 100.6 MHz for ^{13}C measurements). First lyophilized PCA extracts were dissolved in 0.6 mL D_2O and spectra acquisition was performed with a 5-mm 1H/13C dual probe (Flogel *et al.*, 2005). ^{1}H NMR spectra were recorded with a flip angle of 90°, repetition time 15 seconds, low power water presaturation, 512 scans, spectral width 5580 Hz, data size 16 K, zero filling to 32 K. Chemical shifts were referenced to (trimethylsilyl)-propionic-2,2,3,3d4-acid (TSP) at 0 ppm. For ^{13}C NMR spectra 20 K scans were accumulated with a flip angle of 30º, repetition time 1.7 seconds, composite pulse decoupling with Waltz16, spectral width 25062 Hz, data size 32 K, zero filling to 64 K, exponential weighting resulting in a 1 Hz line broadening. Chemical shifts were referenced to C3 of lactate at 21.3 ppm. The relative consumptions of palmitate, glucose and endogenous sources to total amount of acetyl-CoA entering the TCA cycle were calculated from isotopomeric pattern analysis of glutamate carbon 3 (C3) and 4 (C4).

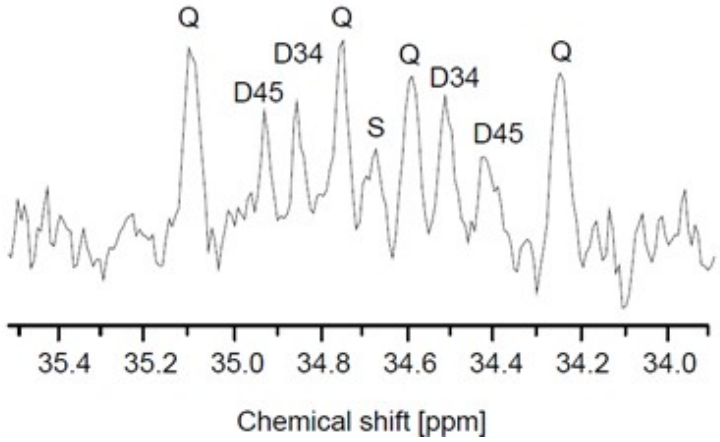

Figure 3.3: Representative section of ^{13}C NMR spectra showing the glutamate C4 isotopomer pattern for a heart extract, perfused with insulin. D34 indicates doublet because of J_{34} coupling (34 Hz); D45, doublet because of J_{45} coupling (51 Hz); Q, quartet (doublet of doublet) because of J_{345} coupling (J_{34} 34 Hz, J_{45} 51 Hz); S, singlet (from (Flogel *et al.*, 2005)).

Fluxes (F) from doublet (D34 due to J_{34} coupling, 34 Hz) and quartet (Q, due to J_{345} coupling, J_{34} 34 Hz, J_{45} 51 Hz)) were normalized to the total resonance of glutamate carbons (C4 divided by C3) (Figure 3.3) leading to following equations:

$$F_{Glucose} = \frac{D34}{C4/C3}$$

$$F_{Palmitate} = \frac{Q}{C4/C3}$$

$$F_{Endogenous} = 1 - F_{Glucose} - F_{Palmitate}$$

3.10 Statistics

All data are presented as mean ±standard deviation (SD). Statistical analysis was performed using Graph Pad Prism 6. Repeated measurements were analyzed by two-way ANOVA followed by Bonferoni post test. Two groups were compared with Student's t-test. For comparison of more than two groups, we used One-way ANOVA followed by Tukey post test. Differences of $p < 0.05$ were considered statistically significant (* $p < 0.05$*, ** $p < 0.01$, *** $p < 0.001$).

4 Results

4.1 Validation of cardiomyocyte specific p38 MAPKα Knock-out (KO) in the heart

The inducible cardiomyocyte specific p38 MAPKα KO mouse model (described in section 1.8.1), thereafter referred to as iCMp38 MAPKα KO, was previously established in our laboratory (Bottermann *et al.*, submitted). To induce the KO, 6-8 week old mice (genotype: p38 MAPKα$^{flox/flox}$ and α-MHC merCremer$^{wt/hemi}$) were intraperitoneally injected for 10 consecutive days with OH-Tamoxifen (500 µg/d dissolved in 100 µL peanut oil), followed by 4 weeks of recovery period. As controls, p38 MAPKα$^{flox/flox}$ litter mates lacking the Cre-recombinase were treated equally to rule out any tamoxifen related effects. To first validate successful deletion of p38 MAPKα in the heart, western blot analysis was performed. As shown in Figure 4.1 p38 MAPKα protein levels in whole heart tissues were significantly reduced to 0.26 ±0.08 of the protein levels in control tissues (Figure 4.1A). Analysis of various tissues regarding p38 MAPKα protein levels showed no changes in skeletal muscle, liver, white adipose tissue (WAT) in iCMp38 MAPKα KO mice compared to control animals (Figure 4.1B).

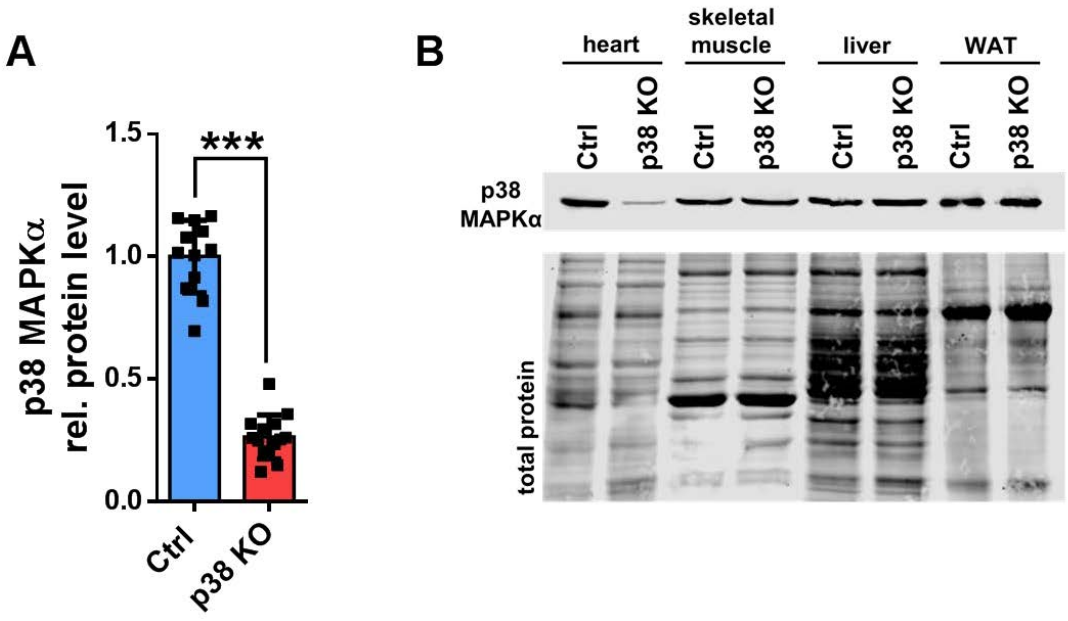

Figure 4.1: Validation of inducible p38 MAPKα KO in heart tissue

(A) Western blot analysis exhibit that protein levels of p38 MAPKα in heart were strongly reduced compared to control. (B) KO of p38 MAPKα in heart but not skeletal muscle, liver and white adipose tissue of iCMp38 MAPKα mice compared to control animals. Total protein stain was used as loading control. Each value was normalized to mean baseline value of controls, which was set equal to 1. Data are presented as mean ±SD, n = 12-14. Statistical significance between two groups was calculated using unpaired two-tailed Student's t-test (*** p <0.001*).*

4.2 Investigations of cardiac metabolic processes in iCMp38 MAPKα KO hearts

The heart has a high metabolic rate and uses different substrates to maintain its contractility. Central to achieve this goal is the metabolic flexibility of the heart (described in section 1.2). It has been shown that the stress kinase p38 MAPKα is an important mediator regulating cellular responses to various stress stimuli (Kumphune *et al.*, 2013). The activation of p38 MAPKα was suggested to play a regulatory role in adapting myocardial metabolism to increased energy demand (Bottermann *et al*., submitted). Another essential player regulating increased cardiac substrate uptake is insulin, mediating enhanced translocation of the glucose transporter 4 (Glut4) and the fatty acid translocase (FAT/CD36) to the plasma membrane (see sections 1.2.1 and 1.2.2). Furthermore, a linkage between activation of cardiac p38 MAP kinases and insulin resistance was described (Liu *et al.*, 2009) Therefore,

the question arose if insulin dependent metabolic processes are affected in the absence of p38 MAPKα in cardiomyocytes.

4.2.1 Insulin-dependent increase in glucose utilization is impaired in iCMp38 MAPKα KO hearts

To get a better understanding of the preferred cardiac substrate utilization, glucose and fatty acid metabolism of iCMp38 MAPKα KO in response to insulin stimulation was investigated. To measure relative substrate utilization, hearts were perfused *ex vivo* using a Langendorff set up (described in section 3.5) with buffer containing [1,6-$^{13}C_2$]glucose and [U-$^{13}C_{16}$]palmitate and either 10 mU/L or 100 mU/L insulin. The relative contribution of palmitate (FA), glucose (G) and endogenous (E) sources to the total acetyl-CoA pool entering the TCA cycle was measured by NMR spectroscopy (described in section 3.9). Analysis of isotopomer patterns of glutamate carbons C3 and C4 (Figure 4.2A) exhibited that control hearts preferred fatty acids as main energy source under non-insulin stimulated (10 mU/L) conditions (FA: 48.6% ±4.4; G: 36.4% ±5.1; E 15.0 % ±4.3) whereas they switched their preference towards glucose (FA: 34.8% ±7.6; G: 49.9% ±9.7; E: 15.3% ±2.1) after stimulation with insulin (100 mU/L). Interestingly, iCMp38 MAPKα KO hearts mainly utilized fatty acids under non-insulin stimulated conditions (FA: 57.2% ±3.8; G: 25.5% ±4.4; E: 17.3% ±1.1) as well as after insulin stimulation (FA: 53.2% ±10.3; G: 30.7% ±12.4; E: 16.1% ±4.6) as depicted in Figure 4.2B. Figure 4.2C summarizes a significant higher FA oxidation in iCMp38 MAPKα KO hearts when stimulated with insulin and significant less glucose oxidation compared to insulin stimulated controls. Sample preparation was done in cooperation with Dr. K. Bottermann. NMR spectroscopy measurements and data quantification were performed in cooperation with Prof. U. Flögel from the Department of Molecular Cardiology at Heinrich-Heine University.

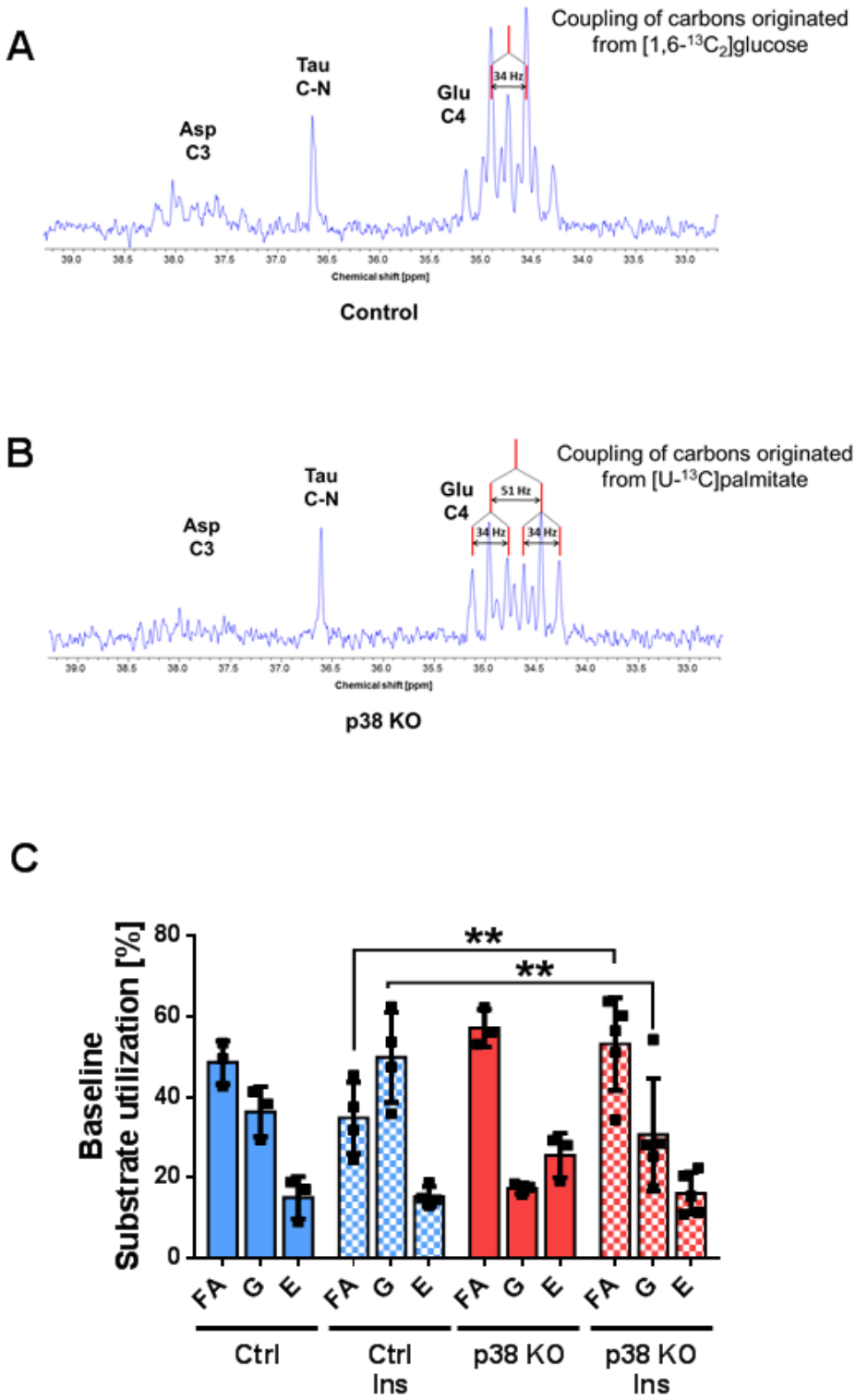

Figure 4.2: Analysis of relative substrate consumption in iCMp38 MAPKα KO and control hearts in response to insulin stimulation

(A) Representative NMR spectrum of carbon C4 of glutamate shows that the specific coupling pattern for carbon derived from [1,6 $^{13}C_2$]glucose in control hearts (Singlet S, Doublet D34) and (B)

from [U $^{13}C_{16}$]palmitate in in iCMp38 MAPKα KO hearts (Doublet D45 and Quartet Q). (C) Quantification of utilization of labeled glucose, palmitate and endogenous substrates exhibit significantly increased palmitate utilization and in turn significantly reduced glucose utilization in iCMp38 MAPKα KO hearts compared to controls in response to insulin. Fatty acids/palmitate (FA), glucose (G), endogenous sources (E). Data are presented as mean ±SD, n = 4-5. Statistical significance was calculated using Two-way ANOVA (** $p < 0.01$). Measurements were performed in cooperation with Prof. U. Flögel.

4.2.2 iCMp38 MAPKα KO influenced protein levels and transcript expression of Glut1 and Glut4, but not of FAT/CD36 in heart

Cardiac metabolism and substrate preference is regulated by secreted hormones such as insulin mediating the presence of glucose and fatty acid transporters in the plasma membrane adjusting substrate uptake into the cell (described in section 1.4). Since iCMp38 MAPKα KO hearts fail to increase glucose oxidation in response to insulin stimulation (see section 4.2.1), transcript expression and protein levels of Glut1, Glut4 and FAT/CD36 were analyzed. Figure 4.3A-C shows representative western blot images demonstrating increased Glut1, decreased Glut4 and no changes in FAT/CD36 protein level in iCMp38 MAPKα KO hearts. Quantification of immunoblotting) revealed that protein levels of the insulin-independent Glut1 were significantly increased (by 1.4 ±0.2-fold), whereas the insulin-dependent Glut4 showed decreased protein levels (to 0.5 ±0.2-fold) in iCMp38 MAPKα KO hearts compared to control hearts (Figure 4.3D-F). FAT/CD36, which increases fatty acid uptake stimulated by insulin showed no difference in protein levels. Transcript expression levels (Figure 4.3G-I) of *Glut1* were increased (by 1.8 ±0.4-fold). In turn, *Glut4* and *FAT/CD36* relative expressions were not altered in iCMp38 MAPKα KO hearts.

These results suggest a connection between impaired insulin sensitivity and the reduced levels of proteins whose translocation is insulin mediated. In addition, these results also lead to the question if insulin signal transduction is affected by the deletion of p38 MAPKα.

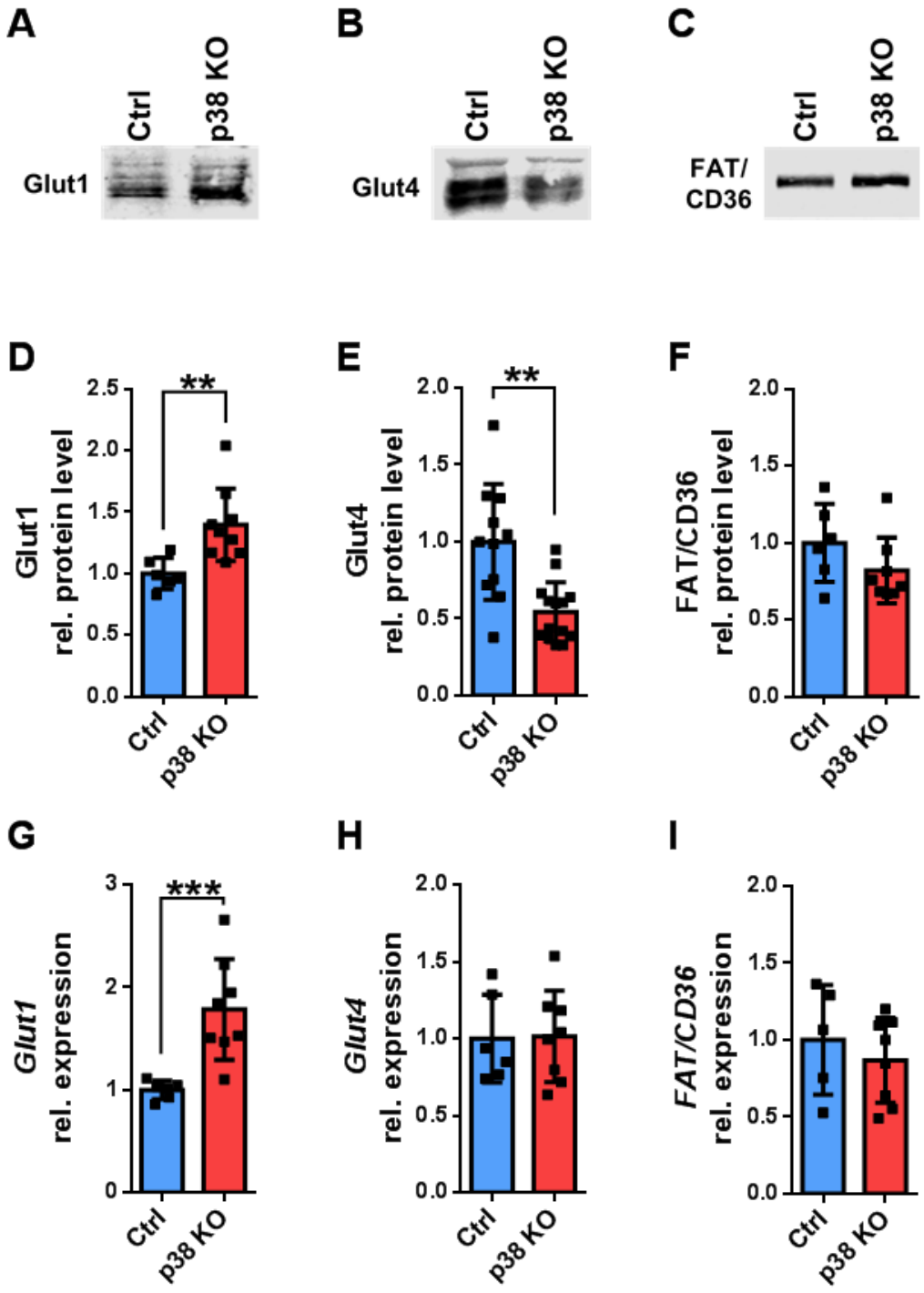

Figure 4.3: Protein and transcript expression levels of Glut1, Glut4 and FAT/CD36 in iCMp38 MAPKα KO hearts

Representative western blot images of (A) Glut1, (B) Glut4 and (C) FAT/CD36 in iCMp38 MAPKα KO and control hearts. Quantitative analyses of western blots exhibit that (D) Glut1 protein levels were significantly increased in iCMp38 MAPKα KO, (E) Glut4 protein levels were significantly reduced in iCMp38 MAPKα KO and (F) FAT/CD36 protein levels were not altered. Total protein stain was used as loading control. All values were normalized to mean value of controls, which was

set equal to 1. Transcript expression of (G) *Glut1* was significantly upregulated in iCMp38 MAPKα KO, whereas relative expression levels of (H) *Glut4* and (I) *FAT/CD36* were not altered. Data were assessed using qPCR. The values of each gene were normalized to mean value of controls. Data are presented as mean ±SD, n = 6-8. Statistical significance between two groups was calculated using unpaired two-tailed Student's t-test (** $p < 0.01$, *** $p < 0.001$).

4.2.3 iCMp38 MAPKα KO hearts showed no alteration in insulin/Akt signaling

The intracellular insulin signaling cascade gets activated by insulin binding to its receptor located in the plasma membrane. Binding of its ligand causes auto phosphorylation of tyrosine residues in the insulin receptor. This activation in turn triggers an intracellular phosphorylation cascade of proteins regulating glucose homeostasis. This leads to exocytosis of Glut4 and FAT/CD36 containing vesicles from cytoplasmic storage increasing transporter presence in the plasma membrane (described in section 1.4.1). Phosphorylation of proteins involved in insulin mediated signaling cascade was measured by western blot analysis (Figure 4.4A-B). The level of phosphorylation was measured in response to *ex vivo* insulin stimulation (described in section 3.5). Interestingly, iCMp38 MAPKα KO hearts showed similar upregulation in phosphorylation levels of Akt^{T308} (Ctrl: 5.5 ±1.0-fold; KO: 4.0 ±2.4-fold), $Akt1^{S473}$ (Ctrl: 2.3 ±0.6-fold; KO: 1.7 ±0.3-fold), $Akt2^{S474}$ (Ctrl: 3.7 ±1.9-fold; KO: 5.6 ±2.8-fold), $AS160^{T642}$ (Ctrl: 3.1 ±1.7-fold; KO: 2.8 ±1.9-fold), Gsk3-β^{S9} (Ctrl: 1.5 ±0.3-fold; KO: 1.6 ±0.4-fold) and $Pras40^{T246}$ (Ctrl: 3.4 ±1.8-fold; KO: 2.5 ±1.2-fold) compared to controls in response to insulin stimulation (Figure 4.4C-H).

In summary, there was no sign of an impairment of the intracellular insulin signal transduction up to AS160 in iCMp38 MAPKα KO hearts compared to control hearts.

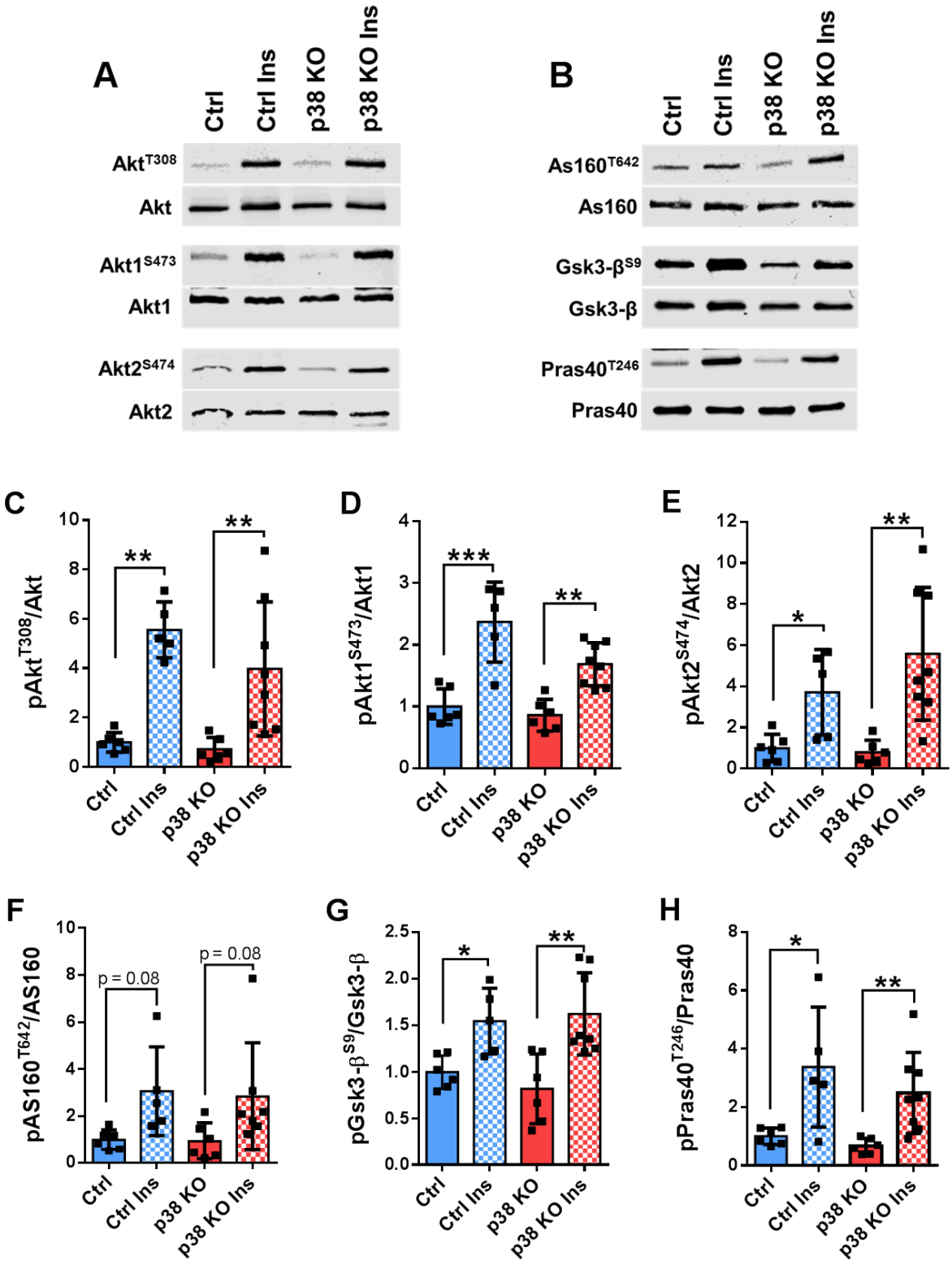

Figure 4.4: Phosphorylation levels of various proteins involved in insulin signaling

Investigation of phosphorylation levels of proteins mediating signal transduction in response to insulin stimulation. (A/B) Western blot analysis exhibit clearly higher phosphorylation levels in control and iCMp38 MAPKα KO hearts after insulin stimulation compared to non-insulin stimulated

samples. Quantification of (C) Akt^{T308}, (D) Akt1^{S473}, (E) Akt2^{S474}, (F) AS160^{T642}, (G) Gsk-3β^{S9} and (H) Pras40^{T246} phosphorylation exhibit similar increase in control and iCMp38 MAPKα KO hearts in response to insulin. Total protein stain was used as loading control. Each value was normalized to mean baseline value of controls, which was set equal to 1. Data are presented as mean ±SD, n = 6-8. Statistical significance was calculated using One-way ANOVA (* $p < 0.05$, ** $p < 0.01$, *** $p < 0.001$)

4.2.4 Subcellular fractionation to analyze insulin induced Glut4 translocation

Since signaling transduction of the insulin/Akt signaling cascade up to AS160 works properly in iCMp38 MAPKα KO hearts, the question arose if p38 MAPKα affected translocation of Glut4 from intracellular stores to the plasma membrane. Therefore, a closer look on exocytosis of insulin dependent Glut4 was taken. For this purpose, a subcellular fractionation protocol was established to separate the pool of transporters located within storage vesicles in the cytoplasm from the pool located in the plasma membrane (described in section 3.7.3). Western blot analysis was used to first validate the fractionation protocol. Four distinct fractions were obtained: total cell lysate (TCL), heavy membrane (HM), light membrane (LM) and cytoplasm (CP). To evaluate the separation quality of the isolated fraction, antibodies against specific marker proteins for each fraction were used to test non-insulin stimulated and insulin stimulated control hearts. The plasmalemmal protein Na^+/K^+-ATPase as well as caveolin3, a cardiomyocyte specific protein concentrated in caveolae in the plasma membrane, were predominantly found in the HM fraction. Immunoblotting analysis against ATP-synthase revealed that mitochondria were primarily found in the HM fraction and Glut4 was found in the HM and the LM fraction. Importantly, the relative amounts of Glut4 in these fractions varied depending on the stimulation conditions. In insulin stimulated samples, the amount of Glut4 is reduced compared to non-insulin stimulated heart lysates (Figure 4.5A). Additionally, quantification of HM to LM signal intensity showed comparable ratios in Na^+/K^+-ATPase, ATP-Synthase, caveolin3 but an increased ratio of Glut4 in insulin stimulated controls (Figure 4.5B). The enzyme PDI (protein disulfide isomerase) is located in the lumen of the intact endoplasmic reticulum. After homogenizing and fractionating cells, it could be detected in the cytoplasmic fraction, because this enzyme is not connected or bound to any kind of membrane.

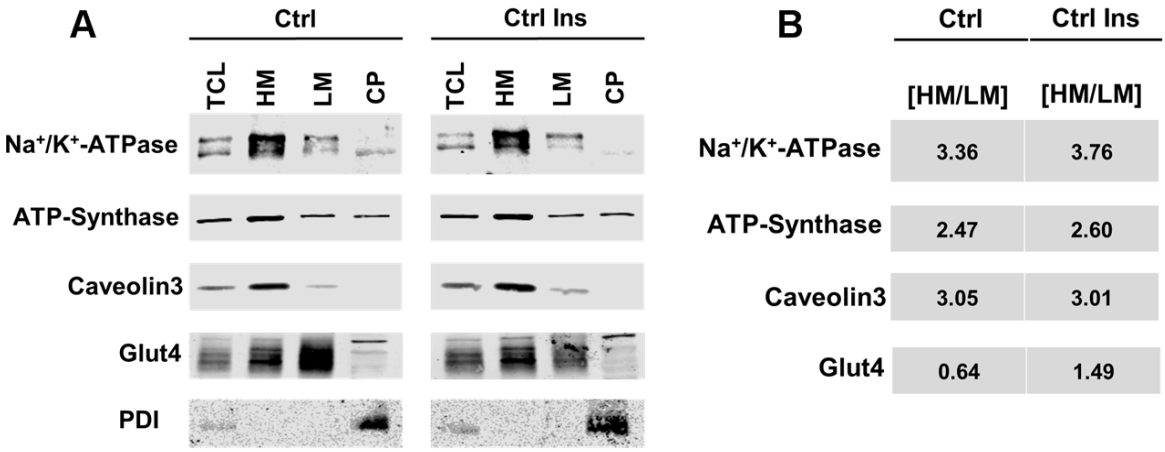

Figure 4.5: Subcellular fractionation analysis of protein composition in obtained fractions

(A) Western blot analysis of tissue lysates subjected to subcellular fractionation protocol to divide cellular compartments into four distinct fractions: total cell lysate (TCL), heavy membrane (HM), light membrane (LM), and cytoplasm (CP). Immunoblotting against Na^+/K^+-ATPase, ATP-Synthase, Caveolin3, PDI, and Glut4 was used to define cellular compartments in each fraction. (B) Ratio of signal intensity of HM/LM in control and insulin stimulated controls.

Since the heavy membrane fraction includes plasma membrane proteins and mitochondria it is hereafter referred to as plasma membrane (PM). The Light membrane fraction contained Glut4 vesicle and is referred to as storage vesicles (SV) in the following. By subjecting insulin-stimulated versus unstimulated tissue lysates to this protocol, the mobilization of proteins out of the Glut4 pool could be assessed.

4.2.5 Insulin induced Glut4 translocation is impaired in iCMp38 MAPKα KO hearts

To measure translocation efficiency, Glut4 stored in cytoplasmic vesicles was separated from Glut4 located in plasma membrane of cardiomyocytes. For this purpose, *ex vivo* insulin stimulated hearts were homogenized and processed according to the fractionation protocol (described in section 3.7.3). Western blot experiments (Figure 4.6A) demonstrated that in control hearts the Glut4 amount in the PM is higher in insulin stimulated heart lysates compared to non-insulin stimulated control samples while iCMp38 MAPKα KO heart lysates display an equal amount of Glut4 in PM and SV with and without insulin stimulation. Quantification of western blot measurements showed that control hearts significantly increased the presence of Glut4 proteins in the PM in response to insulin (Ctrl Ins: 3.1 ±0.9-

fold increase), whereas in the plasma membrane of iCMp38 MAPKα KO hearts only a slight, non-significant Glut4 elevation was detected (KO Ins: 1.6 ±0.4-fold increase) in comparison to non-stimulated samples (Figure 4.6B). Moreover, comparing insulin stimulated control and iCMp38 MAPKα KO groups, significant less Glut4 protein (approximately 50%) in PM could be observed (Figure 4.6B). The reduced translocation of Glut4 in iCMp38 MAPKα KO hearts exhibited an influence of p38 MAPKα on insulin mediated exocytosis of Glut4 vesicles to fuse with the plasma membrane. Thus, this effect maybe the underlying mechanism explaining the reduced glucose utilization.

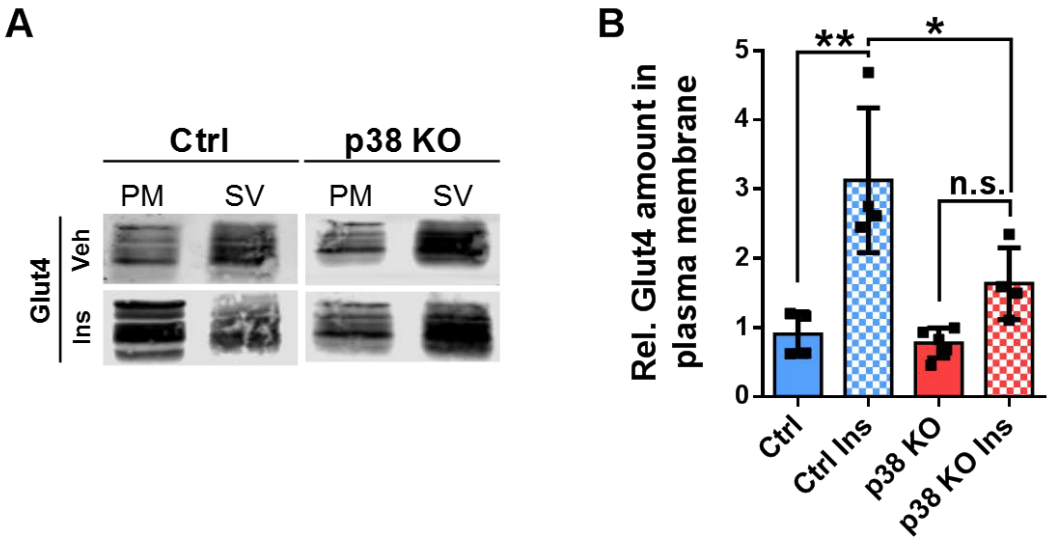

Figure 4.6: Mobilization of glucose transporter 4 (Glut4) out of insulin sensitive storage vesicles (SV) to the plasma membrane (PM)

(A) Vehicle treated control hearts show main presence of Glut4 in storage vesicles (SV) whereas insulin stimulation increased Glut4 pool in plasma membrane (PM). However, iCMp38 MAPKα KO hearts show higher presence of Glut4 in SV under non-stimulated and insulin-stimulated conditions. (B) The amount of Glut4 in PM normalized to Glut4 in SV is significantly increased in control but not in iCMp38 MAPKα KO hearts in response to insulin stimulation. All fractions were diluted in the same volume and signal intensities were normalized to total cell lysate (TCL). Data are presented as mean ±SD, n = 4-5. Statistical significance was calculated using One-way ANOVA (* $p < 0.05$, ** $p < 0.01$)

4.2.6 iCMp38 MAPKα KO hearts showed impaired glucose uptake *in vivo*

As shown before iCMp38 MAPKα KO hearts seem to be insulin resistant. To investigate if a reduced insulin mediated Glut4 translocation also influences glucose uptake into heart tissue *in vivo*, a glucose tolerance test (GTT) was performed (described in section 3.4.4) using [^{3}H]-2-deoxyglucose (2-DG). Control and iCMp38 MAPKα KO mice were fasted for four hours and showed equal baseline blood glucose levels (Ctrl: 129.7 mg/dL ±25.6; KO: 130.2 mg/dL ±17.8). 15 minutes after injection of 2-DG blood glucose levels were strongly increased in both groups (Ctrl: 303.7 mg/dL ±26.7; KO: 238.0 mg/dL ±79.8). Over a time of total 120 minutes three further measurements at 30 minutes (Ctrl: 186.2 mg/dL ±36.3; KO: 172.2 mg/dL ±38.3), 60 minutes (Ctrl: 143.5 mg/dL ±28.6; KO: 142.8 mg/dL ±27.2) and 120 minutes (Ctrl: 127.2 mg/dL ±27.8; KO: 143.6 mg/dL ±31.9) showed that the blood glucose deceased slowly and went back to baseline level (Figure 4.7A). At baseline, 15 minutes and 30 minutes after 2-DG injection blood was sampled to examine plasma insulin levels. Figure 4.7B shows that also plasma insulin exhibited similar levels at baseline (Ctrl: 1.18 µg/L ±0.61; KO: 1.87 µg/L ±0.78) and were increased equally 15 minutes after 2-DG injection in control as well as in iCMp38 MAPKα KO mice (Ctrl: 3,99 µg/L ±1.31; KO:5.45 µg/L ±2.47). After 30 minutes, plasma insulin levels decreased in KO (to 3.09 µg/L ±2.08) and stayed constant in control animals (4.1 µg/L ±1.7). However, no difference in plasma insulin levels over time in control and iCMp38 MAPKα KO mice were found.

2-DG is a glucose analog, which is taken up by cells, phosphorylated by hexokinase to p-2-DG but not further metabolized. Therefore, it accumulates within the cells and glucose uptake can be measured by counting radioactive events using a scintillation counter (described in section 3.4.5). That means the number of scintillation counts correlates with the amount of glucose taken up allowing to measure and analyze tissue specific phospho-2-DG amount. Interestingly, iCMp38 MAPKα KO hearts accumulated significantly less phospho-2-DG compared to control hearts (Ctrl: 0.31 µmol/g/min ±0.09, KO: 0.15 µmol/g/min ±0.06) (Figure 4.7C). Also of interest, various other glucose using organs e.g. liver (L), *musculus gastrocnemius* (M.gastroc), *musculus soleus* (M.soleus), inguinal white adipose tissue (iWAT) and perigonadal white adipose tissue (pWAT) showed similar amount of phospho-2-DG in control as well as iCMp38 MAPKα KO mice (L: Ctrl: 0.03 µmol/g/min ±0.005, KO: 0.03 µmol/g/min ±0.007; M.gastroc: Ctrl:

0.14 µmol/g/min ±0.04, KO: 0.09 µmol/g/min ±0.05; M.soleus: Ctrl: 0.35 µmol/g/min ±0.08, KO: 0.41 µmol/g/min ±0.19; iWAT: Ctrl: 0.05 µmol/g/min ±0.02, KO: 0.06 µmol/g/min ±0.02; pWAT: Ctrl: 0.04 µmol/g/min ±0.03, KO: 0.03 µmol/g/min ±0.01). Organ specific 2-DG uptake is summarized in Figure 4.7C. These experiments were performed and analyzed in Thurl Harris laboratory at the University of Virginia in our collaborators department.

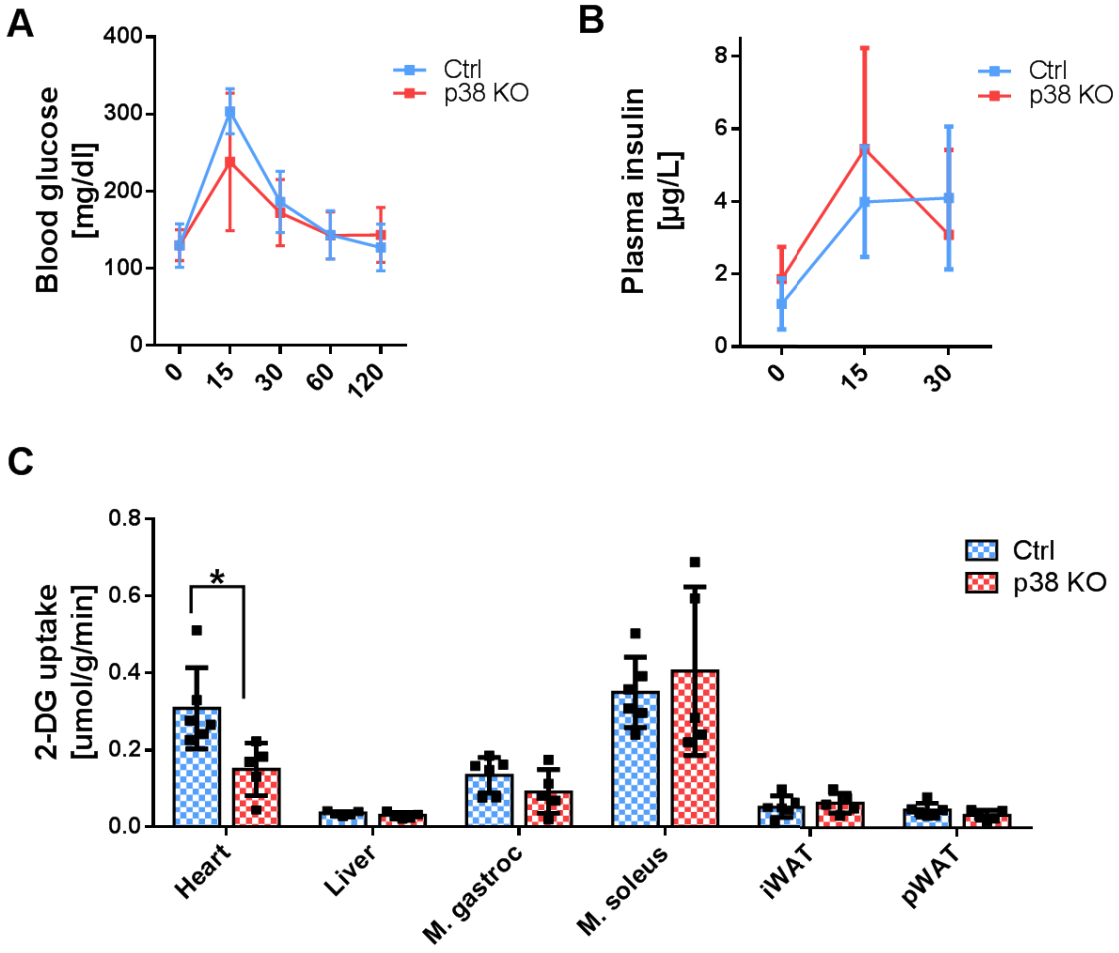

Figure 4.7: Glucose tolerance test performed with using [^{3}H]-2-deoxyglucose (2-DG) to investigate tissue specific 2-DG uptake

(A) Blood glucose levels are strongly increased at 15 minutes, slowly decreased afterwards and are back at baseline level after 120 minutes in control and iCMp38 MAPKα KO mice. (B) Plasma insulin levels equally raise after 15 minutes and slightly decrease in iCMp38 MAPKα KO mice and remain constant in control mice at 30 minutes. (C) iCMp38 MAPKα KO hearts accumulated significant less phospho-2-DG compared to control hearts, whereas liver (L), *musculus gastrocnemius* (M.gastroc), *musculus soleus* (M.soleus), inguinal white adipose tissue (iWAT) and perigonadal white adipose

tissue (pWAT) show a comparable 2-DG uptake. Data are presented as mean ±SD, n = 5-6. Statistical significance was calculated by using Two-way ANOVA (* $p < 0.05$, ** $p < 0.01$)

4.3 Angiotensin II treatment caused heart failure with strongly impaired heart function in iCMp38 MAPKα KO mice

The iCMp38 MAPKα KO mouse model was already established in our laboratory by Dr. Bottermann. Continuous exposure of the vasoconstrictor angiotensin II (AngII) via osmotic mini pumps rapidly induced a dilative phenotype within 48h in iCMp38 MAPKα KO mice, whereas control mice compensated the increased workload (Bottermann *et al.*, submitted). AngII is a vasoconstrictor and causes hypertension through stimulation of the angiotensin receptor AT_1 in the vascular system resulting in an elevated workload for the heart (Crowley *et al.*, 2006; Oliverio *et al.*, 1997). Long term application of AngII under hyperphysiological conditions (1.5 mg/kg/d) leads to vasoconstriction and subsequently to blood pressure overload, ultimately resulting in heart failure. The timeline of p38 MAPKα deletion and heart failure induction is depicted in Figure 4.8. After KO induction by OH-Tx (as described in section 3.2.) osmotic mini pumps were implanted continuously infusing AngII (1.5 µg/g/d) for 48 hours.

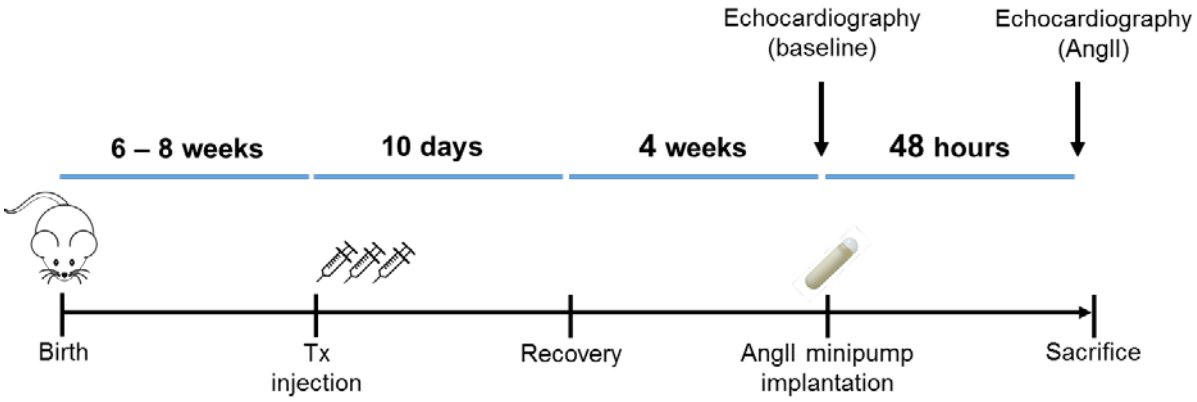

Figure 4.8: Timeline for knock-out establishment and pressure overload induction in iCMp38 MAPKα KO mice

6-8 weeks after birth mice were (i.p.) injected for 10 consecutive days with 500 µL OH-Tamoxifen per day to induce p38 MAPKα KO specifically in cardiomyocytes. After 4 weeks of recovery time echocardiography was performed and AngII mini-osmotic pumps were implanted to continuously infuse AngII (1.5 mg/kg/d). After 48 hours of AngII administration mice were analyzed again using echocardiography and sacrificed to obtain plasma and tissues for subsequent analyses.

The cardiac phenotype of iCMp38 MAPKα KO mice before and 48 hours after the onset of AngII treatment was characterized by echocardiographic analysis and is exemplarily shown in Figure 4.9A. Heart function is summarized in Figure 4.9C-E showing that ejection fraction (EF [%]: Ctrl: 63.6 ±9.2; KO: 59.5 ±7.7, Ctrl AngII: 45.7 ±11.4; KO: 18.5 ±8.9) is significantly reduced in iCMp38 MAPKα KO AngII hearts. The end diastolic volume (EDV [µL]: Ctrl: 84.5 ±13.7; KO: 78.1 ±20.3, Ctrl AngII: 76.9 ±19.4, KO AngII: 125.5 ±14.7) and the end systolic volume (ESV [µL]: Ctrl: 30.5 ±12.2, KO: 32.3 ±13.6, Ctrl AngII: 43.5 ±18.1; KO: 103.0 ±19.8) were significantly increased in iCMp38 MAPKα KO AngII hearts. The body weight over the time period of AngII treatment significantly decreased in control mice (Baseline: 29.1 g ±1.8; AngII: 26.7 g ±1.6) and also iCMp38 MAPKα mice (Baseline: 29.1 g ±2.1; AngII: 24.5 g ±2.3). Interestingly, iCMp38 MAPKα mice lost significant more weight after AngII treatment compared to control animals (Figure 4.9B).

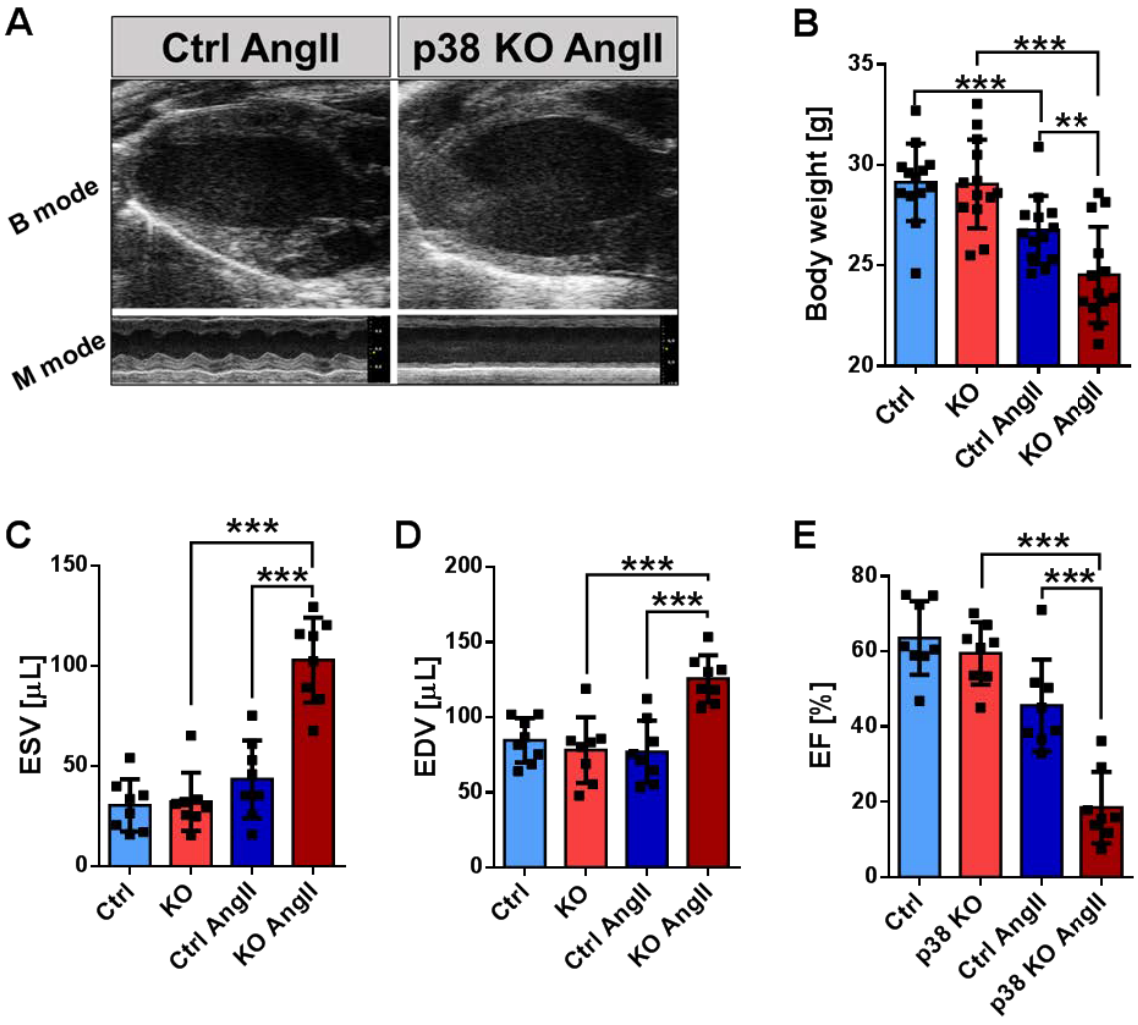

Figure 4.9: Body weight and functional analysis of pressure overloaded iCMp38 MAPKα KO and control hearts induced by 48 hours of AngII treatment

(A) Ultrasound images (parasternal long axis) of control and iCMp38 MAPKα KO hearts after 48 hours of AngII application (upper panel: B mode; lower panel: M Mode). (B) Body weight was significantly reduced in response to AngII in control and even further in iCMp38 MAPKα KO mice. Cardiac dysfunction was clearly demonstrated by significantly increased (C) endsystolic volume (EDV) and (D) enddiastolic volume (ESV) and (E) a severely reduced ejection fraction (EF) in iCMp38 MAPKα KO mice. Data are presented as mean ±SD, n = 8. Statistical significance was calculated using One-way ANOVA (** p <0.01, *** p <0.001).

Moreover, control mice showed that p38 MAPKα$^{T180/Y182}$ phosphorylation is significantly increased in AngII treated animals compared to baseline (by 1.5 ±0.2-fold) confirming the importance of the activation of p38 MAPKα signaling cascade under AngII induced pressure overload (Figure 4.10A-B).

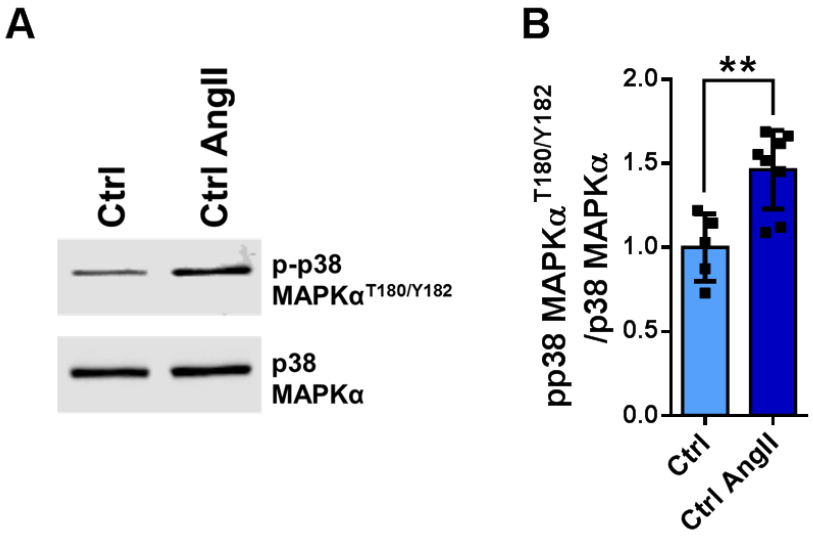

Figure 4.10: Activation of p38 MAPKα signaling in pressure overloaded control hearts

(A) Western blot analysis of control hearts at baseline and after 48 hours of AngII treatment shows (B) significantly increased p38 MAPKα$^{T180/Y182}$ phosphorylation. Data are presented as mean ±SD, n = 5- 12. Statistical significance was calculated using unpaired two-tailed Student's t-test (** p <0.01).

4.4 Pressure overload induced by AngII did not further depress impaired processes in glucose metabolism in iCMp38 MAPKα KO mice

Since cardiac insulin sensitivity is impaired already under baseline conditions in iCMp38 MAPKα KO but does not lead to a functional impairment, the question arose if pressure overload using AngII affects glucose metabolism, particularly insulin dependent substrate preferences. Substrate utilization measurements as described in section 4.2.1, were also performed with AngII hearts stimulated with insulin (described in section 3.5). Quantification of NMR spectra showed that upon insulin stimulation iCMp38 MAPKα KO AngII hearts mainly oxidized fatty acids. In contrast, control AngII hearts preferred glucose after insulin stimulation (Figure 4.11A). The relative fatty acid utilization was significantly increased in iCMp38 MAPKα KO AngII hearts after insulin stimulation (palmitate utilization [%]: Ctrl AngII Ins: 38.9 ±12.3, iCMp38 MAPKα KO AngII Ins: 57.2 ±6.5,). In turn, the relative glucose utilization was reduced in iCMp38 MAPKα KO AngII hearts compared to control AngII hearts (glucose utilization [%]: Ctrl AngII Ins: 49.8 ±13.7,

iCMp38 MAPKα KO AngII Ins: 23.9 ±13.7, p = 0.055). This indicated that the mechanisms adapting cardiac metabolism to increased workload may not work properly, resulting in an impaired metabolic flexibility. Also, insulin sensitivity is reduced in iCMp38 MAPKα KO AngII hearts as already shown for baseline conditions (see section 4.2.1). However, Figure 4.11B illustrates that blood glucose levels after 4 hours of starvation were not affected by metabolic changes in the heart (blood glucose levels [mg/dl]: Ctrl: 95.4 ±10.8, iCMp38 MAPKα KO: 91.3 ±5.6, Ctrl AngII: 83.5 ±11.7, iCMp38 MAPKα KO AngII: 83.6 ±13.2).

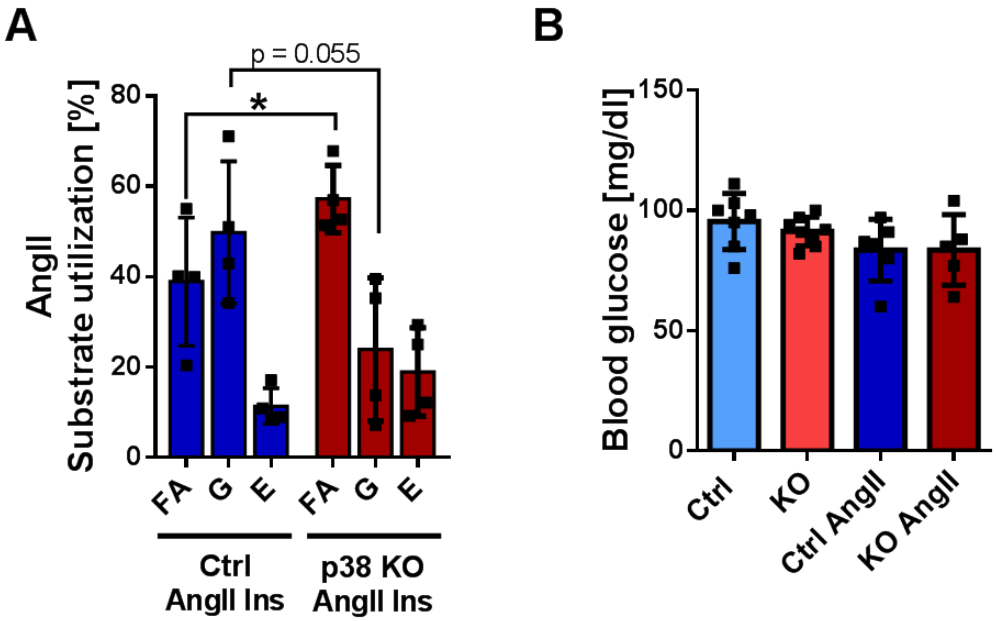

Figure 4.11: Investigation of substrate utilization and blood glucose levels after 48 hours of AngII administration

(A) NMR spectroscopy measurements to identify substrate utilization of labeled palmitate (FA), glucose (G), and endogenous substrates (E). Control hearts prefer glucose, whereas iCMp38 MAPKα KO hearts mainly utilize palmitate after insulin stimulation. Data are presented as mean ±SD, n = 4-5. Statistical significance was calculated using Two-way ANOVA (* $p<0.05$). Measurements were performed in cooperation with Prof. U. Flögel. (B) Blood glucose levels after 4 hours of starvation showed no difference in all measured groups. Data are presented as mean ±SD, n = 5-7.

Glucose uptake by cardiomyocytes is mediated via Glut1 and Glut4, whereas insulin increases glucose uptake by enhancing Glut4 presence in the plasma membrane. Figure 4.12A-B shows cardiac glucose transporter protein levels in all four groups (Baseline

measurements already shown in Figure 4.3). Under baseline conditions Glut1 protein levels were significantly increased (by 1.4 ±0.2-fold) in iCMp38 MAPKα KO, whereas Glut4 protein levels were significantly reduced (to 0.5 ±0.2-fold). Upon AngII treatment Glut1 protein levels were not different between control and iCMp38 MAPKα KO hearts. Glut4 protein levels in AngII-treated iCMp38 MAPKα KO hearts were significantly increased compared to iCMp38 MAPKα KO baseline values (by 1.7 ±0.1-fold) but only up to control baseline level. In addition, Glut4 protein levels were was significantly lower (to 0.7 ±0.06-fold) in iCMp38 MAPKα KO AngII compared to control AngII values. On transcript expression level (Figure 4.12C-D) *Glut1* was increased under baseline conditions (by 1.8 ±0.4-fold) but did not show altered expression levels after AngII treatment. *Glut4* transcript expression, however, was significantly reduced under AngII treatment in iCMp38 MAPKα KO (to 0.1 ±0.05-fold) and control (to 0.4 ±0.2-fold) compared to baseline values. The reduction of *Glut4* expression level was significantly stronger in iCMp38 MAPKα KO AngII compared to control AngII (to additional 0.3 ±0.1-fold).

In summary, these data show that iCMp38 MAPKα KO AngII hearts are not able to increase glucose utilization or increase glucose transporter to enhance glucose uptake under pressure overload conditions.

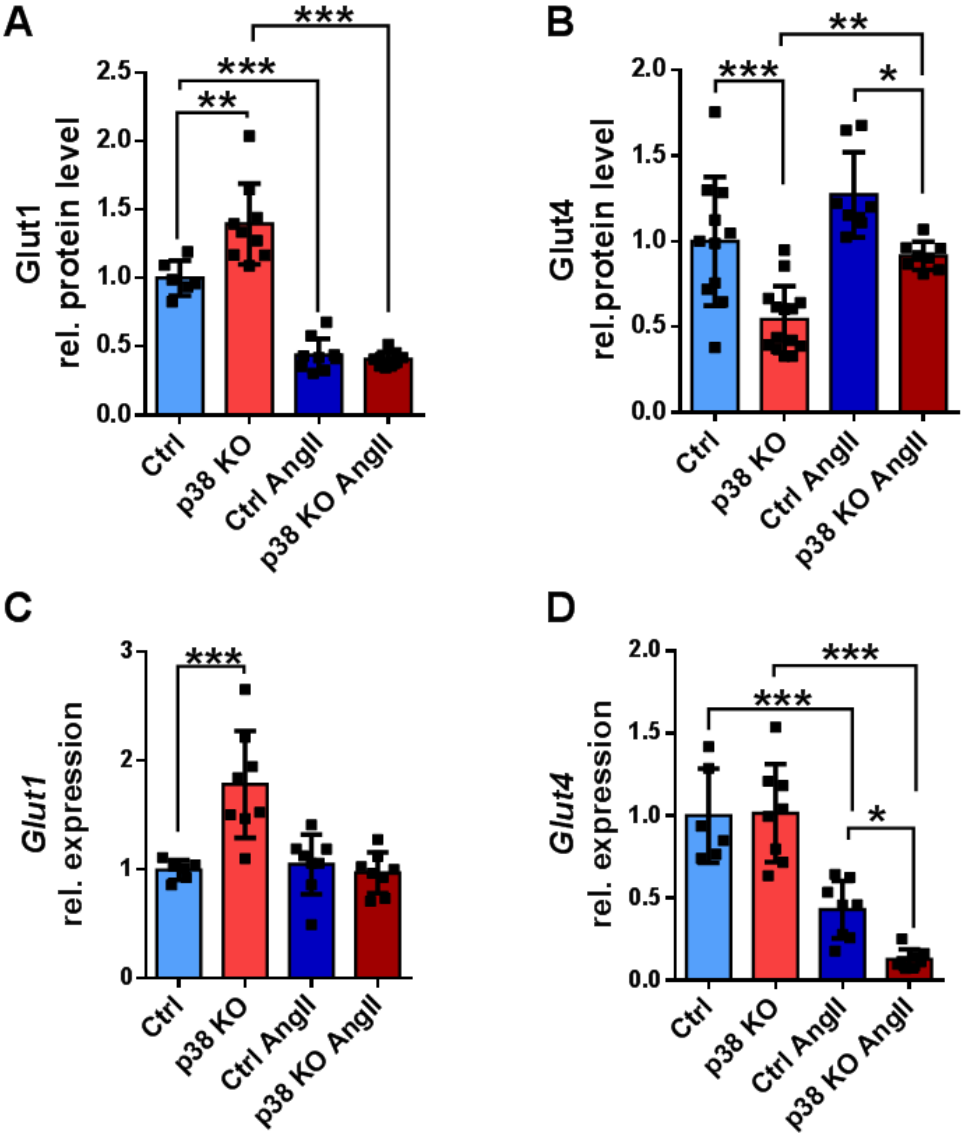

Figure 4.12: Protein and expression levels of Glut1 and Glut4 after AngII treatment

(A) Glut1 protein levels were reduced in response to AngII treatment in control and iCMp38 MAPKα KO hearts, but not on (C) expression level. (B) Glut4 protein levels were significantly reduced in iCMp38 MAPKα KO hearts compared to control at baseline and after AngII treatment. But increased Glut4 protein levels could be measured comparing iCMp38 MAPKα KO hearts at baseline with those after AngII treatment. (D) Relative expression levels of *Glut4* mRNA showed an AngII related downregulation, however, significantly stronger in iCMp38 MAPKα KO hearts. Each value was normalized to baseline value of controls, which was set equal to 1. Data are presented as mean ±SD, n = 8. Statistical significance was calculated using One-way ANOVA (* $p < 0.05$, ** $p < 0.01$, *** $p < 0.001$).

4.5 AngII-induced pressure overload led to lipid droplet accumulation but no changes in protein levels of the fatty acid importing transporter in iCMp38 MAPKα KO AngII hearts

The glucose metabolism in iCMp38 MAPKα KO hearts does not work properly and metabolites from fatty acid oxidation mainly fuel TCA cycle even under insulin stimulated and AngII treated conditions in iCMp38 MAPKα KO mice. Therefore, further experiments were performed to investigate different processes in fatty acid metabolism. Since iCMp38 MAPKα KO hearts mainly utilized fatty acids one may speculate that the rate of fatty acid uptake has to be increased. For initial histological analysis native sections of the heart were stained with sudan red dye marking triglycerides, lipids and lipoproteins. Figure 4.13A (upper panel) shows massive lipid accumulations in cardiac tissue in iCMp38 MAPKα KO AngII but not in control AngII hearts. Furthermore, immunofluorescence staining with anti-perilipin2 (Plin2) antibodies labeling lipid droplets was performed. The Staining shows circular lipid droplets within cardiomyocytes in iCMp38 MAPKα KO AngII hearts (Figure 4.13A, lower panel). These staining were performed in coorperation with Dr. Bottermann. As depicted in Figure 4.13B transcript expression of *Plin2* was significantly increased in iCMp38 MAPKα KO AngII hearts (by 1.9 ±0.7-fold compared to iCMp38 MAPKα KO, by 2.5 ±0.9-fold compared to control AngII). Under basal conditions, the fatty acid transporter FAT/CD36 was not altered in iCMp38 MAPKα KO on protein level. However, after AngII treatment FAT/CD36 protein levels declined compared to baseline values in control (to 0.47 ±0.12-fold) and in iCMp38 MAPKα KO (to 0.7 ±0.07-fold) (Figure 4.13C-D). Also, transcript expression of *FAT/CD36* was significantly downregulated due to AngII exposure in control hearts (to 0.5 ±0.2-fold) and in iCMp38 MAPKα KO hearts (to 0.4 ±0.1-fold) compared to baseline hearts accordingly (Figure 4.13E). These results present the first indications that processes metabolizing fatty acids are altered in iCMp38 MAPKα KO AngII mice. After uptake, fatty acids can be stored as triglyceride or transported into mitochondria. Within the mitochondria, fatty acids undergo beta-oxidation to fuel TCA cycle as acetyl-CoA. To further elucidate the previous results, transcript expression of genes involved in beta-oxidation or genes regulating mitochondrial oxidative phosphorylation was analyzed.

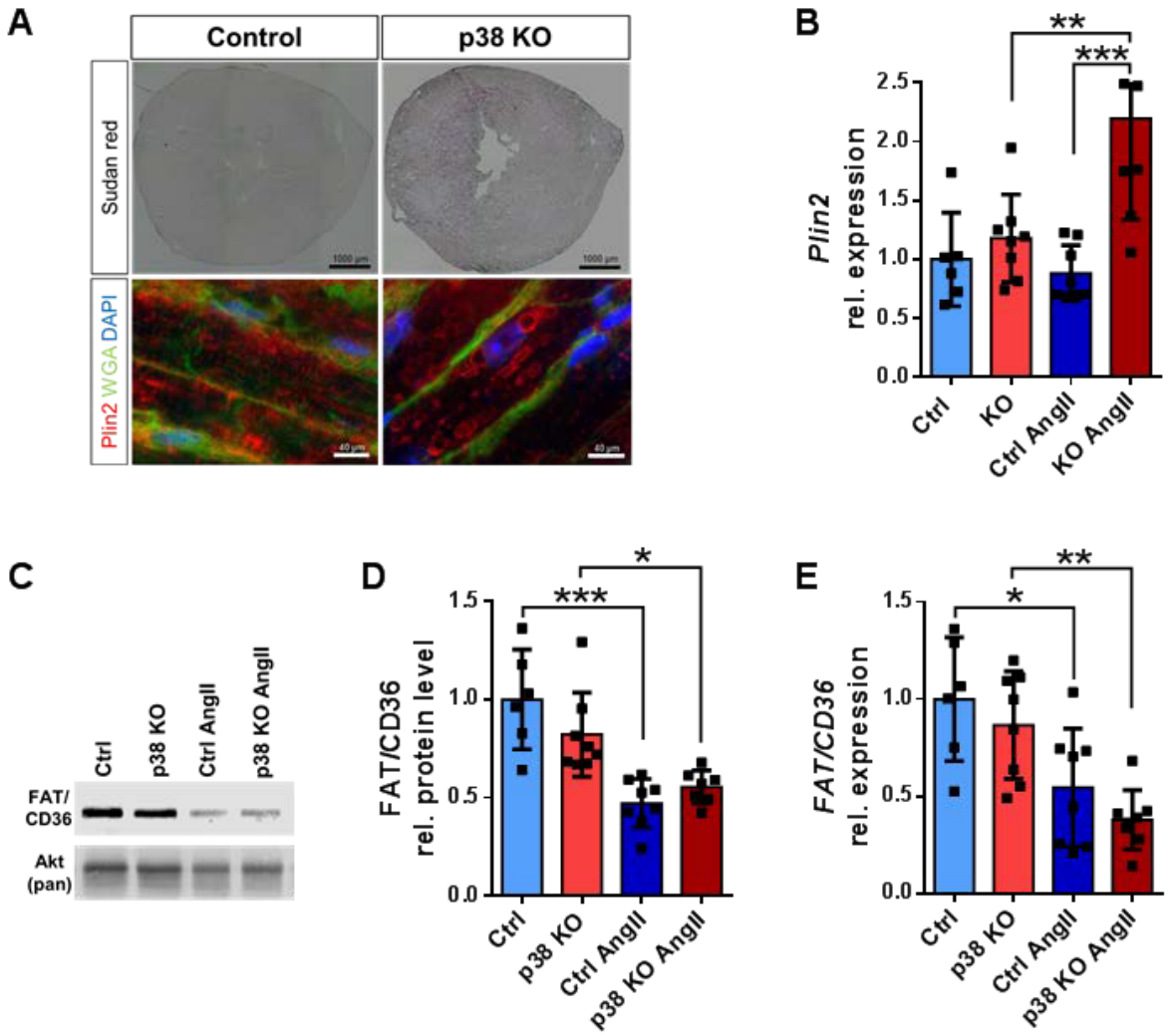

Figure 4.13: Investigation of lipid droplet accumulations and FAT/CD36 protein and transcript levels after 48 hours of AngII exposure

(A) Native sections after sudan red staining (upper panel) show strong lipid droplet accumulation within the heart. Perilipin2 (Plin2) staining demonstrates deposition of lipid droplets in cardiomyocytes detected by immunofluorescence (lower panel; Perilipin2 (red), WGA (green)). These experiments were performed in cooperation with Dr. Bottermann. (B) Relative expression of *Plin2* shows significantly increased transcript expression in iCMp38 MAPKα KO hearts. Protein (C/D) and transcript expression (E) levels of fatty acid translocase (FAT/CD36) exhibit significant reduction in control and iCMp38 MAPKα KO AngII treated groups. Each value was normalized to baseline value of controls, which was set equal to 1. Data are presented as mean ±SD, n = 6-8. Statistical significance was calculated using One-way ANOVA (* $p < 0.05$, ** $p < 0.01$, *** $p < 0.001$).

4.6 Transcript expression profile of genes involved in fatty acid metabolism

Microarray transcript expression profiling prior done in our laboratory by Dr. Bottermann, and Dr. Leitner was performed in cooperation with BMFZ, Heinrich-Heine University Düsseldorf. Transcript analysis using Ingenuity Pathway Analysis (IPA®) software showed that genes summarized under the terms 'mitochondrial dysfunction' and 'oxidative phosphorylation' were highly changed in iCMp38 MAPKα KO AngII hearts (Bottermann *et al*., submitted). In this context the peroxisome proliferator-activated receptor gamma coactivator 1- α (Pgc1-α) was described to be a possible upstream activator highly regulating gene expression of factors involved in these processes. The protein level of Pgc1-α, which is known to be the master regulator of mitochondrial biogenesis, was significantly downregulated in iCMp38 MAPKα KO AngII hearts to 0.41 ±0.1-fold compared to baseline and to 0.53 ±0.1-fold compared to control AngII hearts. Also *Pgc1-α* expression levels were downregulated to 0.25 ±0.04-fold compared to baseline and to 0.19 ±0.03-fold compared to control AngII (Figure 4.14A-C).

When activated Pgc1-α interacts with the peroxisome proliferator-activated receptor-γ (PPARγ). Subsequently, PPARγ activates multiple transcription factors regulating expression pattern of proteins involved in fatty acid storage and glucose metabolism. Transcript expression analysis using qPCR exhibited that relative expression of *PPARγ* was significantly downregulated in iCMp38 MAPKα KO AngII hearts (to 0.5 ±0.29-fold compared to baseline and to 0.45 ±0.26-fold compared to control AngII) (Figure 4.14D). The carnitine palmitoyltransferase II (CPTII), a membrane protein located at the inner mitochondrial membrane, catalyzes the transformation of acylcarnitine to acetyl-CoA and is therefore part of the transportation process of fatty acids into the mitochondria. CPTII relative expression was downregulated due to AngII treatment (to 0.31 ±0.08-fold in iCMp38 MAPKα KO and to 0.41 ±0.08 in control hearts compared to baseline values) (Figure 4.14E). The acetyl-CoA carboxylase 1 (ACC) catalyzes the carboxylation of acetyl-CoA to malonyl-CoA, which represents the rate limiting step in fatty acid synthesis. The acetyl-CoA synthase long chain family member 1 (Acsl1) converting free long-chain fatty acids into fatty acid esters. Thus, ACC and Acsl1 play a key role in lipid biosynthesis and fatty acid degradation. ACC and Acsl1 were significantly downregulated again only after AngII treatment (ACC: to 0.11 ±0.06-fold in iCMp38 MAPKα KO, to 0.1 ±0.06 in control;

Acsl1: to 0.18 ±0.08-fold in iCMp38 MAPKα KO, to 0.36 ±0.17-fold in control) compared to baseline values (Figure 4.14F-G).

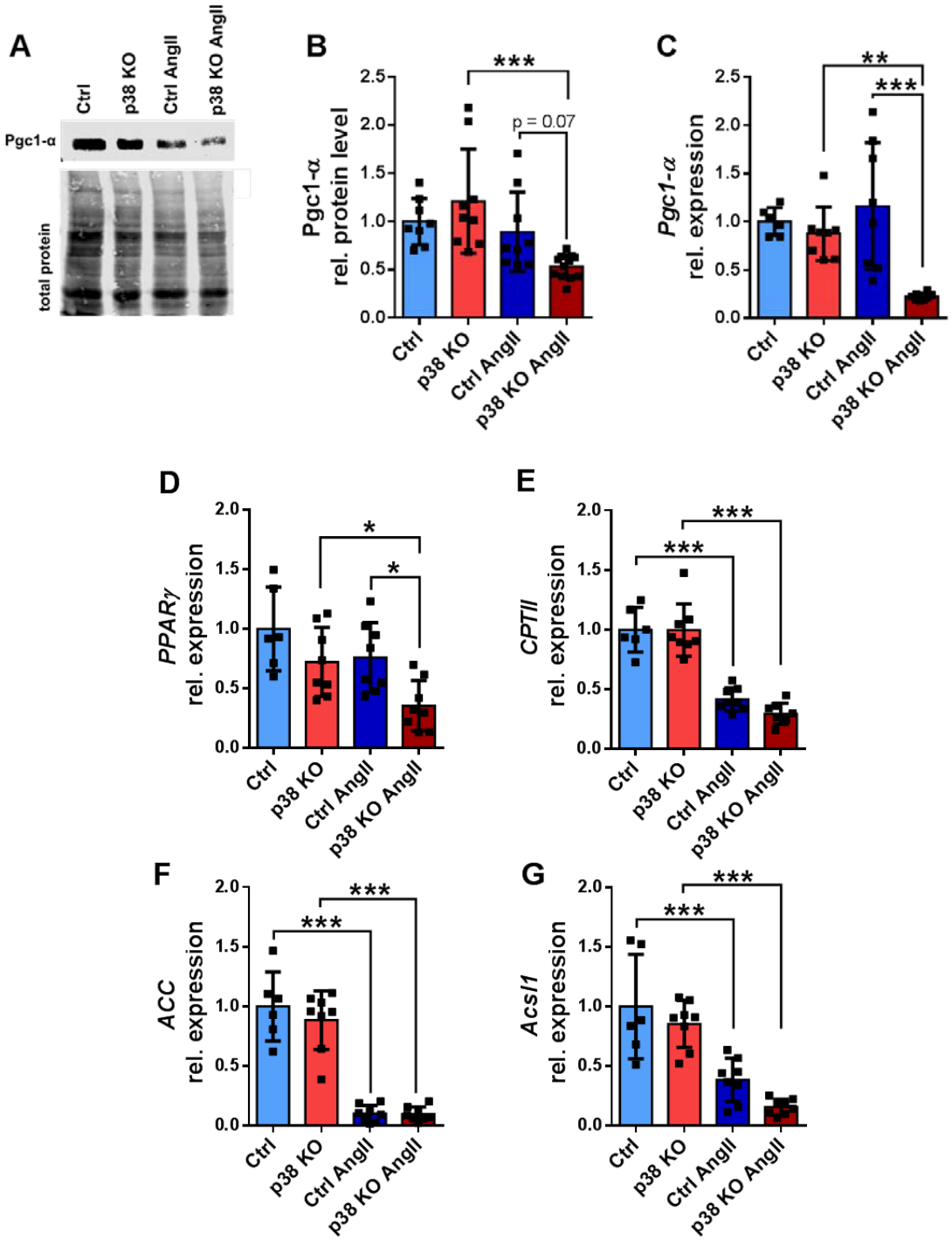

Figure 4.14: Transcript expression profile of factors involved in cardiac lipid metabolism and mitochondrial function

(A) Representative western blot, (B) quantification of relative protein levels and (C) relative expression levels of peroxisome proliferator-activated receptor-γ coactivator 1-α (Pgc1-α). Pgc1-α

protein and expression levels were significantly reduced in iCMp38 MAPKα KO hearts after AngII exposure. (D) Relative transcript expression of peroxisome proliferator-activated receptor-γ (PPARγ) was significantly reduced in iCMp38 MAPKα KO hearts after AngII treatment, whereas expression levels of (E) carnitine palmitoyltransferase II (CPTII), (F) acetyl-CoA carboxylase 1 (ACC), and (G) long-chain-fatty-acid-CoA ligase 1 (Acsl1) are downregulated in response to AngII in control and iCMp38 MAPKα KO hearts. Each value was normalized to baseline value of controls, which was set equal to 1. Data are presented as mean ±SD, n = 6-8. Statistical significance was calculated using One-way ANOVA (* $p < 0.05$, ** $p < 0.01$, *** $p < 0.001$).

These results suggest strong metabolic changes after AngII treatment. In addition, it indicates for a metabolic dysfunction of processes influenced by Pgc1-α including the observed decrease in Glut4 expression (depicted in Figure 4.12). This arose the suggestion that the metabolic dysfunction observed in iCMp38 MAPKα KO hearts is characterized by a reduced glucose uptake and compromised use of fatty acids which might cause the failure to adapt to pressure overload.

4.7 AMPK signaling was not activated in iCMp38 MAPKα KO hearts in response to AngII administration

iCMp38 MAPKα KO hearts showed an impaired insulin response under baseline conditions (shown in section 4.2.1) as well as after AngII treatment (shown in section 4.4). In addition, expression levels of proteins involved in beta-oxidation, transport and storage of fatty acid were altered in iCMp38 MAPKα KO hearts after AngII treatment (see section 4.5). It is known that, besides insulin signaling, metabolic adaptions to various stimuli can be regulated via different signaling pathways. In this context, AMPK signaling is an important regulatory pathway which gets activated by stimuli that increase cellular AMP/ATP ratios. AMPK signaling mediates increased glucose and fatty acid uptake and oxidation by regulating metabolic enzymes through phosphorylation (described in section 1.6).

iCMp38 MAPKα KO mice showed a strong dilative phenotype, maybe due to a state of energy depletion after AngII treatment. That means iCMp38 MAPKα KO hearts are not able to produce sufficient ATP to match increased energy demands due to enhanced workload and to maintain contractility. To investigate AMPKα activation, phosphorylation of the activating phosphorylation site AMPKα^{T172} and the inhibitory phosphorylation site AMPKα^{S485} were measured as surrogated parameters. Immunoblotting showed that

AMPKα^{T172} was surprisingly less phosphorylated, whereas AMPKα^{S485} was higher phosphorylated (Figure 4.15 A and C) in iCMp38 MAPKα KO AngII hearts. Normalization of phosphorylation levels of AMPKα^{T172} and AMPKα^{S485} to total AMPKα protein showed that iCMp38 MAPKα KO AngII hearts have significantly less AMPKα^{T172} phosphorylation compared to control AngII (to 0.66 ±0.17-fold) (Figure 4.15B). In turn, phosphorylation levels of the inhibitory AMPKα^{S485}site were significantly increased by 1.77 ±0.59-fold in iCMp38 MAPKα KO AngII hearts in comparison to AngII treated controls (Figure 4.15D). Thus, AMPKα is not activated in iCMp38 MAPKα KO AngII hearts despite the suggested metabolic need for it.

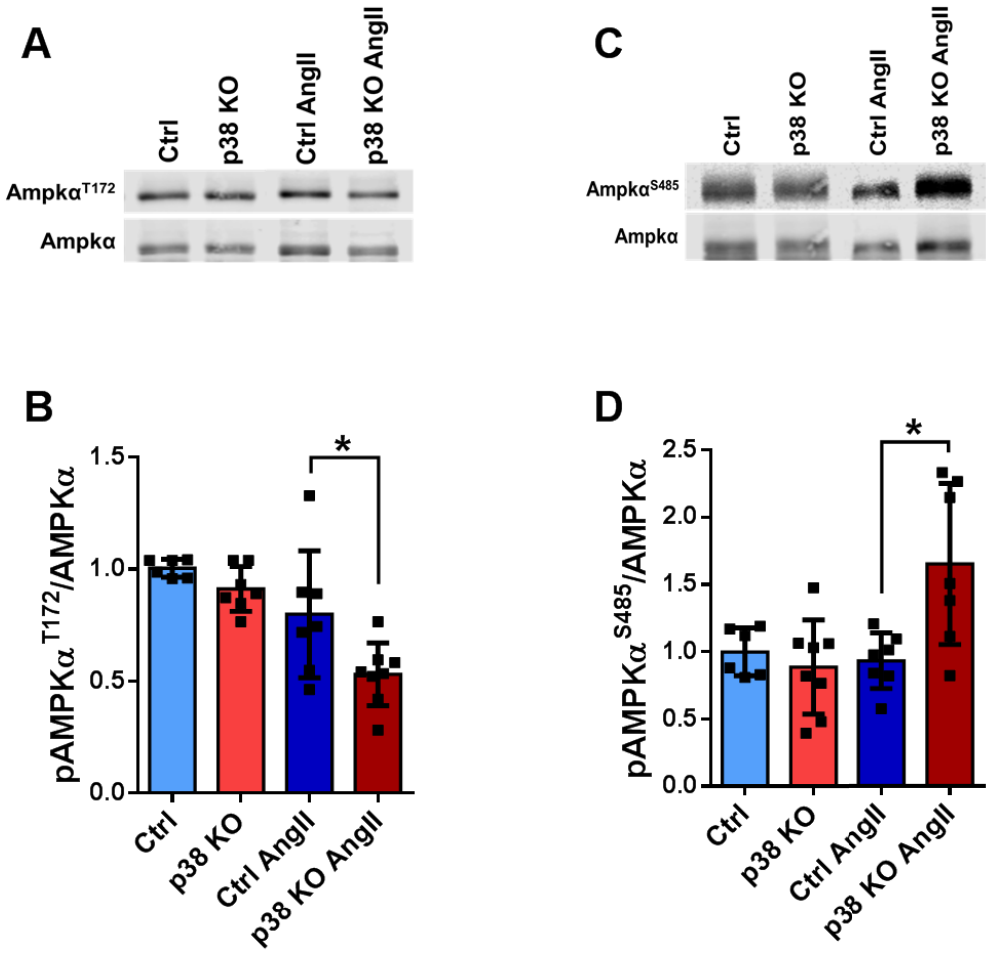

Figure 4.15: Western blot analysis of AMPKα activity in iCMp38 MAPKα KO AngII hearts

(A/B) Phosphorylation levels of the activating phosphorylation site AMPKα^{T172} sre significantly reduced, whereas (C/D) phosphorylation levels of inhibitory phosphorylation site AMPKα^{S485} are significantly higher in iCMp38 MAPKα KO AngII hearts. Each value was normalized to baseline

value of controls, which was set equal to 1. Data are presented as mean ±SD, n = 6-8. Statistical significance was calculated using One-way ANOVA (* $p < 0.05$).

4.8 Akt signaling was highly activated in AngII-induced pressure overloaded iCMp38 MAPKα KO hearts

To investigate the mechanism behind the reduced activity of AMPKα in the hearts of iCMp38 MAPKα KO mice, Akt signaling was analyzed. Akt is an important factor to increase glucose transport by transducing the insulin receptor induced signaling pathway (described in section 1.5). Investigation of Akt signaling in iCMp38 MAPKα KO AngII hearts using western blotting showed that Akt^{S473} and its downstream targets Gsk3-β^{S9} and $Pras40^{T246}$ showed elevated phosphorylation only in iCMp38 MAPKα KO AngII hearts (Figure 4.16A). The calculated ratio of phosphorylated to non-phosphorylated protein levels demonstrated that Akt^{S473} was 2.46 ±0.71-fold higher phosphorylated in iCMp38 MAPKα KO AngII hearts compared to control AngII hearts and 2.71 ±0.78–fold higher compared to iCMp38 MAPKα KO baseline values (Figure 4.16B). Moreover, the selective downstream target of Akt, Pras40, showed significantly higher phosphorylation at threonine 246 in iCMp38 MAPKα KO AngII, by 2.44 ±1.68-fold in comparison to control AngII and by 2.53 ±1.75-fold compared to baseline values (Figure 4.16C). The downstream target of Akt, Gsk3-β^{S9}, was higher phosphorylated in iCMp38 MAPKα KO AngII hearts by 1.39 ±0.44–fold compared to control AngII hearts and significantly higher phosphorylated compared to iCMp38 MAPKα KO baseline values (by 1.8 ±0.57–fold) (Figure 4.16D). However, compared to other proteins of insulin signaling the increase in Gsk3-β^{S9} phosphorylation was relatively low. The regulatory mechanism of Gsk3-β is complex and is mediated via multiple kinases. Besides Akt (Cross *et al.*, 1995), also cAMP-dependent kinase A (PKA) phosphorylates and inactivates Gsk3-β independent of a functional PI3K-Akt pathway (Fang *et al.*, 2000). Interestingly, the Akt substrate of 160 kDa (AS160) was not differentially phosphorylated at its threonine 642 residue in all four groups (Figure 4.16E). The phosphorylation of AS160 at threonine 642 is regulated via distinct signals such as Akt (Peck *et al.*, 2009), contraction (Bruss *et al.*, 2005) and also AMPKα (Kramer *et al.*, 2006). Since AMPKα was shown to have a reduced activity (see Figure 4.15) in iCMp38 MAPKα KO AngII hearts one may speculate an effect on AS160 phosphorylation via the AMPKα-AS160 axis.

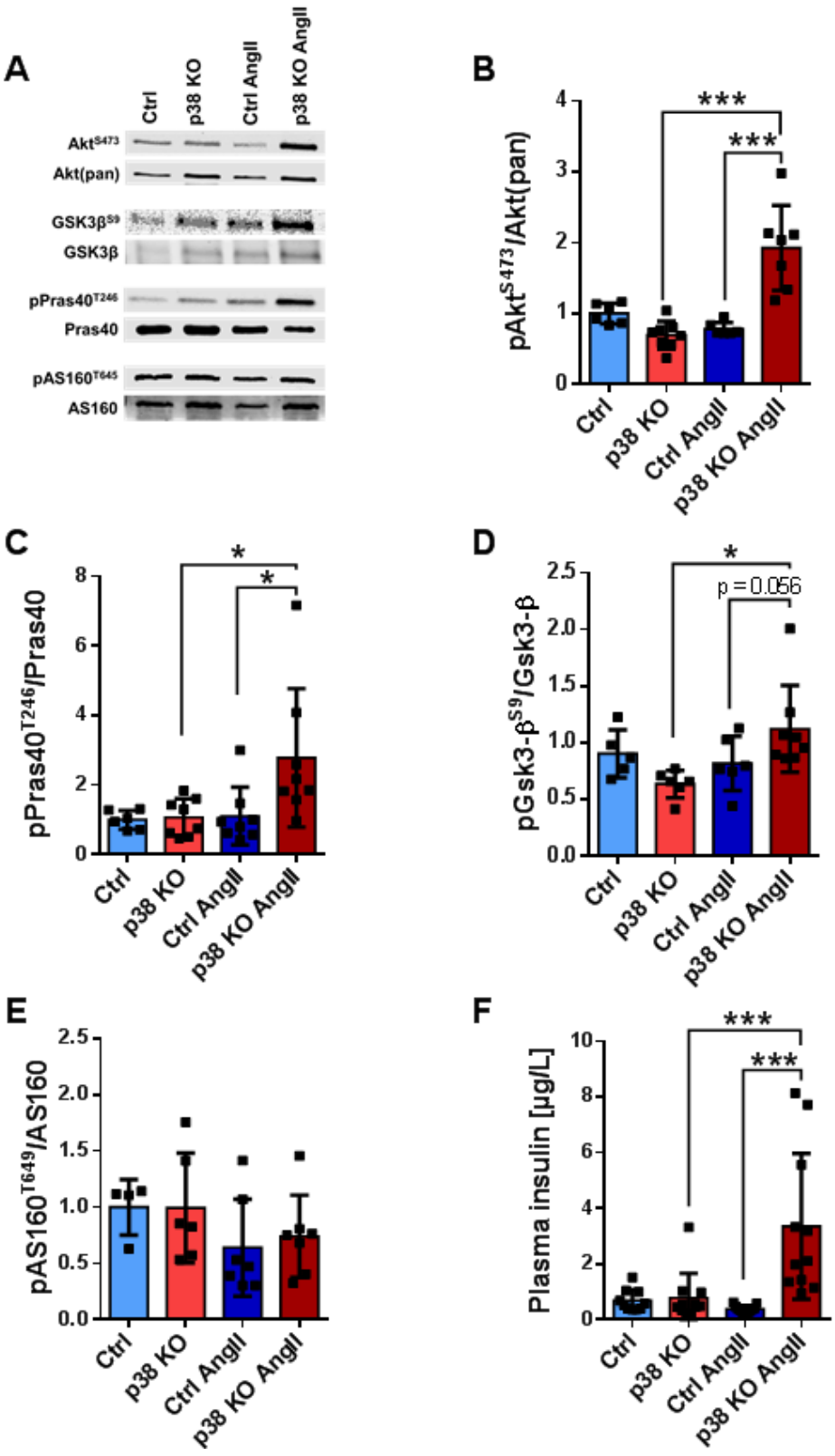

Figure 4.16: Western blot analysis evaluating activation of Akt signaling in iCMp38 MAPKα KO AngII hearts

(A) Investigation of phosphorylation levels of proteins involved in insulin/Akt signal transduction exhibit, that phosphorylation of (B) Akt^{S473}, (C) Gsk3-β^{S9}, (D) Pras40^{T246} but not (E) AS160^{T642} are

significantly higher only in iCMp38 MAPKα KO AngII hearts. Each value was normalized to baseline value of controls, which was set equal to 1. (F) Enzyme-linked immunosorbent assay exhibit that plasma insulin levels were strongly increased in iCMp38 MAPKα KO AngII hearts. Data are presented as mean ±SD, n = 6-8. Statistical significance was calculated using One-way ANOVA (* $p < 0.05$, ** $p < 0.01$, *** $p < 0.001$).

Interestingly, plasma insulin levels were highly increased only in AngII-treated iCMp38 MAPKα KO mice (plasma insulin [µg/L]: Ctrl: 0.68 ±0.36, iCMp38 MAPKα KO: 0.78 ±0.84, Ctrl AngII: 0.38 ±0.12, iCMp38 MAPKα KO AngII: 3.36 ±2.5) as depicted in Figure 4.16F. These results suggest that Akt signaling is activated by high amounts of circulating insulin.

4.9 Investigation of inducible cardiomyocyte specific Akt1 and Akt2 double Knock-out (iCMAkt1/2 KO)

Earlier work has shown that insulin dependent Akt activation inhibits AMPKα activity (Kovacic *et al.*, 2003). To test the influence of Akt on AMPKα activity, a mouse model with an inducible and cardiomyocyte specific KO of Akt1 and Akt2 (iCMAkt1/2 KO) was investigated. Both isoforms are expressed in cardiac tissue and get phosphorylated by insulin receptor mediated signaling cascade. This mouse model was previously established in our laboratory (Gödecke *et al.*, in preparation). To induce the cardiomyocyte specific KO, 12 week old mice ($Akt1^{flox/flox}$, $Akt2^{flox/flox}$ and α-MHC $merCremer^{wt/hemi}$) were injected with OH-Tamoxifen (500 µg/d in peanut oil) (described in section 3.2). After 7 days of recovery time mice were stimulated with i.p. insulin (1 µg/g body weight). As control, litter mates lacking Cre-recombinase were treated equally ($Akt1^{flox/flox}$, $Akt2^{flox/flox}$).

4.9.1 Validation of Akt1/2 KO in the heart and investigation of Akt signaling after insulin stimulation

To first validate the successful deletion of Akt, western blotting analysis was performed. The resulting blots confirmed that the protein levels of Akt were significantly reduced in iCMAkt1/2 KO (to 0.23 ±0.14–fold) compared to control animals (Figure 4.17A und B). After insulin stimulation, Akt^{S473} phosphorylation was significantly increased by

1.82 ±0.26–fold in control animals compared to non-stimulated controls (Figure 4.17C). As Figure 4.17D und E demonstrate, also downstream targets of Akt signaling were significantly higher phosphorylated in insulin stimulated controls compared to control animals injected with vehicle substance (Gsk3-β^{S9}: by 1.67 ±0.84 –fold, AS160^{T642}: by 2.31 ±0.69-fold). As expected, an insulin dependent increase of phosphorylation of Gsk3-β^{S9} and AS160^{T642} was not detectable in the absence of Akt (Figure 4.17A and D-E).

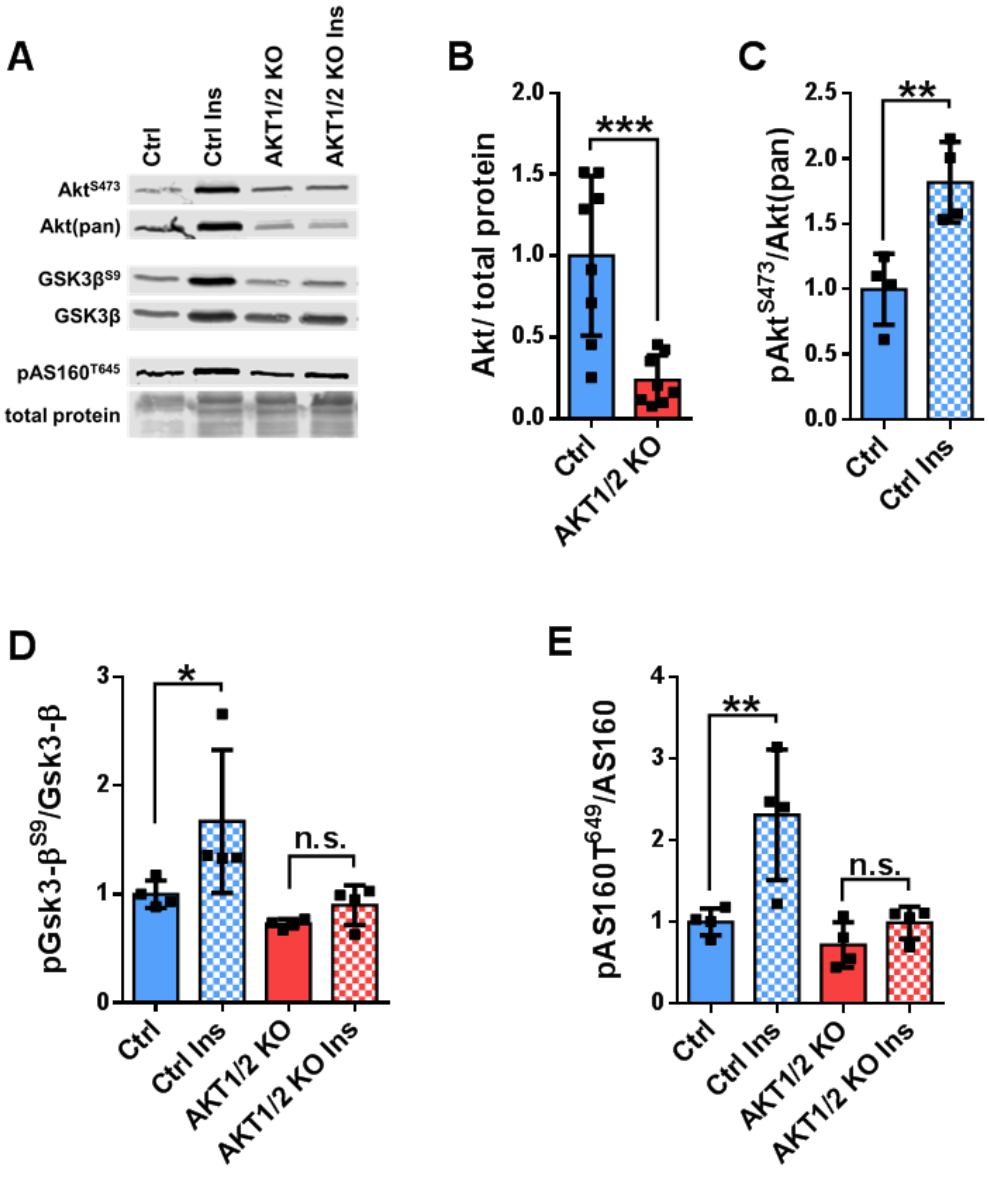

Figure 4.17: Validation of iCMAkt1/2 KO and analysis of Akt signal transduction after insulin stimulation

(A) Immunoblotting of control and iCMAkt1/2 KO hearts before and after insulin stimulation. (B) Protein amount of Akt shows significant reduction in iCMAkt1/2 KO hearts. (C) Phosphorylation

of Akt^{S473} is significantly increased after insulin stimulation in control hearts. Absence of Akt1 and Akt2 leads to loss of insulin induced phosphorylation of (D) Gsk3-β^{S9} and (E) AS160^{T642}. Each value was normalized to baseline value of controls, which was set equal to 1. Data are presented as mean ±SD, n = 4. Statistical significance was calculated using One-way ANOVA (* p <0.05, ** p <0.01, *** p <0.001).

4.9.2 Akt1 and Akt2 deletion led to increased AMPKα protein levels

Further analysis revealed that iCMAkt1/2 KO hearts had significantly increased protein levels of total AMPKα in the basal and insulin stimulated state (iCMAkt1/2 KO: by 1.89 ±0.11–fold; iCMAkt1/2 KO Ins: 1.78 ±0.08–fold) compared to equally treated controls, respectively (Figure 4.18A and B). Since AMPKα signaling shifts metabolic processes to a more catabolic direction the shown increase in total AMPKα protein levels maybe results of an altered energy status in the heart due to the loss of Akt.

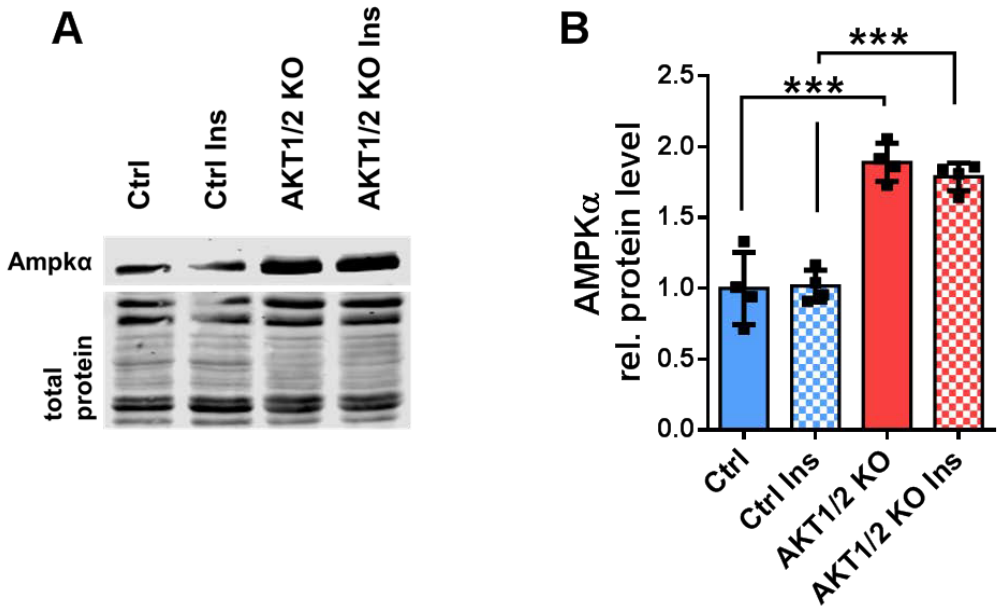

Figure 4.18: Western blot analysis of AMPKα protein levels in iCMAkt1/2 KO

(A) Representative western blot of control and iCMAkt1/2 KO hearts under baseline conditions and after insulin stimulation. (B) Quantification of relative AMPKα protein levels reveale significantly increased protein amount in iCMAkt1/2 KO hearts under baseline and insulin stimulated conditions compared to control hearts, respectively. Each value was normalized to baseline value of controls, which was set equal to 1. Data are presented as mean ±SD, n = 4. Statistical significance was calculated using One-way ANOVA (*** p <0.001).

4.9.3 Loss of Akt1 and Akt2 inhibited reduced AMPKα^{T172} phosphorylation, but had no effect on AMPKα^{S485} phosphorylation after insulin stimulation

In a next step the impact on the absence of Akt1 and Akt2 isoforms on AMPKα phosphorylation after insulin stimulation was analyzed. Interestingly, western blot analysis showed that the activating AMPKα^{T172} phosphorylation was strongly reduced (to 0.35 ±0.15–fold) in control insulin stimulated hearts. In the absence of Akt1 and Akt2, however, this reduction was lost (Figure 4.19A-B), showing the importance of Akt on regulating reduced AMPKα^{T172} phosphorylation. In addition, iCMAkt1/2 KO hearts showed reduced AMPKα^{T172} phosphorylation already under baseline as well as after insulin stimulated conditions that results from significantly increased AMPKα protein levels due to the deletion of Akt1 and Akt2 (depicted in Figure 4.18). To test if the effect of Akt on AMPKα^{T172} phosphorylation is mediated via inhibitory AMPKα^{S485} phosphorylation further western blot analyses were performed. Surprisingly, AMPKα^{S485} phosphorylation was not changed by insulin stimulation or the absence of Akt1 and Akt2 (Figure 4.19C and D). This may indicate that the absence of p38 MAPKα influences reduced AMPKα^{S485} phosphorylation under certain conditions and thus is not affected in iCMAkt1/2 KO hearts where p38 MAPKα is normally present.

These results show that insulin dependent Akt activation influences the reduced AMPKα^{T172} phosphorylation. However, it has no regulatory effect on AMPKα^{S485} phosphorylation.

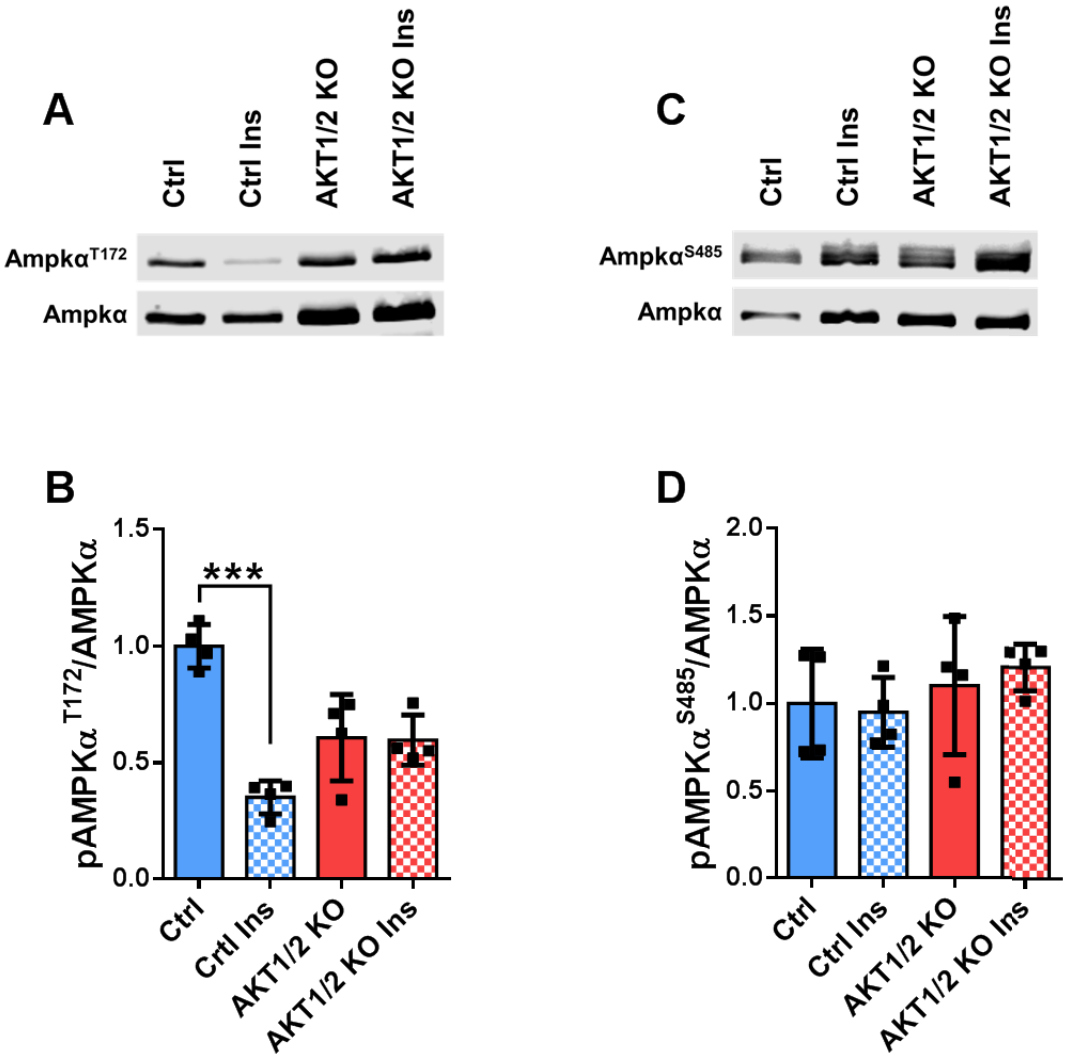

Figure 4.19: Western blot analysis of AMPKα activity in iCMAkt1/2 KO hearts in response to insulin stimulation

(A/B) Phosphorylation levels of the activating phosphorylation site AMPKα^{T172} are significantly reduced in control hearts after insulin stimulation. Reduction in phosphorylation is not detected in iCMAkt1/2 KO after insulin stimulation. (C/D) Phosphorylation levels of inhibitory phosphorylation site AMPKα^{S485} are not altered in all groups independent of the treatment. Each value was normalized to baseline value of controls, which was set equal to 1. Data are presented as mean ±SD, n = 4. Statistical significance was calculated using One-way ANOVA (*** p <0.001).

4.10 Interorgan communication between the failing heart and the pancreatic tissue

As mentioned in section 4.8, iCMp38 MAPKα mice showed highly increased plasma insulin levels after AngII treatment. This finding arose the suggestion about a potential communication between the pancreas and the failing heart. The endocrine pancreas has the major function to regulate blood glucose levels. Its pancreatic islets, also known as islets of Langerhans, secrete hormones like glucagon and insulin in response to changing blood glucose levels. Insulin is released from pancreatic beta-cells to stimulate glucose uptake into body cells (described in section 1.3).

To first validate that p38 MAPKα is only absent in heart but not in pancreatic tissue, western blot analysis was performed using anti-p38 MAPKα antibody. Cardiac protein levels of p38 MAPKα dropped to approximately 26% (see Figure 4.1) in iCMp38 MAPKα KO compared to control level, whereas the p38 MAPKα protein levels in pancreatic tissue remain unaltered (Figure 4.20). Akt(pan) was used as loading control.

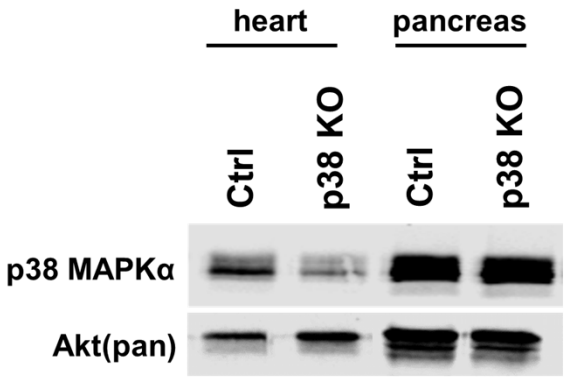

Figure 4.20: Validation of p38 MAPKα KO in heart but not in pancreas

Western blot analysis shows that protein levels of p38 MAPKα are strongly reduced in iCMp38 MAPKα KO hearts compared to control heart but not in pancreatic tissue. As loading control Akt(pan) was used.

4.10.1 Expression levels of *Ins1*, *Ins2* and *Pgc1-α* in pancreatic islets showed no changes in iCMp38 MAPKα KO mice

The hormone insulin is exclusively produced and released from beta-cells located in islets of Langerhans (described in section 1.3.1). Insulin expression and release is triggered by various stimuli including circulating factors secreted by other tissues to achieve cross organ communication. To investigate transcript expression exclusively in islets of Langerhans, first pancreatic tissues were isolated by intraductal perfusion using proteolytic enzymes and afterwards islets were separated using gradient centrifugation (described in section 3.6). After isolation, islets were placed in TRIzol for RNA isolation (see section 3.8.1).

In contrast to humans, the murine pancreas expresses to isoforms of insulin (*Ins1* and *Ins2*), both leading to a functional hormone (Duvillie *et al.*, 1997; Soares *et al.*, 1985). The analysis of mRNA levels of *Ins1* and *Ins2* using qPCR revealed no altered gene expression in iCMp38 MAPKα KO after AngII treatment (Figure 4.21A-B). The comparison of *Ins1* to *Ins2* transcript expression clearly showed that *Ins2* is the higher abundant isoform (4.21D). Its transcript expression levels were more than 1000-fold higher than that of *Ins1*. Additionally, transcript expression of *Pgc1-α* was analyzed. The co-transcription factor Pgc1-α was described to be involved in insulin secretion or processing (De Souza *et al.*, 2005). However, also *Pgc1-α* expression levels was unaltered in all four groups (Figure 4.21C)

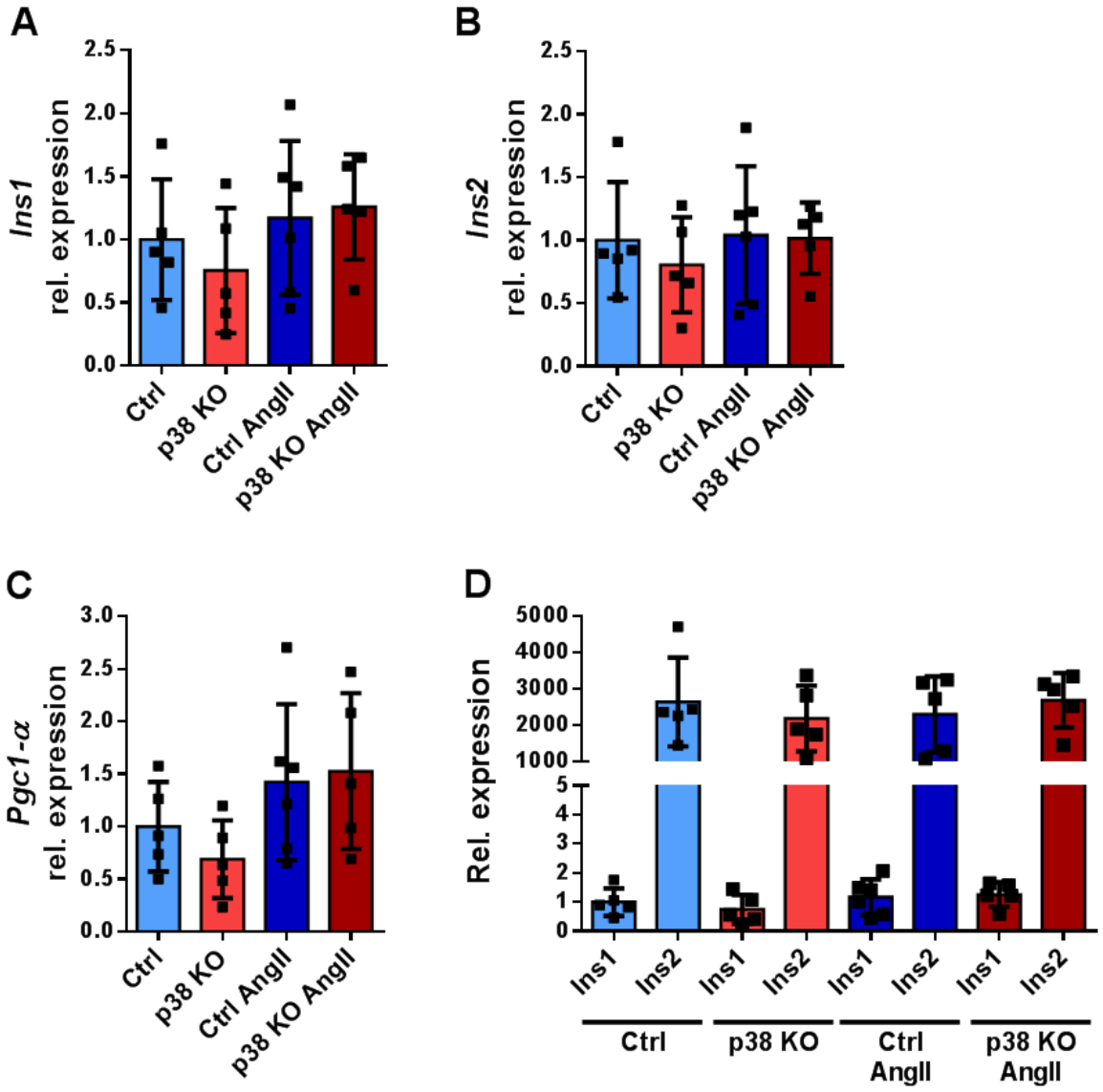

Figure 4.21: Expression profile of Langerhans islets under baseline and AngII treated conditions

Relative expression levels (assessed by qPCR) of (A) *Ins1* and (B) *Ins2* remain unaltered in islets of control and iCMp38 MAPKα KO mice under baseline and AngII treated conditions. (C) Also *Pgc1-α* expression levels are not changed in all four groups. Each value was normalized to baseline value of controls, which was set equal to 1. (D) Comparison of relative expression levels of *Ins1* and *Ins2* clearly shows that *Ins2* is more abundant isoform in pancreatic tissue. Each *Ins2* value was normalized to *Ins1* mean value, which was set equal to 1. Data are presented as mean ±SD, n = 5-6.

4.10.2 Insulin content was reduced in beta-cells of iCMp38 MAPKα KO hearts after AngII-induced pressure overload

Insulin biosynthesis is regulated at both transcriptional and translational level (Fu *et al.*, 2013). After transcript expression insulin is highly processed on translational and posttranslational level (described in section 1.3.1). Briefly, beta-cells synthesize insulin as preproinsulin, which is processed to proinsulin. Proinsulin is then transformed to insulin and C-peptide and stored in secretory vesicles until it gets released (Steiner, 2008). To investigate insulin and proinsulin protein levels in pancreatic beta-cells a combination of ELISA and western blot analysis of whole pancreatic tissue was performed. To measure insulin concentrations, there is a need for a highly sensitive method such as ELISA. Furthermore, to quantify insulin levels to the amount of beta-cells, the tissue lysate was also used to perform immunoblotting using anti-Glut2 antibodies, because the glucose transporter 2 is only expressed in beta-cells within the pancreas. At first, Glut2 content was quantified from the signal intensity normalized to total protein stain (Figure 4.22A). Analysis showed no difference in Glut2-amount in iCMp38 MAPKα KO mice compared to control animals (Ctrl: 1.0 ±0.58; KO: 1.02 ±0.22) (Figure 4.22B). Subsequently, insulin concentrations measured with ELISA were normalized to the Glut2 signal to calculate insulin content in pancreatic beta-cells. This analysis exhibits significantly reduced insulin levels (to 0.33 ±0.11–fold) in iCMp38 MAPKα KO mice after AngII treatment (Figure 4.22C).

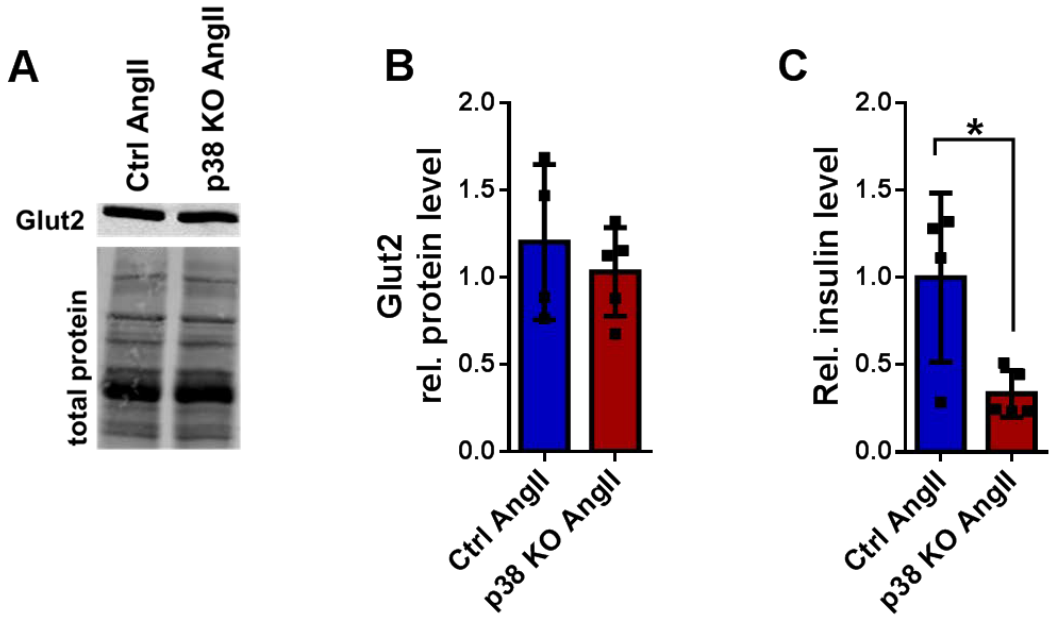

Figure 4.22: Analysis of insulin amount in pancreatic beta-cells

Immunoblotting using anti-Glut2 antibody (A) was used to calculate Glut2 amount and to normalize insulin levels from the same tissue lysate. (B) Calculation of Glut2 amount in pancreatic tissue lysates shows no difference in iCMp38 MAPKα KO AngII mice compared to control animals. (C) Quantification of relative insulin levels exhibit significantly reduced insulin amount in pancreatic beta-cells of iCMp38 MAPKα KO AngII mice. Each value was normalized to AngII value of controls, which was set equal to 1. Data are presented as mean ±SD, n = 4-5. Statistical significance was calculated using unpaired two-tailed Student's t-test (* $p < 0.05$).

5 Discussion

Cardiovascular diseases such as heart failure, myocardial infarction and atherosclerosis have become a social burden, because they are the leading and even increasing cause of morbidity and mortality worldwide. The incidence of cardiovascular complications is strongly increased in people with metabolic disorders such as diabetes mellitus or metabolic syndrome. Thereby, early alterations in cardiac metabolism drive the progression of disorders such as diabetic cardiomyopathy, which represents a comorbidity promoting the establishment of cardiac failure (Boudina *et al.*, 2010; Metra *et al.*, 2017; Stanley *et al.*, 2005; Wende *et al.*, 2017) (described in section 1.7). In general, the heart is capable of consuming different substrates like fatty acids, carbohydrates and lactic acids, and the utilization of these substrates is tightly linked and co-regulated. This extensive metabolic flexibility ensures a high rate of ATP production according to the workload and/or substrate availability (Randle, 1998; Randle *et al.*, 1988). Heart failure is characterized by a permanent shift from the usually preferred fatty acids (FAs) to glucose oxidation (Taegtmeyer, 2002), which has been described as an essential part of a complex cardiac metabolic reprogramming (Akki *et al.*, 2008). Several studies using different models of cardiac hypertrophy and failure have shown that the loss of metabolic flexibility impairs cardiac energy metabolism and drives the progression of heart failure (Bugger *et al.*, 2014; Doenst *et al.*, 2010; Osorio *et al.*, 2002; Riehle *et al.*, 2011; Zhabyeyev *et al.*, 2013). However, the underlying mechanisms promoting the metabolic remodeling still remain unclear.

In this study, the influence of the stress kinase p38 MAPKα on cardiac metabolism under non-stressed conditions and after pressure overload-induced heart failure was investigated. The findings from the present study show that 1) the cardiomyocyte-specific loss of p38 MAPKα leads to cardiac insulin resistance defined by reduced Glut4 amount and impaired Glut4 translocation, 2) p38 MAPKα signaling plays a cardio-protective role in AngII-induced pressure overloaded hearts by regulating metabolic adaptions and 3) the

involvement of an interorgan communication of the failing heart with the endocrine pancreas leads to hyperinsulinemia. These results make the iCMp38 MAPKα KO mouse model a promising system to investigate the role of the stress kinase p38 MAPKα during the establishment of heart failure. Because many of the described aspects are also found in humans, and particularly in patients with diabetes, the present mouse model represents a highly reproducible and reliable model to investigate metabolic remodeling in the early and adaptive phase of heart failure and diabetic cardiomyopathy.

5.1 Deletion of cardiomyocyte-specific p38 MAPKα leads to insulin resistance in the heart

Heart failure in general is known to be frequently associated with an insulin resistance (Riehle *et al.*, 2016) and it was proposed that the p38 MAPKα might be an important regulator linking insulin resistance and cardiovascular dysfunction (Liu *et al.*, 2009).

To investigate substrate utilization under non-stressed conditions and in response to insulin NMR spectroscopy was used (cooperation with Prof. Flögel). This analysis showed that control hearts switch from fatty acid to glucose as main energy source in response to insulin. Interestingly, the loss of cardiac p38 MAPKα impaired the ability to increase glucose utilization relative to fatty acid after insulin stimulation (Figure 4.2). This suggests that iCMp38 MAPKα KO hearts are insulin resistant already under baseline conditions without showing any contractile impairments in the non-stressed state.

In principle, insulin controls the switch between oxidation and uptake/storage of predominantly carbohydrates, but also of fatty acids (Saltiel *et al.*, 2001). It mediates increased glucose uptake by stimulating translocation of the Glut4 glucose transporter to the cell membrane (Kraegen *et al.*, 1993). Insulin also stimulates glycolysis by increasing the activity of PFK-2 (Beitner *et al.*, 1971), and fatty acid uptake is regulated through enhanced surface exposure of FAT/CD36 (Luiken *et al.*, 2002). Concomitantly, fatty acid oxidation is decreased through inhibition of CPTI located at the mitochondrial membrane (Gamble *et al.*, 1997). Thus, the cardiac function of insulin is to regulate anabolic processes when substrate availability is high.

Insulin-mediated actions have been shown to be important in cardiovascular protection. It is well known for decades that insulin with its metabolic modulation can be used to improve recovery from acute myocardial infarction (Gao *et al.*, 2002; Sodi-Pallares *et al.*, 1962; Yu *et al.*, 2011). Therefore, the mechanisms causing insulin resistance in iCMp38 MAPKα KO hearts were intensively analyzed on multiple levels and the findings are described below.

Cardiac glucose uptake is mainly achieved by two glucose transporter isoforms: Glut1 and Glut4. To understand the influence of cardiac p38 MAPKα on cardiac insulin signaling, the insulin dependent Glut4 was analyzed. Interestingly, quantification of protein levels showed significantly reduced Glut4 amounts in iCMp38 MAPKα KO hearts (Figure 4.3). Although Glut4 was downregulated on the protein level, *Glut4* mRNA expression levels were not altered. The decreased Glut4 protein levels can explain at least partly the reduced insulin mediated glucose oxidation without affecting basal insulin independent glucose uptake and cardiac performance, respectively. In that respect, the phenotype of iCMp38 MAPKα KO mice is similar to cardiac specific Glut4 KO mice which exhibited unaltered contractile performance and cardiac glucose uptake shown by baseline measurements in isolated perfused hearts (Abel *et al.*, 1999). Taken together, cardiac p38 MAPKα regulates glucose transporter amounts in the heart. However, Glut4 protein levels seem to be of minor impact on the contractile function under basal conditions (Figure 4.9). Of note, iCMp38 MAPKα KO hearts showed an increased *Glut1* transcript expression (Figure 4.3G) and Glut1 protein levels (Figure 4.3D) which might compensate for the lack of Glut4 under basal conditions.

Upregulation of Glut1 as a compensatory mechanism was also reported in mice lacking Glut4 (Weiss *et al.*, 2002) and after myocardial ischemia in mice with cardiac specific Glut4 deletion (Tian *et al.*, 2001). Furthermore, increased *Glut1* expression levels appeared to maintain basal glucose uptake in animal studies of cardiac hypertrophy (Abel *et al.*, 1999) or transverse aortic constriction (TAC)-induced heart failure (Pereira *et al.*, 2013; Pereira *et al.*, 2014).

Insulin resistance is used as a broad term to describe a variety of pathomechanisms leading to reduced glucose uptake in response to increased concentrations of circulating insulin. Therefore, all steps in the signaling cascade from the insulin receptor to the fusion of Glut4

storage vesicles could be affected by the loss of p38 MAPKα. Insulin induces a variety of downstream effectors by activation of PI3K and its downstream targets including Akt. This raised the question if impaired Akt signal transduction contributes to the underlying mechanism for the insulin resistance in iCMp38 MAPKα KO mice. To analyze insulin signal transduction, control and iCMp38 MAPKα KO hearts were insulin stimulated *ex vivo* (described in section 3.5), and phosphorylation levels of proteins mediating intracellular insulin signal transduction were quantified. Surprisingly, all measured proteins mediating insulin/Akt signaling including $AS160^{T649}$ were phosphorylated in a comparable manner in iCMp38 MAPKα KO and control hearts after insulin stimulation (Figure 4.4). AS160 is located at intracellular storage vesicles and initiates Glut4 storage vesicle exocytosis to the plasma membrane (Ramm *et al.*, 2006). These analyses demonstrated that p38 MAPKα does not affect the canonical insulin receptor mediated signal transduction. It also rules out that mechanisms of insulin resistance identified in other models including the insulin/Akt signal transduction were affected by p38 MAPKα.

Similar to the present findings, other studies showed that insulin signal transduction worked normal although glucose uptake was impaired. Insulin resistance was described without affecting the insulin receptor or IRS1 phosphorylation (Hansen *et al.*, 1998) and insulin induced Akt phosphorylation at serine 473 and threonine 308 was normal in rat skeletal muscle (Tremblay *et al.*, 2001) despite insulin resistance.

The switch from fatty acids to glucose as primary substrate can be realized partially by an increment of Glut4 transporters in the plasma membrane to enhance glucose uptake into the cell to fuel glycolysis and glucose oxidation. Insulin triggered signaling is known to induce the Glut4 movement (Hoffman *et al.*, 2011). As mentioned above, decreased Glut4 protein levels partly explain reduced glucose oxidation in response to insulin stimulation in iCMp38 MAPKα KO hearts. To further characterize reduced insulin sensitivity, subcellular fractionation with *ex vivo* insulin stimulated hearts was performed (described in section 3.5). In contrast to control hearts, the ratio of Glut4 present in the plasma membrane fraction to Glut4 located in storage vesicles was not significantly increased in iCMp38 MAPKα KO hearts after insulin stimulation (Figure 4.6). These findings demonstrate that Glut4 translocation is impaired in iCMp38 MAPKα KO hearts. Importantly, the cardiac insulin resistance was proven to occur *in vivo*. In a glucose tolerance test using radioactive glucose

tracers, iCMp38 MAPKα KO mice showed a significantly reduced glucose uptake by the heart but not by other tissues such as skeletal muscle, liver, or fat depots (Figure 4.7C). This demonstrated that insulin sensitivity of other organs was not compromised in iCMp38 MAPKα KO mice. Importantly, *in vivo* blood glucose and plasma insulin levels behaved in a comparable manner in iCMp38 MAPKα KO and control mice (Figure 4.7A and B). This clearly confirms the cardiac specific effect on insulin sensitivity in the absence of p38 MAPKα defined by impaired Glut4 translocation followed by decreased glucose uptake *in vivo*.

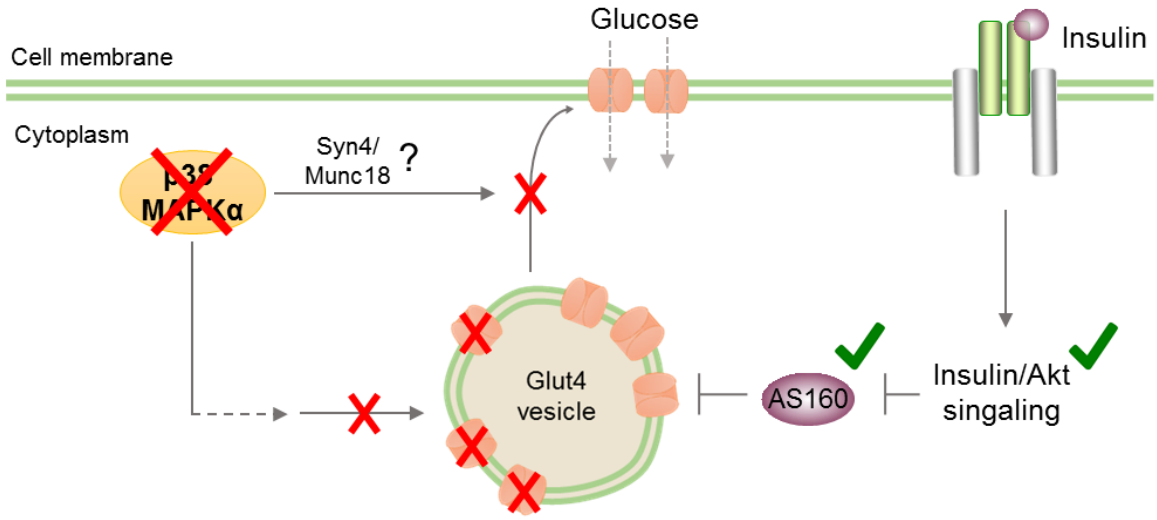

Figure 5.1: Summary of processes mediating cardiac insulin resistance in the absence of p38 MAPKα in cardiomyocytes.

The deletion of p38 MAPKα leads to a reduced Glut4 amount and impaired translocation of Glut4 storage vesicles to the plasma membrane in cardiomyocyte, possibly mediated via Syn4/Munc18, whereas insulin/Akt signal transduction is not affected. Glucose transporter 4 (Glut4), Akt substrate 160 (AS160, p38 mitogen-activated protein kinase α (p38 MAPKα), Syntaxin 4 (Syn4), Mammalian uncoordinated 18 (Munc18).

Although the regulatory function of p38 MAPKα in glucose uptake was shown to be downstream of AS160, the direct target remains to be identified. Possibly, an altered regulation of SNARE proteins mediating intracellular membrane fusion could occur. It was demonstrated before that SNAP23 is required for insulin induced Glut4 translocation by mediating the formation of a complex consisting of syntaxin4 (Syn4) and VAMP2 (Kawanishi *et al.*, 2000). Perturbed *Syn4* expression in the heart of obese mice suggested

that the primary mechanism underlying myocardial insulin resistance in diabetes relates to Glut4 vesicle dysfunction (Cook *et al.*, 2010). In turn, overexpression of *Syn4* in skeletal muscle cells led to an accelerated glucose uptake, which makes *Syn4* a positive regulator of insulin stimulated Glut4 translocation. In the same study Syn4 was also suggested to dictate *Munc18c* expression (Spurlin *et al.*, 2004). Interestingly, p38 MAPKα was suggested to directly phosphorylate and activate Syn4 and Munc18, however, in leukocyte degranulation (Nanamori *et al.*, 2007).

Additionally, other studies proposed that p38 MAPKα mediates the activation of the recruited Glut4 transporter at the membrane without affecting the translocation process itself via a pathway independent of PI3/Akt signaling. However, these data were generated using p38 MAPKα inhibitors, which not specifically affect p38 MAPKα in cardiomyocytes (Somwar *et al.*, 2001; Sweeney *et al.*, 1999) or *in vitro* in 3T3-L1 adipocytes overexpressing dominant-negative p38 MAPKα mutation (Somwar *et al.*, 2002). Nevertheless, an influence on Glut4 activation mediated via p38 MAPKα dependent phosphorylation cannot be precluded from the data in the present study and therefore requires further investigations.

In summary the data provided in this study strongly evidence that p38 MAPKα mainly contributes to cardiac insulin sensitivity by regulating Glut4 protein levels and translocation and thus regulates insulin-mediated myocardial glucose uptake, without affecting insulin/Akt signaling.

5.2 Cardiac p38 MAPKα has a strong cardio-protective role by mediating metabolic remodeling to maintain cardiac performance after AngII-induced pressure overload

Insulin resistance and metabolic remodeling have been excessively investigated and shown to promote cardiac dysfunction and to impair contractility. Likewise, iCMp38 MAPKα KO mice treated with the vasoconstrictor AngII to increase blood pressure showed a severely reduced cardiac function 48 hours after the onset of AngII treatment (Figure 4.9). Hence, the impact of metabolic alterations caused by cardiac p38 MAPKα deletion under stress conditions was investigated. The data provided in this study uncovered novel mechanisms

showing that p38 MAPKα controls metabolic processes on multiple levels during heart failure development.

Insulin resistance is known to be tightly connected with hyperglycemia and hyperinsulinemia. In several studies prolonged hyperglycemia and/or hyperinsulinemia were shown to cause insulin resistance in muscle tissue (Lee *et al.*, 2017) and in circulating cells like monocytes (Vaidyula *et al.*, 2006) in mouse models, but also in insulin-sensitive tissues in humans (Rizza *et al.*, 1985). The present study clearly demonstrates that insulin resistance can result from a p38 MAPKα defect and develops independent of hyperinsulinemia. In consistency with these findings, Ginsberg and colleagues reviewed that hyperinsulinemic conditions should be seen as a marker rather than a direct mediator of insulin resistance (Ginsberg, 2000). Additionally, other studies on non-cardiac tissues demonstrated that locally acting p38 MAPKα may contribute to insulin resistance in skeletal muscle (de Alvaro *et al.*, 2004) and in adipocytes (Bluher *et al.*, 2009; Jager *et al.*, 2007).

iCMp38 MAPKα KO hearts are insulin resistant already under baseline conditions (section 4.2 results and section 5.1). Surprisingly, after AngII treatment iCMp38 MAPKα KO mice showed significantly increased insulin plasma levels compared to AngII-induced pressure overloaded controls demonstrating that heart failure either directly or indirectly affected pancreatic beta-cell function (Figure 4.16F). Blood glucose levels were unaltered in control and iCMp38 MAPKα KO mice under baseline conditions and after AngII exposure (Figure 4.11B). Thus, the cardiac specific insulin resistance did not cause glucose levels to rise. Of note, in the present study hyperinsulinemia only occurred under stress conditions although cardiac insulin resistance was already present in the basal state. The high plasma insulin levels measured in iCMp38 MAPKα KO AngII mice explain the highly increased Akt phosphorylation observed in heart tissue (Figure 4.16B). Moreover, also downstream targets of Akt signaling, such as Gsk3-β and Pras40, were highly phosphorylated (Figure 4.16C and D) demonstrating the full activation of canonical insulin signaling induced by hyperinsulinemia.

Another important impact of this study is the finding that hyperinsulinemia via Akt activation appears to inhibit the activity of AMP-dependent protein kinase α (AMPKα) and may thereby accelerate a metabolic dysfunction in heart failure development. AMPKα is a central regulator of energy homeostasis in the heart. It gets activated under conditions of

cellular energy depletion mediated by various stimuli (described in section 1.6). Following activation, AMPKα signaling ensures sufficient ATP production and contractile function by promoting increased glucose and fatty acid uptake and oxidation by the heart (Abel *et al.*, 2012; Luiken *et al.*, 2003; Russell *et al.*, 1999). Similar to insulin, AMPKα signaling is an alternative inducer of Glut4 translocation and thus increases glucose uptake. In contrast to the insulin pathway which has more anabolic functions, AMPKα shifts the metabolism to a more catabolic direction, which should enhance energy generation. Therefore, it rather had to be expected that AMPKα was activated during heart failure development in AngII treated iCMp38 MAPKα KO mice. Generally, phosphorylation of AMPKα at threonine residue 172 is essential for AMPKα downstream targeting and is usually used as a readout for its activity (Coughlan *et al.*, 2016). However, the data provided in this study indicate a reduced activating AMPKα^{T172} and increased inhibitory AMPKα^{S485} phosphorylation in iCMp38 MAPKα KO AngII hearts (Figure 4.15), suggesting a reduced AMPKα downstream signaling. Insulin stimulation also decreased AMPKα^{T172} phosphorylation in control mice, but not in cardiomyocyte specific Akt1 and 2 (iCMAkt1/2) KO mice (Figure 4.19).

Taken together, the findings shown in the present study clearly demonstrate that the deletion of cardiomyocyte p38 MAPKα leads to hyperinsulinemia in response to cardiac pressure overload induced by AngII. Hyperinsulinemia in turn drives metabolic remodeling in the heart, because intracellular insulin signaling mediated the inhibition of AMPKα signaling via Akt activation in iCMp38 MAPKα KO AngII hearts (Figure 5.2).

The molecular regulation of Akt mediated inhibition of AMPKα was already investigated in various studies: The activation of Akt mediates phosphorylation of AMPKα, which in turn inhibits the activating phosphorylation by LKB1 at threonine 172 and thus blocks AMPKα activity (Kovacic *et al.*, 2003). Furthermore, inactivation of the AMPKα2 isoform has been described to be mediated through inhibitory phosphorylation at the serine residue, 491, and thus impairs insulin signaling in skeletal muscle (Coughlan *et al.*, 2016). However, it was also shown that phosphorylation of serine 491 at the α-subunit alone can inhibit AMPKα activity independent of changes in threonine 172 phosphorylation (Valentine *et al.*, 2014). This shows that the mechanism of Akt influcening AMPKα activity is still unclear and seems to be a multi-factor process. Another interesting finding is that AngII signaling was reported to suppress AMPKα activity in cardiomyocytes by phosphorylation of AMPKα1^{S485} and

AMPKα2^{S491} and subsequently induced hypertrophy (Stuck *et al.*, 2008; Zhang *et al.*, 2017). However, an effect of p38 MAPKα signaling was not considered in these studies and the present study distinctly shows that hyperinsulinemia in AngII treated iCMp38 MAPKα KO mice mediated the effect on AMPKα, because AngII treated control mice exhibit no effect on AMPKα activity.

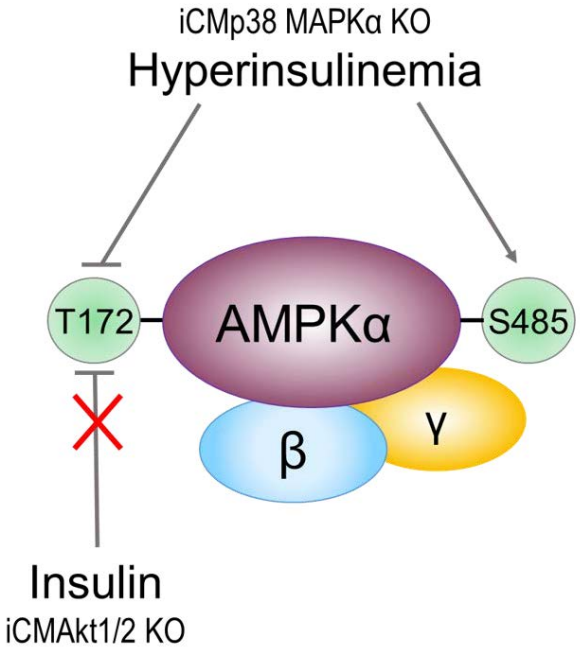

Figure 5.2: Regulation of AMPKα catabolic activity by p38 MAPKα and Akt.

iCMp38 MAPKα KO induced hyperinsulinemia in response to pressure overload leads to decreased AMPKα^{T172} and increased AMPKα^{S485} phosphorylation and thus AMPKα inactivity. iCMAkt1/2 KO leads to loss of insulin mediated reduction in AMPKα^{T172} phosphorylation in the heart.inducible cardiomyocyte (iCM), Knock out (KO), p38 mitogen-activated protein kinase α (p38 MAPKα), AMP-activated protein kinase α (AMPKα).

Hyperinsulinemia dependent Akt phosphorylation is proposed to inhibit AMPKα activity. Thus, despite energy depletion, iCMp38 MAPKα KO AngII hearts are not capable of adapting metabolic processes mediated by AMPKα. Besides regulating Glut4 translocation, AMPK contributes to the regulation of glucose uptake also by promoting *Glut1* expression (Wu *et al.*, 2013). Several studies confirm the finding that AMPK signaling influences glucose uptake via Glut1 and *Glut1* expression was found to be upregulated in the progression from compensated remodeling to overt heart failure post myocardial infarction

(Rosenblatt-Velin *et al.*, 2001). In iCMp38 MAPKα KO mice, however, *Glut1* expression and Glut1 protein levels were unaltered after 48 hours of AngII administration (Figure 4.12A and C). Therefore, one may speculate that insulin dependent inhibition of AMPKα also prevents Glut1 upregulation.

It was further demonstrated that the transcription factor Pgc1-α and its binding partner PPARγ were downregulated in hearts of AngII treated iCMp38 MAPKα KO mice (Figure 4.14C and D). This may have further important implications for the iCMp38 MAPKα KO AngII phenotype. Pgc1-α is a regulator of *Glut4* expression and mediates this effect by MEF2. Therefore, reduced Pgc1-α levels may explain the reduced Glut4 levels also because earlier work in our group has shown that also MEF2 expression is lower in iCMp38 MAPKα KO AngII hearts (Bottermann *et al*., submitted). In addition, pathway analysis had identified Pgc1-α as one of the top regulators which could explain the transcriptomic alterations observed in iCMp38 MAPKα KO AngII hearts (causal network analysis, IPA). The concerted action of Pgc1-α and PPARγ controls mitochondrial biogenesis. The above mentioned transcriptomic analysis revealed that genes summarized under the terms 'mitochondrial dysfunction', 'oxidative phosphorylation' and 'TCA cycle' were substantially affected. The causal network analysis also defined Pgc1-α as a potent factor mainly driving the mitochondrial gene expression alterations in iCMp38 MAPKα KO hearts (Botterman *et al*., submitted). Interestingly, it was published that insulin reduces *Pgc1-α* gene expression (Cho *et al.*, 2001a), which may explain reduced *Pgc1-α* expression found in iCMp38 MAPKα KO hearts after AngII treatment. Additionally, Pcg1-α activation via phosphorylation and thus its transcriptional activity was characterized to be mediated through the p38 MAPKα pathway (Puigserver *et al.*, 2001). Also AMPK and SIRT1 were described to have a major impact on Pgc1-α to transcriptionally regulate metabolic adaptions. AMPK and SIRT1 act as metabolic sensors and mediate Pgc1-α activation through direct phosphorylation (Jager *et al.*, 2007) and deacetylation (Rodgers *et al.*, 2005), respectively.

Furthermore, lipid metabolism seems to be impaired in iCMp38 MAPKα KO mice. As shown by earlier work in our group (Bottermann *et al.*, submitted), iCMp38 MAPKα KO hearts showed severe lipid droplet accumulation after AngII administration. Histological

sections stained for perilipin2 showed a high amount of lipid droplets within the cardiomyocytes of iCMp38 MAPKα KO (Figure 4.13A). In line with these findings, increased perilipin2 mRNA expression levels were found in cardiac tissue of iCMp38 MAPKα KO AngII hearts (Figure 4.13B). Interestingly, ACC, CPTII and Acsl1 expression levels were also reduced in response to AngII in control and iCMp38 MAPKα KO hearts. These results show that these hearts shift their metabolism towards a reduced fatty acid usage under stress conditions. NMR data showed that under AngII treated conditions iCMp38 MAPKα KO hearts still utilize more FAs relative to glucose (Figure 4.11A). This suggests that iCMp38 MAPKα KO hearts fail to maintain ATP production from glucose and fatty acid substrates and even accumulate lipid droplets.

Other studies showed that insulin induced inhibition of AMPKα reduces inhibitory phosphorylation of ACC, which catalyzes the conversion of acetyl-CoA to malonyl-CoA. Malonyl-CoA inhibits CPTI, which appears to exert the rate limiting step of FA import to mitochondria before oxidation (Awan *et al.*, 1993; Gamble *et al.*, 1997; Hardie *et al.*, 2002). Consequently, CPTI inhibition is accompanied by an increase in storage of intracellular TAG, because inhibition of FA oxidation stimulates FA esterification and synthesis (Lopaschuk *et al.*, 2010; Muoio *et al.*, 1999). It would be interesting to analyze if this mechanism contributes to the enhanced lipid storage in iCMp38 MAPKα KO AngII hearts.

In addition, fatty acid uptake was investigated by analyzing the fatty acid transporter FAT/CD36. Interestingly, transcript and protein levels were significantly downregulated in response to AngII in control and in iCMp38 MAPKα KO hearts (Figure 4.13C-E). Insulin and AMPKα both promote translocation of FAT/CD36 to increase fatty acid uptake. Both signaling pathways show an interdependency and are impaired in iCMp38 MAPKα KO AngII hearts. Thus, one may speculate a reduced FAT/CD36 translocation in AngII treated iCMp38 MAPKα KO hearts. However, the FA usage and less the uptake were suggested to have a higher impact on the phenotype in iCMp38 MAPKα KO AngII hearts. Because, it was shown in earlier work that cardiac lipids derived from fat tissue since inhibiting lipolysis clearly reduced lipid accumulation in iCMp38 MAPKα KO AngII hearts (Oenarto, 2020).

Taken together, under stress conditions iCMp38 MAPKα KO hearts exhibit an inhibition of AMPKα activity. These hearts are not able to promote glucose uptake because induction of Glut4 transporter translocation to the plasma membrane is p38 MAPKα dependent or

induced via AMPKα signaling. Moreover, they are unable to enhance fatty acid utilization possibly due to the hyperinsulinemia and Akt-dependent inhibition of the AMPKα- Pgc1-α-mitochondrial axis. This results in a lack of ATP for maintaining cardiac contractility. On the basis of the findings in the present study it was hypothesized that Pgc1-α is a key mediator of p38 MAPKα signaling to increase target expression and to maintain ATP production in pressure overloaded hearts, probably through AMPKα signaling.

Cardiac lipid accumulation in heart failure has already been described in the clinical context. In patients with non-ischemic heart failure a clear connection between cardiac dysfunction and accumulation of intramyocardial lipids has been investigated clinically and experimentally (Sack *et al.*, 1996). 30 % of non-ischemic heart failure patients exhibited high intramyocardial and 44 % moderate intramyocardial lipid deposition, caused by an impaired fatty acid oxidation in heart failure (Sharma *et al.*, 2004). This cardiac lipid accumulation can have toxic effects on cellular function and promote cardiac dysfunction. Therefore, is has been called lipotoxicity (Drosatos *et al.*, 2011; Son *et al.*, 2010).

The loss of cardiac p38 MAPKα results in a phenotype combining insulin resistance and possibly lipotoxicity. Therefore, it represents an interesting model for investigating metabolic remodeling occurring in diabetic cardiomyopathy.

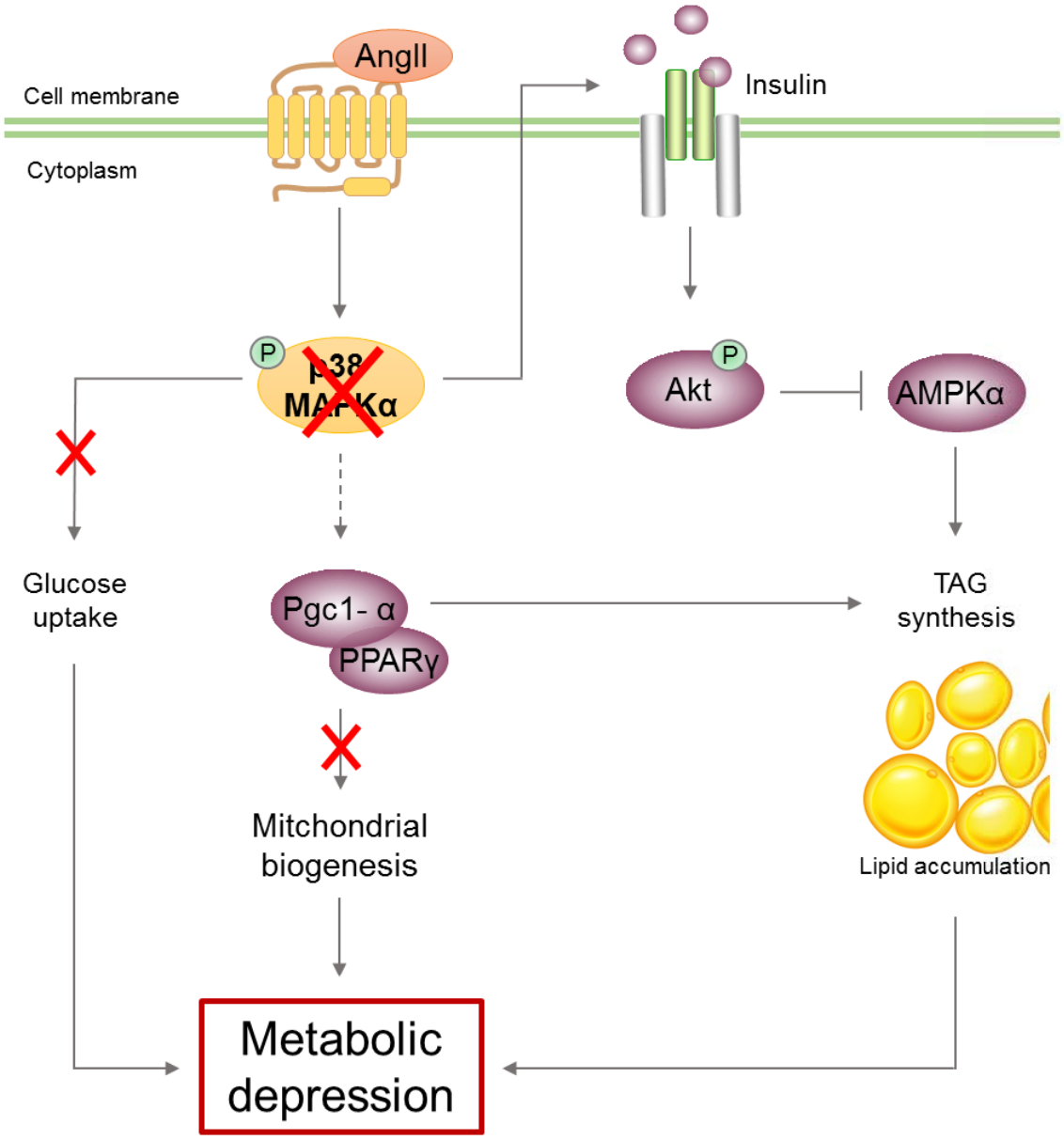

Figure 5.3: Overview of cardiac metabolic remodeling in response to AngII-induced pressure overload in the absence of p38 MAPKα.

AngII-treated iCMp38 MAPKα KO mice develop hyperinsulinemia, which in turn inhibits AMPKα activity via Akt phosphorylation in cardiomyocytes. AMPKα inhibition allows increased TAG synthesis which promotes intramyocardial lipid accumulation. Loss of p38 MAPKα also downregulates glucose uptake and disturbs the activation of Pgc1-α resulting in an impaired mitochondrial biogenesis promoting ATP lack and lipid accumulation. These impaired p38 MAPKα-dependent mechanisms are suggested to drive metabolic depression, strongly promoting cardiac dysfunction. Angiotensin II (AngII), peroxisome proliferator-activated receptor gamma coactivator 1-α (Pgc1-α), persoxisome proliferator-activated receptor γ (PPARγ), triacylglycerol (TAG), p38 mitogen-activated protein kinase α (p38 MAPKα), =AMP-activated protein kinase α (AMPKα).

5.3 The failing heart communicates with the endocrine pancreas

An unexpected result of this work was the finding of elevated plasma insulin levels after AngII-induced pressure overload in iCMp38 MAPKα KO mice (Figure 4.16F). Since insulin is exclusively expressed in beta-cells located in pancreatic islets (Melloul *et al.*, 2002), it was hypothesized that the failing heart promotes insulin secretion by the endocrine pancreas. This effect was not mediated by an ectopic activity of the α-MHC merCremer deleter in beta-cells, because no alteration in p38 MAPKα protein levels were detected in pancreas (Figure 4.20). Also insulin expression was not affected, since *Ins1* and *Ins2* expression levels in isolated pancreatic islets were unaltered in iCMp38 MAPKα KO mice under baseline as well as after AngII treatment (Figure 4.21A and B). Additionally, the transcription factor Pgc1-α, which is suggested to control insulin expression in several organs (Puigserver *et al.*, 2003), was not differentially expressed (Figure 4.21C). Therefore, Pgc1-α related mechanisms which have been demonstrated to contribute to type 2 diabetes in other models (De Souza *et al.*, 2005; Soyal *et al.*, 2006; Valtat *et al.*, 2013; Yoon *et al.*, 2003) seem not to cause the observed hyperinsulinemia.

However, insulin is highly controlled not only on translational but also on posttranslational and secretory level to guarantee a sufficiently large hormone amount and a fast insulin release when needed. Indeed, iCMp38 MAPKα KO mice showed a significantly reduced insulin amount in beta-cells compared to AngII treated controls (Figure 4.22C), suggesting that an enhanced release of stored insulin accounted for the elevated plasma levels. The mechanism underlying the heart failure related insulin secretion in our mouse model is presently unknown.

Increased levels of circulating glucose can be excluded as the trigger to release insulin from pancreatic islets, because blood glucose levels were unaltered in iCMp38 MAPKα KO mice (Figure 4.11B). However, high induction of cytokine expression in iCMp38 MAPKα KO hearts was measured in expression profiling experiments performed previously in our laboratory. Dr. Leitner found that proinflammatory cytokines such as IL-1β, IL-6 and Cxcl5 were upregulated during the 48 hours of AngII treatment in iCMp38 MAPKα KO hearts (Leitner, 2018). Others have shown that elevated serum IL-1β and IL-6 concentrations directly stimulated increased insulin secretion by islets of Langerhans isolated from db/db mice (Spinas *et al.*, 1986). It was described that IL-1β and IL-6 *in vivo* at low concentration and short exposure time stimulated the release of insulin, whereas a high concentration and

long exposure strongly inhibited insulin secretion (Jeong *et al.*, 2002; Palmer *et al.*, 1989). Also, increased Cxcl5 serum levels and Cxcl5 exposure can directly impact islet function (Nunemaker *et al.*, 2014).

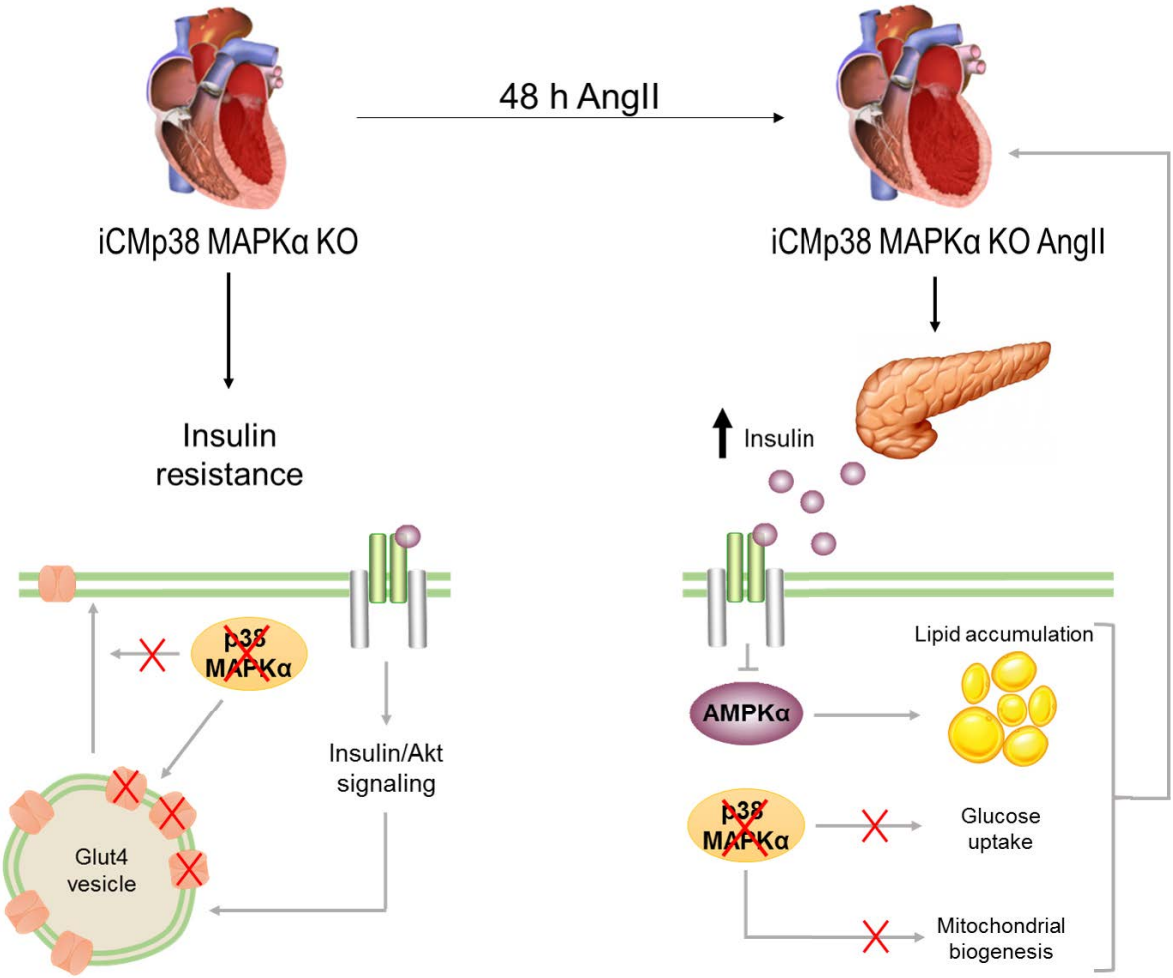

Figure 5.4: Summarized overview of processes influenced by the cardiac p38 MAPKα KO under baseline and AngII-induced stress conditions.

Left side: cardiomyocyte specific deletion of the stress kinase p38 MAPKα promotes cardiac insulin resistance defined by a reduced Glut4 protein amount and an impaired Glut4 translocation without influencing contractile performance or cardiac structure under not stressed conditions.

Right side: 48 hours of AngII exposure leads to a left ventricular dilative phenotype with severely impaired contractility in iCMp38 MAPKα KO hearts. The failing heart communicates with the endocrine pancreas promoting hyperinsulinemia. As a result, insulin induced AMPKα inhibition promotes lipid droplet accumulation. Loss of p38 MAPKα also impairs glucose uptake and reduces mitochondrial biogenesis. inducible cardiomyocyte specific (iCM), Knock out (KO), p38 mitogen-activated protein kinase α (p38 MAPKα), AMP-activated protein kinase α (AMPKα).

In summary, highly increased insulin plasma levels are proposed to be the result of an enhanced insulin release from the endocrine pancreas triggered by secreted factors from the failing heart. However, the regulatory mechanism of insulin secretion in the context of diabetic cardiomyopathy and cardiac dysfunction still remains unclear. Hence, the iCMp38 MAPKα KO mouse model represents a promising tool to further analyze the heart-pancreas interorgan communication and to investigate chemokines/cytokines released from the failing iCMp38 MAPKα KO hearts executing this communication.

5.4 The iCMp38 MAPKα KO mouse model represents a valuable tool to investigate cardiac specific role of p38 MAPKα in the early and adaptive phase of heart failure

In contrast to the frequently used pressure overload model of transverse aortic constriction (TAC), the cardiac specific p38 MAPKα KO mouse model of heart failure using AngII infusion is a less invasive animal model, which develops a highly reproducible dilative phenotype after 48 hours of AngII administration. Under non-stressed conditions, however, cardiac function is not affected (Figure 4.9). The AngII-induced pressure overload leads to a rapidly developing left ventricular dilation without an initial hypertrophic growth. Moreover, these hearts showed a severely impaired heart function (Figure 4.9C-E), which clearly demonstrates that p38 MAPKα activation contributes to the early adaption of the heart to AngII-induced heart failure. In line with this assumption, AngII significantly increased p38 MAPKα phosphorylation in the heart of control animals (Figure 4.10) which maintained cardiovascular performance under AngII-mediated increase in total peripheral resistance.

In general, AngII is an important factor of the renin-angiotensin-aldosterone system (RAAS), which physiologically gets activated upon a drop in blood pressure or loss of volume (described in section 1.1). The activity of the RAAS, however, is also associated with the development of cardiovascular disease (Ayada *et al.*, 2015). Moreover, AngII administration in other animal models markedly increased the levels of phosphorylated p38 MAPKα in the heart (Sugden *et al.*, 1998), in progressive and sustained hypertension, and in cardiac hypertrophy (Bao *et al.*, 2007). In accordance, several studies have already shown that the stress kinase p38 MAPKα is activated in cardiac hypertrophy and remodeling

during the establishment of heart failure (Bao *et al.*, 2007; Nemoto *et al.*, 1998; Sopontammarak *et al.*, 2005). Studies using animal models with TAC-induced pressure overload also showed that p38 MAPKα was clearly activated in the early phase of LV hypertrophy, remodeling, and development of contractile dysfunction (Lei *et al.*, 2008; Liu *et al.*, 2009; Wang *et al.*, 1998). Whereas there is a broad consent in the literature that p38 MAPKα is activated in heart failure, the functional role is still not unambiguously resolved. Some studies showed that p38 MAPKα signaling protects the heart from enhanced hypertrophy in response to pressure overload (Nishida *et al.*, 2004; Zhang *et al.*, 2003). In contrast to our iCMp38 MAPKα KO mouse model, Nishida and colleagues found cardiac hypertrophy, dysfunction and dilation one week after TAC. Our iCMp38 MAPKα KO mice showed a similar cardiac phenotype already within 2 days of AngII-induced pressure overload. Similar to our iCMp38 MAPKα KO AngII mice, a dysregulation of glucose metabolism and significant cell signaling changes were described to be present 1 day after TAC surgery (Kundu *et al.*, 2015).

However, p38 MAPKα was also claimed to be detrimental in myocardial infarction. The targeted inhibition of p38 MAPKα activity reduced cardiac injury and cell death after ischemia-reperfusion experiments *in vivo* (Chai *et al.*, 2008; Kaiser *et al.*, 2004; Li *et al.*, 2006). Thus, the different outcomes require further investigation to find out the reason for the divergent results.

5.5 iCMp38 MAPKα KO mice: A promising mouse model for investigating diabetic cardiomyopathy

Diabetic cardiomyopathy was first described as myocardial changes in diabetic patients without coronary artery disease or hypertension (Rubler *et al.*, 1972). Today it is known that diabetic cardiomyopathy has a long subclinical progression during which the disease proceeds without any outer symptoms. The late appearance of the first visual alterations in cardiac contractility and structure impede an early detection and treatment of the disease (Zamora *et al.*, 2019). Insulin resistance has been excessively described as a main characteristic of diabetic conditions and was mentioned to promote the pathogenesis of diabetic cardiomyopathy (Zamora *et al.*, 2019).

In the basal state iCMp38 MAPKα KO mice showed metabolic alterations such as insulin resistance without diminishing cardiac function. Under stress conditions such as AngII-induced pressure overload iCMp38 MAPKα KO mice exhibited metabolic remodeling leading to e.g. lipotoxicity and metabolic inflexibility. This in turn promoted cardiac dysfunction making iCMp38 MAPKα KO mice a highly promising mouse model to investigate mechanisms promoting a diabetic cardiomyopathy. Moreover, it raises the question to what extent p38 MAPKα contributes to the observed metabolic remodeling.

So far various animal models have been used to investigate diabetic cardiomyopathy. Studies using mice lacking specific factors mediating insulin signal transduction such as insulin receptor (Belke *et al.*, 2002; Boudina *et al.*, 2009), IRS1 and IRS2 (Qi *et al.*, 2013) or PDK1 (Ito *et al.*, 2009) only confirm the relevance of proper insulin signaling for cardiac function. However, due to genetic inactivation of the insulin signaling cascade, these models do not include the systemic influences by elevated insulin levels. Potentially, the hyperinsulinemia in iCMp38 MAPKα KO AngII mice led to inhibition of AMPKα and all the shown consequences for cardiac metabolic adaption to increased workload. Further investigation of the insulin/AMPKα interaction in iCMp38 MAPKα KO and in additional mouse models of heart failure or in human heart disease could show if the identified mechanism is of general and even medical importance. In patients, diabetic cardiomyopathy is often diagnosed as a complication of diabetes, but is also found in heart failure patients without any pre-existing clinical diagnosis of diabetes mellitus (Itzhaki Ben Zadok *et al.*, 2017). This shows that there is an urgent need for further animal models which fulfill various characteristics of diabetic cardiomyopathy.

Taken together, the iCMp38 MAPKα KO model represents the option for a very rapid induction of a left ventricular dilation and a diabetic cardiac phenotype, which comes with advantages but also limitations. The advantage is a precisely inducible phenotype that can help understanding the rapid response of the heart to stress stimuli and metabolic remodeling. The limitation of the mouse model is that it lacks a key feature of human disease since heart failure is a slowly progressing condition which is established over decades.

6 Outlook

The iCMp38 MAPKα KO mouse model emerged as a promising model to investigate metabolic remodeling in the early response to stress stimuli in the heart. It basically offers many possibilities to investigate the altered metabolism in the non-stressed heart influenced by p38 MAPKα and to analyze metabolic remodeling in the development of heart failure. Additionally, it enables the investigation of heart-failure induced interorgan communication with peripheral tissues, such as skeletal muscle, adipose tissue, and endocrine pancreas. This may offer the opportunity to identify mechanisms to improve therapeutic interventions in heart failure and evaluate novel approaches for an earlier diagnosis.

6.1 Approaches to further investigate influence of p38 MAPKα on translocation of substrate transporters

Loss of p38 MAPKα signaling leads to reduced insulin sensitivity in the heart. It was shown in this study that the reduced insulin response is caused by impaired Glut4 translocation already under baseline conditions but the exact mechanism and the p38 MAPKα targets remain to be identified. Further subcellular fractionation experiments combined with quantitative phosphoproteomics of control and iCMp38 MAPKα KO hearts might represent an unbiased approach to identify p38 MAPKα targets involved in Glut4 translocation. This kind of analysis could also be extended to investigate FAT/CD36 translocation in iCMp38 MAPKα KO hearts under baseline as well as AngII treated conditions since FAT/CD36 also translocates to the membrane in response to insulin.

6.2 Measurements of energy metabolism in the living cell

A large number of mitochondrially located proteins was downregulated on protein and transcription level in pressure overloaded iCMp38 MAPKα KO hearts. To analyze the consequences for key cellular functions such as mitochondrial respiration and glycolysis

oxygen consumption rate (OCR) and extracellular acidification (ECAR) can be measured to provide a more precise definition of metabolic status in these hearts.

6.3 Perspectives to clarify the long distance communication of the failing heart with other organs

As mentioned, heart failure results from and causes a multi-level contribution of different tissues and organs. High amounts of released insulin seem to further worsen cardiac remodeling by inhibiting AMPKα activity through Akt. However, it is not fully clear how the failing heart communicates with other organs. Inflammatory cytokines secreted from the heart are likely factors contributing to the inter organ cross talk.

6.3.1 Assays to measure circulating factors

Analyzing circulating factors from blood (plasma or serum) of iCMp38 MAPKα KO mice would allow to estimate circulating cytokine concentrations for subsequently *in vitro* cell culture experiments. But it would also confirm whether inflammatory cytokines directly modulating insulin release or change expression pattern indirectly influence insulin secretion by pancreatic islets. Since the concentration of circulating factors, especially cytokines are rather low, highly sensitive methods like mass spectrometry should be considered and the effect on insulin secretion can be measured.

6.3.2 *In vitro* approaches to investigate impact of circulating factors

To test the potency of circulating factors secreted by the heart *in vitro* cell culture experiments can be performed. Primary isolated cardiomyocytes and isolated pancreatic islets from iCMp38 MAPKα animals can be cultured for at least two days. Plasma (or serum) collected previously from iCMp38 MAPKα mice could be used to conclude whether humoral factors are sufficient to induce increased insulin secretion.

In a second approach cultured cells could be exposed to eluates collected from hearts (in an isolated perfused Langendorff assay) to investigate factors which are exclusively released from the diseased heart.

6.3.3 Profiling transcript expression in pancreatic islets

Until now only a reduced insulin amount could be detected to be altered in pancreas of iCMp38 MAPKα KO AngII mice compared to control animal. To investigate the whole expression profile of pancreatic tissue from iCMp38 MAPKα KO compared to control animals would provide more insights. It might reveal possible candidates regulating enhanced insulin secretion in response to heart failure.

6.4 Rescue experiments using AAV

The iCMp38 MAPKα KO mouse model also offers the opportunity to perform rescue approaches with candidate genes that might successfully restore a normal phenotype. For this project adeno-associated virus (AAV) vectors with cardiomyocyte specific promotors can be used. AAV-mediated gene expression could be used to increase the amount of proteins essential in regulating energy metabolism (potential candidates are: Glut1, Pgc1-α or AMPKα). These approaches can help to interfere with the progression of heart and prevent a systemic condition affecting whole body. A beneficial effect on cardiac function could be basis for new therapeutic options.

7 References

Abel E.D., Kaulbach H.C., Tian R., Hopkins J.C., Duffy J., Doetschman T., Minnemann T., Boers M.E., Hadro E., Oberste-Berghaus C., Quist W., Lowell B.B., Ingwall J.S., and Kahn B.B. (1999). Cardiac hypertrophy with preserved contractile function after selective deletion of GLUT4 from the heart. *J Clin Invest, 104*(12), 1703-1714.

Abel E.D., O'Shea K.M., and Ramasamy R. (2012). Insulin resistance: metabolic mechanisms and consequences in the heart. *Arterioscler Thromb Vasc Biol, 32*(9), 2068-2076.

Adams R.H., Porras A., Alonso G., Jones M., Vintersten K., Panelli S., Valladares A., Perez L., Klein R., and Nebreda A.R. (2000). Essential role of p38alpha MAP kinase in placental but not embryonic cardiovascular development. *Mol Cell, 6*(1), 109-116.

Akki A., Smith K., and Seymour A.M. (2008). Compensated cardiac hypertrophy is characterised by a decline in palmitate oxidation. *Mol Cell Biochem, 311*(1-2), 215-224.

Alessi D.R., James S.R., Downes C.P., Holmes A.B., Gaffney P.R., Reese C.B., and Cohen P. (1997). Characterization of a 3-phosphoinositide-dependent protein kinase which phosphorylates and activates protein kinase Balpha. *Curr Biol, 7*(4), 261-269.

Allard M.F., Schonekess B.O., Henning S.L., English D.R., and Lopaschuk G.D. (1994). Contribution of oxidative metabolism and glycolysis to ATP production in hypertrophied hearts. *Am J Physiol, 267*(2 Pt 2), H742-750.

Allen M., Svensson L., Roach M., Hambor J., McNeish J., and Gabel C.A. (2000). Deficiency of the stress kinase p38alpha results in embryonic lethality: characterization of the kinase dependence of stress responses of enzyme-deficient embryonic stem cells. *J Exp Med, 191*(5), 859-870.

Ammon H.P., Reiber C., and Verspohl E.J. (1991). Indirect evidence for short-loop negative feedback of insulin secretion in the rat. *J Endocrinol, 128*(1), 27-34.

Arany Z., He H., Lin J., Hoyer K., Handschin C., Toka O., Ahmad F., Matsui T., Chin S., Wu P.H., Rybkin, II, Shelton J.M., Manieri M., Cinti S., Schoen F.J., Bassel-Duby R., Rosenzweig A., Ingwall J.S., and Spiegelman B.M. (2005). Transcriptional coactivator PGC-1 alpha controls the energy state and contractile function of cardiac muscle. *Cell Metab, 1*(4), 259-271.

Arany Z., Novikov M., Chin S., Ma Y., Rosenzweig A., and Spiegelman B.M. (2006). Transverse aortic constriction leads to accelerated heart failure in mice lacking PPAR-gamma coactivator 1alpha. *Proc Natl Acad Sci U S A, 103*(26), 10086-10091.

Ashrafian H. (2002). Cardiac energetics in congestive heart failure. *Circulation, 105*(6), e44-45.

Awan M.M., and Saggerson E.D. (1993). Malonyl-CoA metabolism in cardiac myocytes and its relevance to the control of fatty acid oxidation. *Biochem J, 295 (Pt 1)*(Pt 1), 61-66.

Ayada C., Toru U., and Korkut Y. (2015). The relationship of stress and blood pressure effectors. *Hippokratia, 19*(2), 99-108.

Balaban R.S. (1990). Regulation of oxidative phosphorylation in the mammalian cell. *Am J Physiol, 258*(3 Pt 1), C377-389.

Bao W., Behm D.J., Nerurkar S.S., Ao Z., Bentley R., Mirabile R.C., Johns D.G., Woods T.N., Doe C.P., Coatney R.W., Ohlstein J.F., Douglas S.A., Willette R.N., and Yue T.L. (2007). Effects of p38 MAPK Inhibitor on angiotensin II-dependent hypertension, organ damage, and superoxide anion production. *J Cardiovasc Pharmacol, 49*(6), 362-368.

Beer M., Seyfarth T., Sandstede J., Landschütz W., Lipke C., Köstler H., von Kienlin M., Harre K., Hahn D., and Neubauer S. (2002). Absolute concentrations of high-energy phosphate metabolites in normal, hypertrophied, and failing human myocardium measured noninvasively with 31P-SLOOP magnetic resonance spectroscopy. *Journal of the American College of Cardiology, 40*(7), 1267-1274.

Behr T.M., Nerurkar S.S., Nelson A.H., Coatney R.W., Woods T.N., Sulpizio A., Chandra S., Brooks D.P., Kumar S., Lee J.C., Ohlstein E.H., Angermann C.E., Adams J.L., Sisko J., Sackner-Bernstein J.D., and Willette R.N. (2001). Hypertensive end-organ damage and premature mortality are p38 mitogen-activated protein kinase-dependent in a rat model of cardiac hypertrophy and dysfunction. *Circulation, 104*(11), 1292-1298.

Beitner R., and Kalant N. (1971). Stimulation of glycolysis by insulin. *J Biol Chem, 246*(2), 500-503.

Belke D.D., Betuing S., Tuttle M.J., Graveleau C., Young M.E., Pham M., Zhang D., Cooksey R.C., McClain D.A., Litwin S.E., Taegtmeyer H., Severson D., Kahn C.R., and Abel E.D. (2002). Insulin signaling coordinately regulates cardiac size, metabolism, and contractile protein isoform expression. *J Clin Invest, 109*(5), 629-639.

Bernardo B.C., Weeks K.L., Pretorius L., and McMullen J.R. (2010). Molecular distinction between physiological and pathological cardiac hypertrophy: experimental findings and therapeutic strategies. *Pharmacol Ther, 128*(1), 191-227.

Betts J.G., DeSaix P., Johnson E., Johnson J.E., Korol O., Kruse D.H., Poe B., Wise J.A., and Young K.A. (2014). Anatomy and physiology.

Bluher M., Bashan N., Shai I., Harman-Boehm I., Tarnovscki T., Avinaoch E., Stumvoll M., Dietrich A., Kloting N., and Rudich A. (2009). Activated Ask1-MKK4-p38MAPK/JNK stress signaling pathway in human omental fat tissue may link macrophage infiltration to whole-body Insulin sensitivity. *Journal of Clinical Endocrinology and Metabolism, 94*, 2507-2515.

Borlaug B.A., and Paulus W.J. (2011). Heart failure with preserved ejection fraction: pathophysiology, diagnosis, and treatment. *Eur Heart J, 32*(6), 670-679.

Boudina S., and Abel E.D. (2007). Diabetic cardiomyopathy revisited. *Circulation, 115*(25), 3213-3223.

Boudina S., and Abel E.D. (2010). Diabetic cardiomyopathy, causes and effects. *Rev Endocr Metab Disord, 11*(1), 31-39.

Boudina S., Bugger H., Sena S., O'Neill B.T., Zaha V.G., Ilkun O., Wright J.J., Mazumder P.K., Palfreyman E., Tidwell T.J., Theobald H., Khalimonchuk O., Wayment B., Sheng X., Rodnick K.J., Centini R., Chen D., Litwin S.E., Weimer B.E., and Abel E.D. (2009). Contribution of impaired myocardial insulin signaling to mitochondrial dysfunction and oxidative stress in the heart. *Circulation, 119*(9), 1272-1283.

Boulton T.G., Nye S.H., Robbins D.J., Ip N.Y., Radziejewska E., Morgenbesser S.D., DePinho R.A., Panayotatos N., Cobb M.H., and Yancopoulos G.D. (1991). ERKs: a family of protein-serine/threonine kinases that are activated and tyrosine phosphorylated in response to insulin and NGF. *Cell, 65*(4), 663-675.

Broadley K. (1979). The Langendorff heart preparation—reappraisal of its role as a research and teaching model for coronary vasoactive drugs. *Journal of Pharmacological Methods, 2*(2), 143-156.

Bruss M.D., Arias E.B., Lienhard G.E., and Cartee G.D. (2005). Increased phosphorylation of Akt substrate of 160 kDa (AS160) in rat skeletal muscle in response to insulin or contractile activity. *Diabetes, 54*(1), 41-50.

Bryant N.J., and Gould G.W. (2011). SNARE proteins underpin insulin-regulated GLUT4 traffic. *Traffic, 12*(6), 657-664.

Bugger H., and Abel E.D. (2014). Molecular mechanisms of diabetic cardiomyopathy. *Diabetologia, 57*(4), 660-671.

Bui A.L., Horwich T.B., and Fonarow G.C. (2011). Epidemiology and risk profile of heart failure. *Nat Rev Cardiol, 8*(1), 30-41.

Chaanine A.H., and Hajjar R.J. (2011). AKT signalling in the failing heart. *Eur J Heart Fail, 13*(8), 825-829.

Chabowski A., Coort S.L., Calles-Escandon J., Tandon N.N., Glatz J.F., Luiken J.J., and Bonen A. (2004). Insulin stimulates fatty acid transport by regulating expression of FAT/CD36 but not FABPpm. *Am J Physiol Endocrinol Metab, 287*(4), E781-789.

Chai W., Wu Y., Li G., Cao W., Yang Z., and Liu Z. (2008). Activation of p38 mitogen-activated protein kinase abolishes insulin-mediated myocardial protection against ischemia-reperfusion injury. *Am J Physiol Endocrinol Metab, 294*(1), E183-189.

Cho H., Mu J., Kim J.K., Thorvaldsen J.L., Chu Q., Crenshaw E.B., 3rd, Kaestner K.H., Bartolomei M.S., Shulman G.I., and Birnbaum M.J. (2001a). Insulin resistance and a diabetes mellitus-like syndrome in mice lacking the protein kinase Akt2 (PKB beta). *Science, 292*(5522), 1728-1731.

Cho H., Thorvaldsen J.L., Chu Q., Feng F., and Birnbaum M.J. (2001b). Akt1/PKBalpha is required for normal growth but dispensable for maintenance of glucose homeostasis in mice. *J Biol Chem, 276*(42), 38349-38352.

Cook S.A., Varela-Carver A., Mongillo M., Kleinert C., Khan M.T., Leccisotti L., Strickland N., Matsui T., Das S., Rosenzweig A., Punjabi P., and Camici P.G. (2010). Abnormal myocardial insulin signalling in type 2 diabetes and left-ventricular dysfunction. *Eur Heart J, 31*(1), 100-111.

Coughlan K.A., Valentine R.J., Sudit B.S., Allen K., Dagon Y., Kahn B.B., Ruderman N.B., and Saha A.K. (2016). PKD1 Inhibits AMPKalpha2 through Phosphorylation of Serine 491 and Impairs Insulin Signaling in Skeletal Muscle Cells. *J Biol Chem, 291*(11), 5664-5675.

Cross D.A., Alessi D.R., Cohen P., Andjelkovich M., and Hemmings B.A. (1995). Inhibition of glycogen synthase kinase-3 by insulin mediated by protein kinase B. *Nature, 378*(6559), 785-789.

Crowley S.D., Gurley S.B., Herrera M.J., Ruiz P., Griffiths R., Kumar A.P., Kim H.S., Smithies O., Le T.H., and Coffman T.M. (2006). Angiotensin II causes hypertension and cardiac hypertrophy through its receptors in the kidney. *Proc Natl Acad Sci U S A, 103*(47), 17985-17990.

Da Silva Xavier G. (2018). The Cells of the Islets of Langerhans. *J Clin Med, 7*(3).

de Alvaro C., Teruel T., Hernandez R., and Lorenzo M. (2004). Tumor necrosis factor alpha produces insulin resistance in skeletal muscle by activation of inhibitor kappaB kinase in a p38 MAPK-dependent manner. *J Biol Chem, 279*(17), 17070-17078.

De Souza C.T., Araujo E.P., Prada P.O., Saad M.J., Boschero A.C., and Velloso L.A. (2005). Short-term inhibition of peroxisome proliferator-activated receptor-gamma coactivator-1alpha expression reverses diet-induced diabetes mellitus and hepatic steatosis in mice. *Diabetologia, 48*(9), 1860-1871.

DeBosch B., Sambandam N., Weinheimer C., Courtois M., and Muslin A.J. (2006). Akt2 regulates cardiac metabolism and cardiomyocyte survival. *J Biol Chem, 281*(43), 32841-32851.

Derijard B., Raingeaud J., Barrett T., Wu I.H., Han J., Ulevitch R.J., and Davis R.J. (1995). Independent human MAP-kinase signal transduction pathways defined by MEK and MKK isoforms. *Science, 267*(5198), 682-685.

Doenst T., Pytel G., Schrepper A., Amorim P., Färber G., Shingu Y., Mohr F.W., and Schwarzer M. (2010). Decreased rates of substrate oxidation ex vivo predict the onset of heart failure and contractile dysfunction in rats with pressure overload. *Cardiovasc Res, 86*, 461-470.

Drosatos K., Bharadwaj K.G., Lymperopoulos A., Ikeda S., Khan R., Hu Y., Agarwal R., Yu S., Jiang H., Steinberg S.F., Blaner W.S., Koch W.J., and Goldberg I.J. (2011). Cardiomyocyte lipids impair beta-adrenergic receptor function via PKC activation. *Am J Physiol Endocrinol Metab, 300*(3), E489-499.

Drucker D.J. (2013). Incretin action in the pancreas: potential promise, possible perils, and pathological pitfalls. *Diabetes, 62*(10), 3316-3323.

Duvillie B., Cordonnier N., Deltour L., Dandoy-Dron F., Itier J.M., Monthioux E., Jami J., Joshi R.L., and Bucchini D. (1997). Phenotypic alterations in insulin-deficient mutant mice. *Proc Natl Acad Sci U S A, 94*(10), 5137-5140.

Dyck J.R., and Lopaschuk G.D. (2006). AMPK alterations in cardiac physiology and pathology: enemy or ally? *J Physiol, 574*(Pt 1), 95-112.

Dzeja P.P., Redfield M.M., Burnett J.C., and Terzic A. (2000). Failing energetics in failing hearts. *Curr Cardiol Rep, 2*(3), 212-217.

Embi N., Rylatt D.B., and Cohen P. (1980). Glycogen synthase kinase-3 from rabbit skeletal muscle. Separation from cyclic-AMP-dependent protein kinase and phosphorylase kinase. *Eur J Biochem, 107*(2), 519-527.

Estall J.L., Kahn M., Cooper M.P., Fisher F.M., Wu M.K., Laznik D., Qu L., Cohen D.E., Shulman G.I., and Spiegelman B.M. (2009). Sensitivity of lipid metabolism and insulin signaling to genetic alterations in hepatic peroxisome proliferator-activated receptor-gamma coactivator-1alpha expression. *Diabetes, 58*(7), 1499-1508.

Fang X., Yu S.X., Lu Y., Bast R.C., Jr., Woodgett J.R., and Mills G.B. (2000). Phosphorylation and inactivation of glycogen synthase kinase 3 by protein kinase A. *Proc Natl Acad Sci U S A, 97*(22), 11960-11965.

Feil R., Brocard J., Mascrez B., LeMeur M., Metzger D., and Chambon P. (1996). Ligand-activated site-specific recombination in mice. *Proc Natl Acad Sci U S A, 93*(20), 10887-10890.

Feil R., Wagner J., Metzger D., and Chambon P. (1997). Regulation of Cre recombinase activity by mutated estrogen receptor ligand-binding domains. *Biochem Biophys Res Commun, 237*(3), 752-757.

Fernandez-Marcos P.J., and Auwerx J. (2011). Regulation of PGC-1alpha, a nodal regulator of mitochondrial biogenesis. *Am J Clin Nutr, 93*(4), 884s-890.

Flogel U., Decking U.K., Godecke A., and Schrader J. (1999). Contribution of NO to ischemia-reperfusion injury in the saline-perfused heart: a study in endothelial NO synthase knockout mice. *J Mol Cell Cardiol, 31*(4), 827-836.

Flogel U., Laussmann T., Godecke A., Abanador N., Schafers M., Fingas C.D., Metzger S., Levkau B., Jacoby C., and Schrader J. (2005). Lack of myoglobin causes a switch in cardiac substrate selection. *Circ Res, 96*(8), e68-75.

Fountain J.H., and Lappin S.L. (2019). Physiology, Renin Angiotensin System. In *StatPearls [Internet]*: StatPearls Publishing.

Fridlyand L.E., and Philipson L.H. (2016). Pancreatic Beta Cell G-Protein Coupled Receptors and Second Messenger Interactions: A Systems Biology Computational Analysis. *PLoS One, 11*(5), e0152869.

Fu Z., Gilbert E.R., and Liu D. (2013). Regulation of insulin synthesis and secretion and pancreatic Beta-cell dysfunction in diabetes. *Curr Diabetes Rev, 9*(1), 25-53.

Gamble J., and Lopaschuk G.D. (1997). Insulin inhibition of 5' adenosine monophosphate-activated protein kinase in the heart results in activation of acetyl coenzyme A carboxylase and inhibition of fatty acid oxidation. *Metabolism, 46*(11), 1270-1274.

Gao F., Gao E., Yue T.L., Ohlstein E.H., Lopez B.L., Christopher T.A., and Ma X.L. (2002). Nitric oxide mediates the antiapoptotic effect of insulin in myocardial ischemia-reperfusion: the roles of PI3-kinase, Akt, and endothelial nitric oxide synthase phosphorylation. *Circulation, 105*(12), 1497-1502.

Garnier A., Fortin D., Deloménie C., Momken I., Veksler V., and Ventura-Clapier R. (2003). Depressed mitochondrial transcription factors and oxidative capacity in rat failing cardiac and skeletal muscles. *J Physiol, 551*(Pt 2), 491-501.

Gaykema R.P., Newmyer B.A., Ottolini M., Raje V., Warthen D.M., Lambeth P.S., Niccum M., Yao T., Huang Y., Schulman I.G., Harris T.E., Patel M.K., Williams K.W., and

Scott M.M. (2017). Activation of murine pre-proglucagon-producing neurons reduces food intake and body weight. *J Clin Invest, 127*(3), 1031-1045.

Gertz E.W., Wisneski J.A., Stanley W.C., and Neese R.A. (1988). Myocardial substrate utilization during exercise in humans. Dual carbon-labeled carbohydrate isotope experiments. *J Clin Invest, 82*(6), 2017-2025.

Ginsberg H.N. (2000). Insulin resistance and cardiovascular disease. *The Journal of clinical investigation, 106*(4), 453-458.

Glatz J.F., Luiken J.J., and Bonen A. (2010). Membrane fatty acid transporters as regulators of lipid metabolism: implications for metabolic disease. *Physiol Rev, 90*(1), 367-417.

Gowans G.J., Hawley S.A., Ross F.A., and Hardie D.G. (2013). AMP is a true physiological regulator of AMP-activated protein kinase by both allosteric activation and enhancing net phosphorylation. *Cell Metab, 18*(4), 556-566.

Grodsky G.M., Batts A.A., Bennett L.L., Vcella C., McWilliams N.B., and Smith D.F. (1963). Effects of Carbohydrates on Secretion of Insulin from Isolated Rat Pancreas. *Am J Physiol, 205*, 638-644.

Grossman W., Jones D., and McLaurin L.P. (1975). Wall stress and patterns of hypertrophy in the human left ventricle. *J Clin Invest, 56*(1), 56-64.

Guillam M.T., Hummler E., Schaerer E., Yeh J.I., Birnbaum M.J., Beermann F., Schmidt A., Deriaz N., and Thorens B. (1997). Early diabetes and abnormal postnatal pancreatic islet development in mice lacking Glut-2. *Nat Genet, 17*(3), 327-330.

Guillemain G., Loizeau M., Pincon-Raymond M., Girard J., and Leturque A. (2000). The large intracytoplasmic loop of the glucose transporter GLUT2 is involved in glucose signaling in hepatic cells. *J Cell Sci, 113 (Pt 5)*, 841-847.

Han J., Lee J.D., Bibbs L., and Ulevitch R.J. (1994). A MAP kinase targeted by endotoxin and hyperosmolarity in mammalian cells. *Science, 265*(5173), 808-811.

Handschin C., Choi C.S., Chin S., Kim S., Kawamori D., Kurpad A.J., Neubauer N., Hu J., Mootha V.K., Kim Y.B., Kulkarni R.N., Shulman G.I., and Spiegelman B.M. (2007). Abnormal glucose homeostasis in skeletal muscle-specific PGC-1alpha knockout mice reveals skeletal muscle-pancreatic beta cell crosstalk. *J Clin Invest, 117*(11), 3463-3474.

Handschin C., and Spiegelman B.M. (2006). Peroxisome proliferator-activated receptor gamma coactivator 1 coactivators, energy homeostasis, and metabolism. *Endocr Rev, 27*(7), 728-735.

Hansen P.A., Han D.H., Marshall B.A., Nolte L.A., Chen M.M., Mueckler M., and Holloszy J.O. (1998). A high fat diet impairs stimulation of glucose transport in muscle. Functional evaluation of potential mechanisms. *J Biol Chem, 273*(40), 26157-26163.

Hardie D.G., and Pan D.A. (2002). Regulation of fatty acid synthesis and oxidation by the AMP-activated protein kinase. *Biochem Soc Trans, 30*(Pt 6), 1064-1070.

Hardie D.G., Scott J.W., Pan D.A., and Hudson E.R. (2003). Management of cellular energy by the AMP-activated protein kinase system. *FEBS Lett, 546*(1), 113-120.

Hardt S.E., and Sadoshima J. (2002). Glycogen synthase kinase-3beta: a novel regulator of cardiac hypertrophy and development. *Circ Res, 90*(10), 1055-1063.

Hawley S.A., Davison M., Woods A., Davies S.P., Beri R.K., Carling D., and Hardie D.G. (1996). Characterization of the AMP-activated protein kinase kinase from rat liver and identification of threonine 172 as the major site at which it phosphorylates AMP-activated protein kinase. *J Biol Chem, 271*(44), 27879-27887.

Hay C.W., and Docherty K. (2006). Comparative analysis of insulin gene promoters: implications for diabetes research. *Diabetes, 55*(12), 3201-3213.

Heimberg H., De Vos A., Pipeleers D., Thorens B., and Schuit F. (1995). Differences in glucose transporter gene expression between rat pancreatic alpha- and beta-cells are correlated to differences in glucose transport but not in glucose utilization. *J Biol Chem, 270*(15), 8971-8975.

Hoffman N.J., and Elmendorf J.S. (2011). Signaling, cytoskeletal and membrane mechanisms regulating GLUT4 exocytosis. *Trends in Endocrinology & Metabolism, 22*(3), 110-116.

Hue L., and Taegtmeyer H. (2009). The Randle cycle revisited: a new head for an old hat. *Am J Physiol Endocrinol Metab, 297*(3), E578-591.

Huss J.M., Imahashi K., Dufour C.R., Weinheimer C.J., Courtois M., Kovacs A., Giguère V., Murphy E., and Kelly D.P. (2007). The nuclear receptor ERRalpha is required for the bioenergetic and functional adaptation to cardiac pressure overload. *Cell Metab, 6*(1), 25-37.

Huss J.M., and Kelly D.P. (2005). Mitochondrial energy metabolism in heart failure: a question of balance. *J Clin Invest, 115*(3), 547-555.

Ionescu-Tirgoviste C., Gagniuc P.A., Gubceac E., Mardare L., Popescu I., Dima S., and Militaru M. (2015). A 3D map of the islet routes throughout the healthy human pancreas. *Sci Rep, 5*, 14634.

Ito K., Akazawa H., Tamagawa M., Furukawa K., Ogawa W., Yasuda N., Kudo Y., Liao C.H., Yamamoto R., Sato T., Molkentin J.D., Kasuga M., Noda T., Nakaya H., and Komuro I. (2009). PDK1 coordinates survival pathways and beta-adrenergic response in the heart. *Proc Natl Acad Sci U S A, 106*(21), 8689-8694.

Itzhaki Ben Zadok O., Kornowski R., Goldenberg I., Klempfner R., Toledano Y., Biton Y., Fisman E.Z., Tenenbaum A., Golovchiner G., Kadmon E., Omelchenko A., Gal T.B., and Barsheshet A. (2017). Admission blood glucose and 10-year mortality among patients with or without pre-existing diabetes mellitus hospitalized with heart failure. *Cardiovasc Diabetol, 16*(1), 102.

Iwano H., and Little W.C. (2013). Heart failure: what does ejection fraction have to do with it? *J Cardiol, 62*(1), 1-3.

Jager J., Gremeaux T., Cormont M., Le Marchand-Brustel Y., and Tanti J.F. (2007). Interleukin-1beta-induced insulin resistance in adipocytes through down-regulation of insulin receptor substrate-1 expression. *Endocrinology, 148*(1), 241-251.

Jeong I.K., Oh S.H., Chung J.H., Min Y.K., Lee M.S., Lee M.K., and Kim K.W. (2002). The stimulatory effect of IL-1beta on the insulin secretion of rat pancreatic islet is not related with iNOS pathway. *Exp Mol Med, 34*(1), 12-17.

Jia G., DeMarco V.G., and Sowers J.R. (2016). Insulin resistance and hyperinsulinaemia in diabetic cardiomyopathy. *Nat Rev Endocrinol, 12*(3), 144-153.

Kaiser R.A., Bueno O.F., Lips D.J., Doevendans P.A., Jones F., Kimball T.F., and Molkentin J.D. (2004). Targeted inhibition of p38 mitogen-activated protein kinase antagonizes cardiac injury and cell death following ischemia-reperfusion in vivo. *J Biol Chem, 279*(15), 15524-15530.

Kamp F., Zakim D., Zhang F., Noy N., and Hamilton J.A. (1995). Fatty acid flip-flop in phospholipid bilayers is extremely fast. *Biochemistry, 34*(37), 11928-11937.

Kawanishi M., Tamori Y., Okazawa H., Araki S., Shinoda H., and Kasuga M. (2000). Role of SNAP23 in insulin-induced translocation of GLUT4 in 3T3-L1 adipocytes. Mediation of complex formation between syntaxin4 and VAMP2. *J Biol Chem, 275*(11), 8240-8247.

Ke B., Oh E., and Thurmond D.C. (2007). Doc2beta is a novel Munc18c-interacting partner and positive effector of syntaxin 4-mediated exocytosis. *J Biol Chem, 282*(30), 21786-21797.

Kemi O.J., Ceci M., Wisloff U., Grimaldi S., Gallo P., Smith G.L., Condorelli G., and Ellingsen O. (2008). Activation or inactivation of cardiac Akt/mTOR signaling diverges physiological from pathological hypertrophy. *J Cell Physiol, 214*(2), 316-321.

Kerkhof P.L. (2015). Characterizing heart failure in the ventricular volume domain. *Clin Med Insights Cardiol, 9*(Suppl 1), 11-31.

Kerner J., Zaluzec E., Gage D., and Bieber L.L. (1994). Characterization of the malonyl-CoA-sensitive carnitine palmitoyltransferase (CPTo) of a rat heart mitochondrial particle. Evidence that the catalytic unit is CPTi. *J Biol Chem, 269*(11), 8209-8219.

Kienesberger P.C., Pulinilkunnil T., Nagendran J., and Dyck J.R. (2013). Myocardial triacylglycerol metabolism. *J Mol Cell Cardiol, 55*, 101-110.

Kim A.S., Miller E.J., Wright T.M., Li J., Qi D., Atsina K., Zaha V., Sakamoto K., and Young L.H. (2011). A small molecule AMPK activator protects the heart against ischemia-reperfusion injury. *J Mol Cell Cardiol, 51*(1), 24-32.

Kleiner S., Mepani R.J., Laznik D., Ye L., Jurczak M.J., Jornayvaz F.R., Estall J.L., Chatterjee Bhowmick D., Shulman G.I., and Spiegelman B.M. (2012). Development of insulin resistance in mice lacking PGC-1α in adipose tissues. *Proc Natl Acad Sci U S A, 109*(24), 9635-9640.

Kolwicz S.C., Jr., Purohit S., and Tian R. (2013). Cardiac metabolism and its interactions with contraction, growth, and survival of cardiomyocytes. *Circ Res, 113*(5), 603-616.

Koranyi L., James D.E., Kraegen E.W., and Permutt M.A. (1992). Feedback inhibition of insulin gene expression by insulin. *J Clin Invest, 89*(2), 432-436.

Kovacic S., Soltys C.L., Barr A.J., Shiojima I., Walsh K., and Dyck J.R. (2003). Akt activity negatively regulates phosphorylation of AMP-activated protein kinase in the heart. *J Biol Chem, 278*(41), 39422-39427.

Kraegen E.W., Sowden J.A., Halstead M.B., Clark P.W., Rodnick K.J., Chisholm D.J., and James D.E. (1993). Glucose transporters and in vivo glucose uptake in skeletal and cardiac muscle: fasting, insulin stimulation and immunoisolation studies of GLUT1 and GLUT4. *Biochem J, 295 (Pt 1)*, 287-293.

Kramer H.F., Witczak C.A., Fujii N., Jessen N., Taylor E.B., Arnolds D.E., Sakamoto K., Hirshman M.F., and Goodyear L.J. (2006). Distinct signals regulate AS160 phosphorylation in response to insulin, AICAR, and contraction in mouse skeletal muscle. *Diabetes, 55*(7), 2067-2076.

Kumphune S., Chattipakorn S., and Chattipakorn N. (2013). Roles of p38-MAPK in insulin resistant heart: evidence from bench to future bedside application. *Curr Pharm Des, 19*(32), 5742-5754.

Kundu B.K., Zhong M., Sen S., Davogustto G., Keller S.R., and Taegtmeyer H. (2015). Remodeling of glucose metabolism precedes pressure overload-induced left ventricular hypertrophy: review of a hypothesis. *Cardiology, 130*(4), 211-220.

Kurland I.J., and Pilkis S.J. (1995). Covalent control of 6-phosphofructo-2-kinase/fructose-2,6-bisphosphatase: insights into autoregulation of a bifunctional enzyme. *Protein Sci, 4*(6), 1023-1037.

Lakso M., Sauer B., Mosinger B., Jr., Lee E.J., Manning R.W., Yu S.H., Mulder K.L., and Westphal H. (1992). Targeted oncogene activation by site-specific recombination in transgenic mice. *Proc Natl Acad Sci U S A, 89*(14), 6232-6236.

Langendorff O. (1895). Untersuchungen am überlebenden Säugethierherzen. *Pflügers Archiv European Journal of Physiology, 61*(6), 291-332.

Lee Y., Fluckey J.D., Chakraborty S., and Muthuchamy M. (2017). Hyperglycemia- and hyperinsulinemia-induced insulin resistance causes alterations in cellular bioenergetics and activation of inflammatory signaling in lymphatic muscle. *Faseb j, 31*(7), 2744-2759.

Lehman J.J., and Kelly D.P. (2002). Gene regulatory mechanisms governing energy metabolism during cardiac hypertrophic growth. *Heart Fail Rev, 7*(2), 175-185.

Lei B., Chess D.J., Keung W., O'Shea K.M., Lopaschuk G.D., and Stanley W.C. (2008). Transient activation of p38 MAP kinase and up-regulation of Pim-1 kinase in cardiac hypertrophy despite no activation of AMPK. *J Mol Cell Cardiol, 45*(3), 404-410.

Leitner L.M. (2018). *Heart Failure Rapidly Induces Wasting-related Program in Skeletal Muscle.*

Leitner L.M., Wilson R.J., Yan Z., and Godecke A. (2017). Reactive Oxygen Species/Nitric Oxide Mediated Inter-Organ Communication in Skeletal Muscle Wasting Diseases. *Antioxid Redox Signal, 26*(13), 700-717.

Leroux L., Desbois P., Lamotte L., Duvillie B., Cordonnier N., Jackerott M., Jami J., Bucchini D., and Joshi R.L. (2001). Compensatory responses in mice carrying a null mutation for Ins1 or Ins2. *Diabetes, 50 Suppl 1*, S150-153.

Li X., Liu J., Lu Q., Ren D., Sun X., Rousselle T., Tan Y., and Li J. (2019). AMPK: a therapeutic target of heart failure-not only metabolism regulation. *Biosci Rep, 39*(1).

Li X., Monks B., Ge Q., and Birnbaum M.J. (2007). Akt/PKB regulates hepatic metabolism by directly inhibiting PGC-1alpha transcription coactivator. *Nature, 447*(7147), 1012-1016.

Li Z., Ma J.Y., Kerr I., Chakravarty S., Dugar S., Schreiner G., and Protter A.A. (2006). Selective inhibition of p38alpha MAPK improves cardiac function and reduces

myocardial apoptosis in rat model of myocardial injury. *Am J Physiol Heart Circ Physiol, 291*(4), H1972-1977.

Liang Q., and Molkentin J.D. (2003). Redefining the roles of p38 and JNK signaling in cardiac hypertrophy: dichotomy between cultured myocytes and animal models. *J Mol Cell Cardiol, 35*(12), 1385-1394.

Liu C., and Lin J.D. (2011). PGC-1 coactivators in the control of energy metabolism. *Acta Biochim Biophys Sin, 43*(4), 248-257.

Liu M., Feng J., Du Q., Ai J., and Lv Z. (2020). Paeoniflorin Attenuates Myocardial Fibrosis in Isoprenaline-induced Chronic Heart Failure Rats via Inhibiting P38 MAPK Pathway. *Curr Med Sci, 40*(2), 307-312.

Liu Y.H., Wang D., Rhaleb N.E., Yang X.P., Xu J., Sankey S.S., Rudolph A.E., and Carretero O.A. (2005). Inhibition of p38 mitogen-activated protein kinase protects the heart against cardiac remodeling in mice with heart failure resulting from myocardial infarction. *J Card Fail, 11*(1), 74-81.

Liu Z., and Cao W. (2009). p38 mitogen-activated protein kinase: a critical node linking insulin resistance and cardiovascular diseases in type 2 diabetes mellitus. *Endocr Metab Immune Disord Drug Targets, 9*(1), 38-46.

Lopaschuk G.D., Ussher J.R., Folmes C.D., Jaswal J.S., and Stanley W.C. (2010). Myocardial fatty acid metabolism in health and disease. *Physiol Rev, 90*(1), 207-258.

Luiken J.J., Coort S.L., Willems J., Coumans W.A., Bonen A., van der Vusse G.J., and Glatz J.F. (2003). Contraction-induced fatty acid translocase/CD36 translocation in rat cardiac myocytes is mediated through AMP-activated protein kinase signaling. *Diabetes, 52*(7), 1627-1634.

Luiken J.J., Koonen D.P., Willems J., Zorzano A., Becker C., Fischer Y., Tandon N.N., Van Der Vusse G.J., Bonen A., and Glatz J.F. (2002). Insulin stimulates long-chain fatty acid utilization by rat cardiac myocytes through cellular redistribution of FAT/CD36. *Diabetes, 51*(10), 3113-3119.

Luiken J.J., Ouwens D.M., Habets D.D., van der Zon G.C., Coumans W.A., Schwenk R.W., Bonen A., and Glatz J.F. (2009). Permissive action of protein kinase C-zeta in insulin-induced CD36- and GLUT4 translocation in cardiac myocytes. *J Endocrinol, 201*(2), 199-209.

Lyon R.C., Zanella F., Omens J.H., and Sheikh F. (2015). Mechanotransduction in cardiac hypertrophy and failure. *Circ Res, 116*(8), 1462-1476.

Martin E.D., Bassi R., and Marber M.S. (2015). p38 MAPK in cardioprotection - are we there yet? *Br J Pharmacol, 172*(8), 2101-2113.

Melloul D., Marshak S., and Cerasi E. (2002). Regulation of insulin gene transcription. *Diabetologia, 45*(3), 309-326.

Mendis S., Puska P., Norrving B., and Organization W.H. (2011). Global atlas on cardiovascular disease prevention and control: Geneva: World Health Organization.

Metra M., and Teerlink J.R. (2017). Heart failure. *Lancet (London, England), 390*(10106), 1981-1995.

Miller E.J., Li J., Leng L., McDonald C., Atsumi T., Bucala R., and Young L.H. (2008). Macrophage migration inhibitory factor stimulates AMP-activated protein kinase in the ischaemic heart. *Nature, 451*(7178), 578-582.

Milner R.D., and Hales C.N. (1967). The role of calcium and magnesium in insulin secretion from rabbit pancreas studied in vitro. *Diabetologia, 3*(1), 47-49.

Molkentin J.D., Bugg D., Ghearing N., Dorn L.E., Kim P., Sargent M.A., Gunaje J., Otsu K., and Davis J. (2017). Fibroblast-Specific Genetic Manipulation of p38 Mitogen-Activated Protein Kinase In Vivo Reveals Its Central Regulatory Role in Fibrosis. *Circulation, 136*(6), 549-561.

Muoio D.M., Dohm G.L., Tapscott E.B., and Coleman R.A. (1999). Leptin opposes insulin's effects on fatty acid partitioning in muscles isolated from obese ob/ob mice. *Am J Physiol, 276*(5), E913-921.

Nanamori M., Chen J., Du X., and Ye R.D. (2007). Regulation of leukocyte degranulation by cGMP-dependent protein kinase and phosphoinositide 3-kinase: potential roles in phosphorylation of target membrane SNARE complex proteins in rat mast cells. *J Immunol, 178*(1), 416-427.

Navar L.G., Carmines P.K., Huang W.C., and Mitchell K.D. (1987). The tubular effects of angiotensin II. *Kidney Int Suppl, 20*, S81-88.

Nemoto S., Sheng Z., and Lin A. (1998). Opposing effects of Jun kinase and p38 mitogen-activated protein kinases on cardiomyocyte hypertrophy. *Mol Cell Biol, 18*(6), 3518-3526.

Ng Y., Ramm G., Lopez J.A., and James D.E. (2008). Rapid activation of Akt2 is sufficient to stimulate GLUT4 translocation in 3T3-L1 adipocytes. *Cell Metab, 7*(4), 348-356.

Nikolova G., Jabs N., Konstantinova I., Domogatskaya A., Tryggvason K., Sorokin L., Fassler R., Gu G., Gerber H.P., Ferrara N., Melton D.A., and Lammert E. (2006). The vascular basement membrane: a niche for insulin gene expression and Beta cell proliferation. *Dev Cell, 10*(3), 397-405.

Nishida K., Yamaguchi O., Hirotani S., Hikoso S., Higuchi Y., Watanabe T., Takeda T., Osuka S., Morita T., Kondoh G., Uno Y., Kashiwase K., Taniike M., Nakai A., Matsumura Y., Miyazaki J., Sudo T., Hongo K., Kusakari Y., Kurihara S., Chien K.R., Takeda J., Hori M., and Otsu K. (2004). p38alpha mitogen-activated protein kinase plays a critical role in cardiomyocyte survival but not in cardiac hypertrophic growth in response to pressure overload. *Mol Cell Biol, 24*(24), 10611-10620.

Nunemaker C.S., Chung H.G., Verrilli G.M., Corbin K.L., Upadhye A., and Sharma P.R. (2014). Increased serum CXCL1 and CXCL5 are linked to obesity, hyperglycemia, and impaired islet function. *J Endocrinol, 222*(2), 267-276.

O'Neill C.M., Lu C., Corbin K.L., Sharma P.R., Dula S.B., Carter J.D., Ramadan J.W., Xin W., Lee J.K., and Nunemaker C.S. (2013). Circulating levels of IL-1B+IL-6 cause ER stress and dysfunction in islets from prediabetic male mice. *Endocrinology, 154*(9), 3077-3088.

Oenarto V. (2020). *Interorgan Crosstalk between the Heart and Adipose Tissue during Heart Failure Establishment.*

Oh E., Spurlin B.A., Pessin J.E., and Thurmond D.C. (2005). Munc18c heterozygous knockout mice display increased susceptibility for severe glucose intolerance. *Diabetes, 54*(3), 638-647.

Oliverio M.I., Best C.F., Kim H.S., Arendshorst W.J., Smithies O., and Coffman T.M. (1997). Angiotensin II responses in AT1A receptor-deficient mice: a role for AT1B receptors in blood pressure regulation. *Am J Physiol, 272*(4 Pt 2), F515-520.

Ono K., and Han J. (2000). The p38 signal transduction pathway: activation and function. *Cell Signal, 12*(1), 1-13.

Opie L.H. (2004). Heart physiology: from cell to circulation: Lippincott Williams & Wilkins.

Orban P.C., Chui D., and Marth J.D. (1992). Tissue- and site-specific DNA recombination in transgenic mice. *Proc Natl Acad Sci U S A, 89*(15), 6861-6865.

Oropeza D., Jouvet N., Bouyakdan K., Perron G., Ringuette L.J., Philipson L.H., Kiss R.S., Poitout V., Alquier T., and Estall J.L. (2015). PGC-1 coactivators in beta-cells regulate lipid metabolism and are essential for insulin secretion coupled to fatty acids. *Mol Metab, 4*(11), 811-822.

Osorio J.C., Stanley W.C., Linke A., Castellari M., Diep Q.N., Panchal A.R., Hintze T.H., Lopaschuk G.D., and Recchia F.A. (2002). Impaired myocardial fatty acid oxidation and reduced protein expression of retinoid X receptor-alpha in pacing-induced heart failure. *Circulation, 106*(5), 606-612.

Palmer J.P., Helqvist S., Spinas G.A., Molvig J., Mandrup-Poulsen T., Andersen H.U., and Nerup J. (1989). Interaction of beta-cell activity and IL-1 concentration and exposure time in isolated rat islets of Langerhans. *Diabetes, 38*(10), 1211-1216.

Patel M.S., and Korotchkina L.G. (2006). Regulation of the pyruvate dehydrogenase complex. *Biochem Soc Trans, 34*(Pt 2), 217-222.

Patzelt C., Labrecque A.D., Duguid J.R., Carroll R.J., Keim P.S., Heinrikson R.L., and Steiner D.F. (1978). Detection and kinetic behavior of preproinsulin in pancreatic islets. *Proc Natl Acad Sci U S A, 75*(3), 1260-1264.

Peach M.J. (1977). Renin-angiotensin system: biochemistry and mechanisms of action. *Physiol Rev, 57*(2), 313-370.

Peck G.R., Chavez J.A., Roach W.G., Budnik B.A., Lane W.S., Karlsson H.K., Zierath J.R., and Lienhard G.E. (2009). Insulin-stimulated phosphorylation of the Rab GTPase-activating protein TBC1D1 regulates GLUT4 translocation. *J Biol Chem, 284*(44), 30016-30023.

Pereira R.O., Wende A.R., Olsen C., Soto J., Rawlings T., Zhu Y., Anderson S.M., and Abel E.D. (2013). Inducible overexpression of GLUT1 prevents mitochondrial dysfunction and attenuates structural remodeling in pressure overload but does not prevent left ventricular dysfunction. *J Am Heart Assoc, 2*(5), e000301.

Pereira R.O., Wende A.R., Olsen C., Soto J., Rawlings T., Zhu Y., Riehle C., and Abel E.D. (2014). GLUT1 deficiency in cardiomyocytes does not accelerate the transition from compensated hypertrophy to heart failure. *J Mol Cell Cardiol, 72*, 95-103.

Poitout V., Hagman D., Stein R., Artner I., Robertson R.P., and Harmon J.S. (2006). Regulation of the insulin gene by glucose and fatty acids. *J Nutr, 136*(4), 873-876.

Prentki M., and Matschinsky F.M. (1987). Ca2+, cAMP, and phospholipid-derived messengers in coupling mechanisms of insulin secretion. *Physiol Rev, 67*(4), 1185-1248.

Puigserver P., Rhee J., Lin J., Wu Z., Yoon J.C., Zhang C.Y., Krauss S., Mootha V.K., Lowell B.B., and Spiegelman B.M. (2001). Cytokine stimulation of energy expenditure through p38 MAP kinase activation of PPARgamma coactivator-1. *Mol Cell, 8*(5), 971-982.

Puigserver P., and Spiegelman B.M. (2003). Peroxisome proliferator-activated receptor-gamma coactivator 1 alpha (PGC-1 alpha): transcriptional coactivator and metabolic regulator. *Endocr Rev, 24*(1), 78-90.

Qi Y., Xu Z., Zhu Q., Thomas C., Kumar R., Feng H., Dostal D.E., White M.F., Baker K.M., and Guo S. (2013). Myocardial loss of IRS1 and IRS2 causes heart failure and is controlled by p38alpha MAPK during insulin resistance. *Diabetes, 62*(11), 3887-3900.

Raingeaud J., Whitmarsh A.J., Barrett T., Derijard B., and Davis R.J. (1996). MKK3- and MKK6-regulated gene expression is mediated by the p38 mitogen-activated protein kinase signal transduction pathway. *Mol Cell Biol, 16*(3), 1247-1255.

Ramm G., Larance M., Guilhaus M., and James D.E. (2006). A role for 14-3-3 in insulin-stimulated GLUT4 translocation through its interaction with the RabGAP AS160. *J Biol Chem, 281*(39), 29174-29180.

Randle P.J. (1986). Fuel selection in animals. *Biochem Soc Trans, 14*(5), 799-806.

Randle P.J. (1998). Regulatory interactions between lipids and carbohydrates: the glucose fatty acid cycle after 35 years. *Diabetes Metab Rev, 14*(4), 263-283.

Randle P.J., Garland P.B., Hales C.N., and Newsholme E.A. (1963). The glucose fatty-acid cycle. Its role in insulin sensitivity and the metabolic disturbances of diabetes mellitus. *Lancet, 1*(7285), 785-789.

Randle P.J., Kerbey A.L., and Espinal J. (1988). Mechanisms decreasing glucose oxidation in diabetes and starvation: role of lipid fuels and hormones. *Diabetes Metab Rev, 4*(7), 623-638.

Remy G., Risco A.M., Inesta-Vaquera F.A., Gonzalez-Teran B., Sabio G., Davis R.J., and Cuenda A. (2010). Differential activation of p38MAPK isoforms by MKK6 and MKK3. *Cell Signal, 22*(4), 660-667.

Riehle C., and Abel E.D. (2014). Insulin regulation of myocardial autophagy. *Circ J, 78*(11), 2569-2576.

Riehle C., and Abel E.D. (2016). Insulin Signaling and Heart Failure. *Circ Res, 118*(7), 1151-1169.

Riehle C., Wende A.R., Zaha V.G., Pires K.M., Wayment B., Olsen C., Bugger H., Buchanan J., Wang X., Moreira A.B., Doenst T., Medina-Gomez G., Litwin S.E., Lelliott C.J., Vidal-Puig A., and Abel E.D. (2011). PGC-1beta deficiency accelerates the transition to heart failure in pressure overload hypertrophy. *Circ Res, 109*(7), 783-793.

Rizza R.A., Mandarino L.J., Genest J., Baker B.A., and Gerich J.E. (1985). Production of insulin resistance by hyperinsulinaemia in man. *Diabetologia, 28*(2), 70-75.

Rodgers J.T., Lerin C., Haas W., Gygi S.P., Spiegelman B.M., and Puigserver P. (2005). Nutrient control of glucose homeostasis through a complex of PGC-1alpha and SIRT1. *Nature, 434*(7029), 113-118.

Rosenblatt-Velin N., Montessuit C., Papageorgiou I., Terrand J., and Lerch R. (2001). Postinfarction heart failure in rats is associated with upregulation of GLUT-1 and downregulation of genes of fatty acid metabolism. *Cardiovasc Res, 52*(3), 407-416.

Rubler S., Dlugash J., Yuceoglu Y.Z., Kumral T., Branwood A.W., and Grishman A. (1972). New type of cardiomyopathy associated with diabetic glomerulosclerosis. *Am J Cardiol, 30*(6), 595-602.

Russell R.R., 3rd, Bergeron R., Shulman G.I., and Young L.H. (1999). Translocation of myocardial GLUT-4 and increased glucose uptake through activation of AMPK by AICAR. *Am J Physiol, 277*(2), H643-649.

Russell R.R., 3rd, Li J., Coven D.L., Pypaert M., Zechner C., Palmeri M., Giordano F.J., Mu J., Birnbaum M.J., and Young L.H. (2004). AMP-activated protein kinase mediates ischemic glucose uptake and prevents postischemic cardiac dysfunction, apoptosis, and injury. *J Clin Invest, 114*(4), 495-503.

Rutter G.A. (1999). Insulin secretion: feed-forward control of insulin biosynthesis? *Curr Biol, 9*(12), R443-445.

Sack M.N., Rader T.A., Park S., Bastin J., McCune S.A., and Kelly D.P. (1996). Fatty acid oxidation enzyme gene expression is downregulated in the failing heart. *Circulation, 94*(11), 2837-2842.

Saddik M., and Lopaschuk G.D. (1991). Myocardial triglyceride turnover and contribution to energy substrate utilization in isolated working rat hearts. *J Biol Chem, 266*(13), 8162-8170.

Saltiel A.R., and Kahn C.R. (2001). Insulin signalling and the regulation of glucose and lipid metabolism. *Nature, 414*(6865), 799-806.

Sarbassov D.D., Guertin D.A., Ali S.M., and Sabatini D.M. (2005). Phosphorylation and regulation of Akt/PKB by the rictor-mTOR complex. *Science, 307*(5712), 1098-1101.

Schaper J., Meiser E., and Stammler G. (1985). Ultrastructural morphometric analysis of myocardium from dogs, rats, hamsters, mice, and from human hearts. *Circ Res, 56*(3), 377-391.

Schroeder A., Mueller O., Stocker S., Salowsky R., Leiber M., Gassmann M., Lightfoot S., Menzel W., Granzow M., and Ragg T. (2006). The RIN: an RNA integrity number for assigning integrity values to RNA measurements. *BMC Mol Biol, 7*, 3.

See F., Thomas W., Way K., Tzanidis A., Kompa A., Lewis D., Itescu S., and Krum H. (2004). p38 mitogen-activated protein kinase inhibition improves cardiac function and attenuates left ventricular remodeling following myocardial infarction in the rat. *J Am Coll Cardiol, 44*(8), 1679-1689.

Sharma S., Adrogue J.V., Golfman L., Uray I., Lemm J., Youker K., Noon G.P., Frazier O.H., and Taegtmeyer H. (2004). Intramyocardial lipid accumulation in the failing human heart resembles the lipotoxic rat heart. *Faseb j, 18*(14), 1692-1700.

Shi Y., Vattem K.M., Sood R., An J., Liang J., Stramm L., and Wek R.C. (1998). Identification and characterization of pancreatic eukaryotic initiation factor 2 alpha-subunit kinase, PEK, involved in translational control. *Mol Cell Biol, 18*(12), 7499-7509.

Shibata R., Ouchi N., Ito M., Kihara S., Shiojima I., Pimentel D.R., Kumada M., Sato K., Schiekofer S., Ohashi K., Funahashi T., Colucci W.S., and Walsh K. (2004). Adiponectin-mediated modulation of hypertrophic signals in the heart. *Nat Med, 10*(12), 1384-1389.

Shimizu I., and Minamino T. (2016). Physiological and pathological cardiac hypertrophy. *J Mol Cell Cardiol, 97*, 245-262.

Shiojima I., Yefremashvili M., Luo Z., Kureishi Y., Takahashi A., Tao J., Rosenzweig A., Kahn C.R., Abel E.D., and Walsh K. (2002). Akt signaling mediates postnatal heart growth in response to insulin and nutritional status. *J Biol Chem, 277*(40), 37670-37677.

Soares M.B., Schon E., Henderson A., Karathanasis S.K., Cate R., Zeitlin S., Chirgwin J., and Efstratiadis A. (1985). RNA-mediated gene duplication: the rat preproinsulin I gene is a functional retroposon. *Mol Cell Biol, 5*(8), 2090-2103.

Sodi-Pallares D., Testelli M.R., Fishleder B.L., Bisteni A., Medrano G.A., Friedland C., and De Micheli A. (1962). Effects of an intravenous infusion of a potassium-glucose-insulin solution on the electrocardiographic signs of myocardial infarction. A preliminary clinical report. *Am J Cardiol, 9*, 166-181.

Sohal D.S., Nghiem M., Crackower M.A., Witt S.A., Kimball T.R., Tymitz K.M., Penninger J.M., and Molkentin J.D. (2001). Temporally regulated and tissue-specific gene manipulations in the adult and embryonic heart using a tamoxifen-inducible Cre protein. *Circ Res, 89*(1), 20-25.

Somwar R., Kim D.Y., Sweeney G., Huang C., Niu W., Lador C., Ramlal T., and Klip A. (2001). GLUT4 translocation precedes the stimulation of glucose uptake by insulin in muscle cells: potential activation of GLUT4 via p38 mitogen-activated protein kinase. *Biochem J, 359*(Pt 3), 639-649.

Somwar R., Koterski S., Sweeney G., Sciotti R., Djuric S., Berg C., Trevillyan J., Scherer P.E., Rondinone C.M., and Klip A. (2002). A dominant-negative p38 MAPK mutant and novel selective inhibitors of p38 MAPK reduce insulin-stimulated glucose uptake in 3T3-L1 adipocytes without affecting GLUT4 translocation. *Journal of Biological Chemistry, 277*(52), 50386-50395.

Son N.H., Yu S., Tuinei J., Arai K., Hamai H., Homma S., Shulman G.I., Abel E.D., and Goldberg I.J. (2010). PPARgamma-induced cardiolipotoxicity in mice is ameliorated by PPARalpha deficiency despite increases in fatty acid oxidation. *J Clin Invest, 120*(10), 3443-3454.

Sopontammarak S., Aliharoob A., Ocampo C., Arcilla R.A., Gupta M.P., and Gupta M. (2005). Mitogen-activated protein kinases (p38 and c-Jun NH2-terminal kinase) are differentially regulated during cardiac volume and pressure overload hypertrophy. *Cell Biochem Biophys, 43*(1), 61-76.

Sorokina N., O'Donnell J.M., McKinney R.D., Pound K.M., Woldegiorgis G., LaNoue K.F., Ballal K., Taegtmeyer H., Buttrick P.M., and Lewandowski E.D. (2007).

Recruitment of compensatory pathways to sustain oxidative flux with reduced carnitine palmitoyltransferase I activity characterizes inefficiency in energy metabolism in hypertrophied hearts. *Circulation, 115*(15), 2033-2041.

Soyal S., Krempler F., Oberkofler H., and Patsch W. (2006). PGC-1alpha: a potent transcriptional cofactor involved in the pathogenesis of type 2 diabetes. *Diabetologia, 49*(7), 1477-1488.

Spinas G.A., Mandrup-Poulsen T., Molvig J., Baek L., Bendtzen K., Dinarello C.A., and Nerup J. (1986). Low concentrations of interleukin-1 stimulate and high concentrations inhibit insulin release from isolated rat islets of Langerhans. *Acta Endocrinol (Copenh), 113*(4), 551-558.

Spurlin B.A., Park S.Y., Nevins A.K., Kim J.K., and Thurmond D.C. (2004). Syntaxin 4 transgenic mice exhibit enhanced insulin-mediated glucose uptake in skeletal muscle. *Diabetes, 53*(9), 2223-2231.

Stanley W.C., and Chandler M.P. (2002). Energy metabolism in the normal and failing heart: potential for therapeutic interventions. *Heart Fail Rev, 7*(2), 115-130.

Stanley W.C., Recchia F.A., and Lopaschuk G.D. (2005). Myocardial substrate metabolism in the normal and failing heart. *Physiol Rev, 85*(3), 1093-1129.

Steiner D.F. (2008). The biosynthesis of insulin. In *Pancreatic Beta Cell in Health and Disease* (pp. 31-49): Springer.

Stuck B.J., Lenski M., Böhm M., and Laufs U. (2008). Metabolic switch and hypertrophy of cardiomyocytes following treatment with angiotensin II are prevented by AMP-activated protein kinase. *J Biol Chem, 283*(47), 32562-32569.

Sugden P.H., and Clerk A. (1998). "Stress-responsive" mitogen-activated protein kinases (c-Jun N-terminal kinases and p38 mitogen-activated protein kinases) in the myocardium. *Circ Res, 83*(4), 345-352.

Sutherland F.J., Shattock M.J., Baker K.E., and Hearse D.J. (2003). Mouse isolated perfused heart: characteristics and cautions. *Clinical and experimental pharmacology and physiology, 30*(11), 867-878.

Sweeney G., Somwar R., Ramlal T., Volchuk A., Ueyama A., and Klip A. (1999). An inhibitor of p38 mitogen-activated protein kinase prevents insulin-stimulated glucose transport but not glucose transporter translocation in 3T3-L1 adipocytes and L6 myotubes. *J Biol Chem, 274*(15), 10071-10078.

Taegtmeyer H. (2002). Switching metabolic genes to build a better heart. *Circulation, 106*(16), 2043-2045.

Taha M.S., Nouri K., Milroy L.G., Moll J.M., Herrmann C., Brunsveld L., Piekorz R.P., and Ahmadian M.R. (2014). Subcellular fractionation and localization studies reveal a direct interaction of the fragile X mental retardation protein (FMRP) with nucleolin. *PLoS One, 9*(3), e91465.

Taniike M., Yamaguchi O., Tsujimoto I., Hikoso S., Takeda T., Nakai A., Omiya S., Mizote I., Nakano Y., Higuchi Y., Matsumura Y., Nishida K., Ichijo H., Hori M., and Otsu K. (2008). Apoptosis signal-regulating kinase 1/p38 signaling pathway negatively regulates physiological hypertrophy. *Circulation, 117*(4), 545-552.

Thomsen R., Solvsten C.A., Linnet T.E., Blechingberg J., and Nielsen A.L. (2010). Analysis of qPCR data by converting exponentially related Ct values into linearly related X0 values. *J Bioinform Comput Biol, 8*(5), 885-900.

Tian R., and Abel E.D. (2001). Responses of GLUT4-deficient hearts to ischemia underscore the importance of glycolysis. *Circulation, 103*(24), 2961-2966.

Timmermans P.B., Wong P.C., Chiu A.T., Herblin W.F., Benfield P., Carini D.J., Lee R.J., Wexler R.R., Saye J.A., and Smith R.D. (1993). Angiotensin II receptors and angiotensin II receptor antagonists. *Pharmacol Rev, 45*(2), 205-251.

Tran D.H., and Wang Z.V. (2019). Glucose Metabolism in Cardiac Hypertrophy and Heart Failure. *J Am Heart Assoc, 8*(12), e012673.

Tremblay F., Lavigne C., Jacques H., and Marette A. (2001). Defective insulin-induced GLUT4 translocation in skeletal muscle of high fat-fed rats is associated with alterations in both Akt/protein kinase B and atypical protein kinase C (zeta/lambda) activities. *Diabetes, 50*(8), 1901-1910.

Vaidyula V.R., Rao A.K., Mozzoli M., Homko C., Cheung P., and Boden G. (2006). Effects of hyperglycemia and hyperinsulinemia on circulating tissue factor procoagulant activity and platelet CD40 ligand. *Diabetes, 55*(1), 202-208.

Valentine R.J., Coughlan K.A., Ruderman N.B., and Saha A.K. (2014). Insulin inhibits AMPK activity and phosphorylates AMPK Ser(4)(8)(5)/(4)(9)(1) through Akt in hepatocytes, myotubes and incubated rat skeletal muscle. *Arch Biochem Biophys, 562*, 62-69.

Valtat B., Riveline J.P., Zhang P., Singh-Estivalet A., Armanet M., Venteclef N., Besseiche A., Kelly D.P., Tronche F., Ferre P., Gautier J.F., Breant B., and Blondeau B. (2013). Fetal PGC-1alpha overexpression programs adult pancreatic beta-cell dysfunction. *Diabetes, 62*(4), 1206-1216.

Vander Mierde D., Scheuner D., Quintens R., Patel R., Song B., Tsukamoto K., Beullens M., Kaufman R.J., Bollen M., and Schuit F.C. (2007). Glucose activates a protein phosphatase-1-mediated signaling pathway to enhance overall translation in pancreatic beta-cells. *Endocrinology, 148*(2), 609-617.

Ventura J.J., Tenbaum S., Perdiguero E., Huth M., Guerra C., Barbacid M., Pasparakis M., and Nebreda A.R. (2007). p38alpha MAP kinase is essential in lung stem and progenitor cell proliferation and differentiation. *Nat Genet, 39*(6), 750-758.

Verrou C., Zhang Y., Zurn C., Schamel W.W., and Reth M. (1999). Comparison of the tamoxifen regulated chimeric Cre recombinases MerCreMer and CreMer. *Biol Chem, 380*(12), 1435-1438.

Wang Y., Huang S., Sah V.P., Ross J., Jr., Brown J.H., Han J., and Chien K.R. (1998). Cardiac muscle cell hypertrophy and apoptosis induced by distinct members of the p38 mitogen-activated protein kinase family. *J Biol Chem, 273*(4), 2161-2168.

Ward C.W., and Lawrence M.C. (2009). Ligand-induced activation of the insulin receptor: a multi-step process involving structural changes in both the ligand and the receptor. *Bioessays, 31*(4), 422-434.

Weeks K.L., and McMullen J.R. (2011). The athlete's heart vs. the failing heart: can signaling explain the two distinct outcomes? *Physiology (Bethesda), 26*(2), 97-105.

Weiss R.G., Chatham J.C., Georgakopolous D., Charron M.J., Wallimann T., Kay L., Walzel B., Wang Y., Kass D.A., Gerstenblith G., and Chacko V.P. (2002). An increase in the myocardial PCr/ATP ratio in GLUT4 null mice. *Faseb j, 16*(6), 613-615.

Wende A.R., Brahma M.K., McGinnis G.R., and Young M.E. (2017). Metabolic Origins of Heart Failure. *JACC Basic Transl Sci, 2*(3), 297-310.

Wisneski J.A., Gertz E.W., Neese R.A., Gruenke L.D., and Craig J.C. (1985). Dual carbon-labeled isotope experiments using D-[6-14C] glucose and L-[1,2,3-13C3] lactate: a new approach for investigating human myocardial metabolism during ischemia. *J Am Coll Cardiol, 5*(5), 1138-1146.

Woods A., Dickerson K., Heath R., Hong S.P., Momcilovic M., Johnstone S.R., Carlson M., and Carling D. (2005). Ca2+/calmodulin-dependent protein kinase kinase-beta acts upstream of AMP-activated protein kinase in mammalian cells. *Cell Metab, 2*(1), 21-33.

Wright C.V., Schnegelsberg P., and De Robertis E.M. (1989). XlHbox 8: a novel Xenopus homeo protein restricted to a narrow band of endoderm. *Development, 105*(4), 787-794.

Wu C., Okar D.A., Stoeckman A.K., Peng L.J., Herrera A.H., Herrera J.E., Towle H.C., and Lange A.J. (2004). A potential role for fructose-2,6-bisphosphate in the stimulation of hepatic glucokinase gene expression. *Endocrinology, 145*(2), 650-658.

Wu N., Zheng B., Shaywitz A., Dagon Y., Tower C., Bellinger G., Shen C.H., Wen J., Asara J., McGraw T.E., Kahn B.B., and Cantley L.C. (2013). AMPK-dependent degradation of TXNIP upon energy stress leads to enhanced glucose uptake via GLUT1. *Mol Cell, 49*(6), 1167-1175.

Xiao B., Sanders M.J., Carmena D., Bright N.J., Haire L.F., Underwood E., Patel B.R., Heath R.B., Walker P.A., Hallen S., Giordanetto F., Martin S.R., Carling D., and Gamblin S.J. (2013). Structural basis of AMPK regulation by small molecule activators. *Nat Commun, 4*, 3017.

Yancy C.W., Jessup M., Bozkurt B., Butler J., Casey D.E., Drazner M.H., Fonarow G.C., Geraci S.A., Horwich T., and Januzzi J.L. (2013). 2013 ACCF/AHA guideline for the management of heart failure: a report of the American College of Cardiology Foundation/American Heart Association Task Force on Practice Guidelines. *Journal of the American College of Cardiology, 62*(16), e147-e239.

Yang J., and Holman G.D. (2005). Insulin and contraction stimulate exocytosis, but increased AMP-activated protein kinase activity resulting from oxidative metabolism stress slows endocytosis of GLUT4 in cardiomyocytes. *J Biol Chem, 280*(6), 4070-4078.

Yesil P., Michel M., Chwalek K., Pedack S., Jany C., Ludwig B., Bornstein S.R., and Lammert E. (2009). A new collagenase blend increases the number of islets isolated from mouse pancreas. *Islets, 1*(3), 185-190.

Yoon J.C., Xu G., Deeney J.T., Yang S.N., Rhee J., Puigserver P., Levens A.R., Yang R., Zhang C.Y., Lowell B.B., Berggren P.O., Newgard C.B., Bonner-Weir S., Weir G., and Spiegelman B.M. (2003). Suppression of beta cell energy metabolism and insulin release by PGC-1alpha. *Dev Cell, 5*(1), 73-83.

Yu Q., Gao F., and Ma X.L. (2011). Insulin says NO to cardiovascular disease. *Cardiovasc Res, 89*(3), 516-524.

Zamora M., and Villena J.A. (2019). Contribution of Impaired Insulin Signaling to the Pathogenesis of Diabetic Cardiomyopathy. *Int J Mol Sci, 20*(11).

Zarubin T., and Han J. (2005). Activation and signaling of the p38 MAP kinase pathway. *Cell Res, 15*(1), 11-18.

Zeqiraj E., Filippi B.M., Goldie S., Navratilova I., Boudeau J., Deak M., Alessi D.R., and van Aalten D.M. (2009). ATP and MO25alpha regulate the conformational state of the STRADalpha pseudokinase and activation of the LKB1 tumour suppressor. *PLoS Biol, 7*(6), e1000126.

Zhabyeyev P., Gandhi M., Mori J., Basu R., Kassiri Z., Clanachan A., Lopaschuk G.D., and Oudit G.Y. (2013). Pressure-overload-induced heart failure induces a selective reduction in glucose oxidation at physiological afterload. *Cardiovasc Res, 97*(4), 676-685.

Zhang X., Shan P., Otterbein L.E., Alam J., Flavell R.A., Davis R.J., Choi A.M., and Lee P.J. (2003). Carbon monoxide inhibition of apoptosis during ischemia-reperfusion lung injury is dependent on the p38 mitogen-activated protein kinase pathway and involves caspase 3. *J Biol Chem, 278*(2), 1248-1258.

Zhang Z.Z., Cheng Y.W., Jin H.Y., Chang Q., Shang Q.H., Xu Y.L., Chen L.X., Xu R., Song B., and Zhong J.C. (2017). The sirtuin 6 prevents angiotensin II-mediated myocardial fibrosis and injury by targeting AMPK-ACE2 signaling. *Oncotarget, 8*(42), 72302-72314.

Zisman A., Peroni O.D., Abel E.D., Michael M.D., Mauvais-Jarvis F., Lowell B.B., Wojtaszewski J.F., Hirshman M.F., Virkamaki A., Goodyear L.J., Kahn C.R., and Kahn B.B. (2000). Targeted disruption of the glucose transporter 4 selectively in muscle causes insulin resistance and glucose intolerance. *Nat Med, 6*(8), 924-928.

8 List of Abbreviations

Abbreviation	Meaning
^{3}H	Tritium
2-DG	2-deoxyglucose
ACC	Acetyl-CoA carboxylase
ACE	Angiotensin-converting enzyme
Acsl	Long-chain fatty acid -CoA ligase
ADP	Adenosine diphosphate
AMP	Adenosine monophosphate
AMPK	AMP-mediated protein kinase
AngII	Angiotensin II
AS160	Akt substrate 160
AT_1	Angiotensin receptor 1
ATF2	Activating transcription factor 2
ATGL	Adipose triglyceride lipase
ATP	Adenosine triphosphate
Ca^{2+}	Calcium
Na^{+}	Sodium
Na^{+}/K^{+}-ATPase	Sodium-potassium ATPase
K^{+}	Potassium

CACT	Carnitine-acylcarnitin translocase
CaMKK	Ca^{2+}/Calmodulin-dependet protein kinase kinase
cAMP	Cyclic adenosine monophosphate
cDNA	Complementary deoxyribonucleic acid
CM	Cardiomyocyte
CP	Cytoplasma
CPTI	Carnitine palmitoyltransferase I
CPTII	Carnitine palmitoyltransferase II
Cre	Causes recombination
CT	Threshold cycle
Ctrl	Control
CVD	Cardiovascular diseases
D	Doublet
d	Day
ddH_2O	Double deionized water
DGAT	Diglyceride acyltransferase
DNA	Deoxyribonucleic acid
dNTP	Deoxyribonucleic acid triphosphate
DOG	Deoxyglucose
DTT	Dithiothreitol
E	Endogenous
EDTA	Ethylendiamintetraacetate
EDV	End diastolic volume
EF	Ejection fraction
eIF2a	Eukaryotic initiation factor 2a
Elk1	ETS-like 1

ER	Endoplasmatic reticulum
ERK	Extracellular regulated kinase
ERRα	Estrogen related receptor α
ESV	End systolic volume
ETC	Electron transport chain
FA	Fatty acid
$FADH_2$	Dihydro-flavin adenine dinucleotide
FAT/CD36	Fatty acid translocase
FFA	Free fatty acid
FoxO	Forkhead box protein O
G	Glucose
g	Gram
G6P	Glucose-6-phosphate
GAP	GTPase activating protein
Glut1	Glucose transpoter 1
Glut2	Glucose transporter 2
Glut4	Glucose transporter 4
GPCR	G protein coupled receptor
GS	Glycogen synthase
Gsk3-β	Glycogen synthase kinase 3-β
h	hour(s)
HF	Heart failure
HFpEF	Heart failure with preserved ejection fraction
HFrEF	Heart failure with reduced ejection fraction
HM	Heavy membrane

i.p.	intraperitoneal
Ins1	*Insulin 1*
Ins2	*Insulin 2*
IR	Insulin receptor
IRS1	Insulin receptor substrate 1
IRS2	Insulin receptor substrate 2
iWAT	inguinal white adipose tissue
k	Kilo
K_{ATP}	ATP-sensitive potassium channel
KO	Knock out
L	Liter
LDH	Lactate dehydrogenase
LKB1	Liver kinase b1
LM	Light membrane
LV	Left ventricle
LVEDV	Left ventricular end diastolic volume
LVESV	Left ventricular end systolic volume
M	Molar
m	Milli
M.gastroc	*Musculus gastrogenmius*
M.soleus	*Musculus soleus*
MAPK	Mitogen-activated protein kinase
MCT1	Monocarboxylate transporter 1
MEF2	Myocyte enhancer factor 2
mer	Mutagenized estrogenreceptor
MHC	Myosin heavy chain
MKK	MAPK kinase

MKKK	MAPK kinase kinase
mRNA	Messenger RNA
mTOR	Mammalian target of rapamycin
mTORC2	mTOR complex 2
Munc18	Mammalian uncoordinated 18
MW	Molecular weight
n	Nano
NADH	Dihydronicotinamide adenine dinucleotide
NMR	Nuclear magnetic resonance
Nudc	*Nuclear distribution C, dynein somplex regulator*
OH-Tx	Hydrotamoxifen
PBS	Phosphate-buffered saline
PCR	Polymerase chain reaction
PDH	Pyruvate dehydrogenase
PDI	Protein disulfide isomerase
PDK1	Phosphoinositide-dependent protein kinase 1
PDK4	Phosphoinositide-dependent protein kinase 4
PDX1	Pancreatic duodenal homeobox-1
PERK	Pancreatic ER kinase
PFK-2	6-phosphorfructo-2-kinase
Pgc1-α	Peroxisome proliferator-activated receptor gamma coactivator 1-α
PI3K	Phosphoinositide-3 kinase
PKB	Protein kinase b
PKCζ	Protein kinase C-ζ
Plin2	Perilpin 2

PM	Plasma membrane
PP1	Protein phosphatase 1
PPARγ	Persoxisome proliferator-activated receptor γ
Pras40	Proline-rich Akt substrate
pWAT	Perigonadal white adipose tissue
Q	Quartet
qPCR	Quantitative real-time PCR
RAAS	Renin-angiotensin aldosterone system
RNA	Ribonucleic acid
SD	Standard deviation
SDS	Sodium dodecyl sulphate
SIRT1	silent mating type information regulation 2 homolog
SM	Sec1/Munc18-like
SNAP23	Synaptosomal-associated protein 23
SNARE	Snap receptor
STAT1	Signal transducer and activator of transcription 1
SV	Storage vesicle
SV	Stroke volume
Syn4	*Syntaxin 4*
TAC	Transaortic constriction
TAG	Triacylglycerol
TBS	Tris-buffered saline
TCA	Tricarboxylic acid
TCL	Total cell lysate

TGFβ	Transforming growth factor β
TNFα	Tumor necrosis factor α
tSNARE	target snap receptor
Tx	Tamoxifen
u	Unit
VAMP2	Vesicle-associated membrane protein 2
vSNARE	Vesicle snap receptor
wt	Wildtype
µ	Micro

9 Statutory Declaration

Statutory declaration

I declare under oath that I have produced my thesis independently and without any undue assistance by third parties under consideration of the 'Principles for the Safeguarding of Good Scientific Practice' at Heinrich Heine University Düsseldorf. Furthermore, I assure that I did not submit this dissertation, either in full or in part, to any other faculty and did not absolve any promotion trials before.

Düsseldorf,

Lisa Kalfhues

Eidesstattliche Erklärung

Ich versichere an Eides Statt, dass die Dissertation von mir selbstständig und ohne unzulässige fremde Hilfe unter Beachtung der "Grundsätze zur Sicherung guter wissenschaftlicher Praxis an der Heinrich-Heine Universität Düsseldorf" erstellt worden ist. Darüber hinaus versichere ich, dass ich die Dissertation weder in der hier vorgelegten noch in einer ähnlichen Form bei einem anderen Institut eingereicht habe und bisher keine Promotionsversuche unternommen habe.

Düsseldorf,

Lisa Kalfhues

Danksagung

Axel – Danke, dass du mir vor knapp 4 Jahren die großartige Möglichkeit gegeben hast Teil deines Teams zu werden und mir seitdem immer mir Rat und Tat zur Seite gestanden hast. Vielen Dank, dass du mich immer wieder motiviert hast aus meiner Komfortzone zu treten, wodurch ich mich fachlich aber auch persönlich stängig weiterentwickeln konnte.

Prof. Dr. Reza Ahmadian – Danke für die Übernahme des Zweitgutachtens.

Christoph, Vici and Jacqueline – Thank you for being amazing PhD buddies and for the professional and emotional support during all the countless hours we spent in the lab.

Rianne und André -Danke für eure wissenschaftliche Expertise, emotionale Unterstützung und die immer ehrlichen Worte. Ihr habt mich immer wieder inspiriert, motiviert und an mich geglaubt, auch wenn ich mal an mir gezweifelt habe. Danke für eure Freundschaft!

Das ganze Team der HKP – Danke, dass ich Teil dieses großartigen Teams sein konnte und ich immer eine unterstützende Hand in jeder Lage gefunden habe. Danke für euren Zusammenhalt!

Sandra und das gesamte IRTG 1902 – Danke für fast 4 aufregende Jahre voller Herausforderungen und allen Möglichkeiten.

To all my friends in Charlottesville – Thank you for making my stay at UVa such an amazing experience.

All meinen Freunden aus Münster und Düsseldorf und meiner Familie: Mama, Papa, Anna, Stefan und Andi – Danke für eure Liebe und euer Verständnis in jeder Lage. Danke, dass ihr mich immer ausgehalten und wieder aufgebaut habt.